The role of p300 in cardio-oncology: implications for breast and prostate cancer treatments and impact on vascular function

by

Olivia Nicolle Kunkel

B.S., Kansas State University, 2018
M.S., Kansas State University, 2019

AN ABSTRACT OF A DISSERTATION

submitted in partial fulfillment of the requirements for the degree

DOCTOR OF PHILOSOPHY

Department of Kinesiology
College of Health and Human Sciences

KANSAS STATE UNIVERSITY
Manhattan, Kansas

2024

Abstract

In men and women in the United States, prostate and breast cancer account for nearly a third of all new cancer diagnoses each year. Though the five-year survival is over 90% for both, those with metastatic disease have a five-year survival closer to 30%. For many of these individuals, treatment with radiation, chemotherapy, or a combination of several therapies is curative. However, many individuals will experience treatment failure or severe side effects that require early cessation of standard treatment, which is associated with increased recurrence and worse survival outcomes. As such, finding adjuvant treatment options that can enhance treatment efficacy and limit side effects is of critical importance. Given the evidence supporting the role of p300 in DNA damage repair, which is an important factor mediating the efficacy of radiation, we sought to understand whether p300, a histone acetyltransferase and transcriptional coactivator, or its homologue CREB binding protein (CBP), plays a role in the success of radiation therapy in humans by performing a candidate gene association study (Chapter 2). We found that there are several p300 and CBP single nucleotide polymorphisms (SNPs) associated with the odds of diagnosis of a second malignancy after radiation, suggesting that they may play a role in the efficacy of radiation therapy in humans. As a follow-up to these findings, we investigated the role of p300/CBP in the radiosensitivity of human prostate and breast cancer cells *in vitro* through pharmacological inhibition. Results from this work did not reveal any effect of p300/CBP inhibition on prostate or breast cancer cell survival after radiation. In chapter 3, we further investigated the role of p300/CBP in the response to doxorubicin, a first line drug for metastatic breast cancer. First, we investigated whether p300 or CBP plays a role in the success of doxorubicin by performing a candidate gene association study. We found that there are several CBP, but no p300, SNPs that decrease the odds of second malignancy after doxorubicin,

suggesting that CBP may play a role in the efficacy of doxorubicin. We followed these findings with *in vitro* experiments to determine the role of p300/CBP inhibition on breast cancer cell survival after exposure to doxorubicin and found that p300/CBP inhibition had no effect on the efficacy of doxorubicin. We also sought to determine if p300/CBP modulates the effects of doxorubicin on the vasculature, a physiological target for development of adverse cardiotoxicity, by investigating vascular reactivity of the thoracic aorta in rats, finding that there was no effect of either p300/CBP inhibition or doxorubicin *ex vivo*. Finally, in chapter 4, we sought to characterize the vascular, skeletal muscle mass, and cardiac mass changes in an orthotopic model of breast cancer. We found that independent of any treatment, the breast tumor vasculature exhibits impaired α-adrenergic vasoconstriction and that skeletal muscle, but not cardiac muscle, atrophy may occur, mirroring several findings that have been demonstrated in orthotopic prostate cancer models. Together, our findings suggest that there may be an association between p300/CBP and the odds of diagnosis of secondary malignancy after exposure to anti-cancer therapies. However, further investigation is needed to determine the exact role of p300/CBP on the efficacy of current first line anti-cancer therapies. We also determined that the orthotopic breast cancer model extends several findings from orthotopic models of prostate cancer, suggesting it may be useful to study interventions that rely on hemodynamic alterations.

The role of p300 in cardio-oncology: implications for breast and prostate cancer treatments and impact on vascular function

by

Olivia Nicolle Kunkel

B.S., Kansas State University, 2018
M.S., Kansas State University, 2019

A DISSERTATION

submitted in partial fulfillment of the requirements for the degree

DOCTOR OF PHILOSOPHY

Department of Kinesiology
College of Health and Human Sciences

KANSAS STATE UNIVERSITY
Manhattan, Kansas

2024

Approved by:

Major Professor
Bradley J Behnke

Copyright

Abstract

In men and women in the United States, prostate and breast cancer account for nearly a third of all new cancer diagnoses each year. Though the five-year survival is over 90% for both, those with metastatic disease have a five-year survival closer to 30%. For many of these individuals, treatment with radiation, chemotherapy, or a combination of several therapies is curative. However, many individuals will experience treatment failure or severe side effects that require early cessation of standard treatment, which is associated with increased recurrence and worse survival outcomes. As such, finding adjuvant treatment options that can enhance treatment efficacy and limit side effects is of critical importance. Given the evidence supporting the role of p300 in DNA damage repair, which is an important factor mediating the efficacy of radiation, we sought to understand whether p300, a histone acetyltransferase and transcriptional coactivator, or its homologue CREB binding protein (CBP), plays a role in the success of radiation therapy in humans by performing a candidate gene association study (Chapter 2). We found that there are several p300 and CBP single nucleotide polymorphisms (SNPs) associated with the odds of diagnosis of a second malignancy after radiation, suggesting that they may play a role in the efficacy of radiation therapy in humans. As a follow-up to these findings, we investigated the role of p300/CBP in the radiosensitivity of human prostate and breast cancer cells *in vitro* through pharmacological inhibition. Results from this work did not reveal any effect of p300/CBP inhibition on prostate or breast cancer cell survival after radiation. In chapter 3, we further investigated the role of p300/CBP in the response to doxorubicin, a first line drug for metastatic breast cancer. First, we investigated whether p300 or CBP plays a role in the success of doxorubicin by performing a candidate gene association study. We found that there are several CBP, but no p300, SNPs that decrease the odds of second malignancy after doxorubicin,

suggesting that CBP may play a role in the efficacy of doxorubicin. We followed these findings with *in vitro* experiments to determine the role of p300/CBP inhibition on breast cancer cell survival after exposure to doxorubicin and found that p300/CBP inhibition had no effect on the efficacy of doxorubicin. We also sought to determine if p300/CBP modulates the effects of doxorubicin on the vasculature, a physiological target for development of adverse cardiotoxicity, by investigating vascular reactivity of the thoracic aorta in rats, finding that there was no effect of either p300/CBP inhibition or doxorubicin *ex vivo*. Finally, in chapter 4, we sought to characterize the vascular, skeletal muscle mass, and cardiac mass changes in an orthotopic model of breast cancer. We found that independent of any treatment, the breast tumor vasculature exhibits impaired α-adrenergic vasoconstriction and that skeletal muscle, but not cardiac muscle, atrophy may occur, mirroring several findings that have been demonstrated in orthotopic prostate cancer models. Together, our findings suggest that there may be an association between p300/CBP and the odds of diagnosis of secondary malignancy after exposure to anti-cancer therapies. However, further investigation is needed to determine the exact role of p300/CBP on the efficacy of current first line anti-cancer therapies. We also determined that the orthotopic breast cancer model extends several findings from orthotopic models of prostate cancer, suggesting it may be useful to study interventions that rely on hemodynamic alterations.

Table of Contents

List of Figures

List of Tables

Acknowledgements

First, thank you to my mentor, Dr. Brad Behnke, whose KIN 603 class is what started this journey for me. Thank you for the opportunity to join the lab to pursue my master's degree, and for continuing to support me as I stayed for my doctoral degree. To Dr. Carl Ade, thank for not only serving as a member of my committee, but for providing me endless opportunities to spend time in your lab and for truly going above and beyond to provide guidance on many projects. Thank you to the other members of my committee, Drs. Emily Mailey and Nick Wallace; I truly can't thank you enough for all the support you have provided over the last few years. To all of my fellow graduate students, thank you for your support, both scientific and social, with a special thank you to Dr. Dryden Baumfalk for a being a big part of my journey to joining the Behnke Lab. I'd also like to thank the K-State Johnson Cancer Research Center for supporting much of this research, and the members of the K-State College of Veterinary Medicine Radiation Oncology team. A special shoutout to both Vennture and Lake Effect Coffee in Milwaukee for making the writing of this dissertation possible.

To my parents, Dylan and Liza, and my sister, Tori, thank you for your constant support throughout my entire academic journey, but especially throughout the last year. I would not have made it to this point without your love and encouragement. Lastly, to Steve. Thank you doesn't even begin to cover it but thank you; for everything.

Preface

The studies included in this dissertation are written as three independent manuscripts. These manuscripts are not yet submitted in scientific journals for publication, but are in the final stages of preparation for submission.

Chapter 1 - Background

Worldwide, nearly 20 million people are diagnosed with cancer each year, and in the United States, there is nearly a 40% lifetime risk of being diagnosed with cancer. In 2024 alone, there will be over 2 million new diagnoses in the United States [1]. Despite drastic improvements in treatments over the last several hundred years, cancer remains the leading cause of death for Americans under age 85, and for those who do survive cancer, the life-saving treatments they received often lead to life-limiting side effects.

The first known descriptions of cancer (and its treatment) date back to 3000 BC, described in the Edwin Smith Papyrus in Egypt [2]. However, it would be centuries before our understanding of cancer and modern medicine were sufficient to develop curative treatments. Thanks to the adoption of the scientific method, an improved understanding of human physiology, and emergence of pathology and oncology, successful treatments for cancer began to develop. The first documented treatment was surgery—a radical mastectomy performed in 1882 [3] —which has remained a mainstay for the treatment of many cancers today. But for many, surgery alone is not curative or may not be a viable treatment option. Fortunately, a variety of other treatments have been developed as adjuvants or alternatives to surgery, thanks in part to funding created specifically for cancer research. Beyond surgery, radiation was first used to cure cancer in 1899 in a case of squamous cell carcinoma of the skin [4], with hormonal therapy and chemotherapies introduced in the 1940s [5]. As a result of extensive research and development in these new treatment modalities, patients are now treated with regimens tailored for success for their cancer type, stage, and genetic mutations. In addition to the research directed at developing new anti-cancer therapies, significant efforts have also been focused on prevention and early detection, which have significantly contributed to reductions in overall cancer mortality.

Unfortunately, cancer incidence continues to increase for several cancers, and treatment failure, treatment side effects, and early discontinuation remain a significant challenge in oncology.

Of the cancers with an increasing incidence, breast and prostate cancers are the most diagnosed, representing nearly a third of all new diagnoses for women and men, respectively [1]. Despite a five-year survival rate of 91% for all stages combined, breast cancer is the second-leading cause of cancer-related deaths in women in the United States, and the five-year survival rate is much lower (31%) [6] for those with metastatic disease. Like breast cancer, prostate cancer is the second-leading cause of cancer-related deaths for men in the United States. The five-year survival rate is 97% for all stages combined, but as with breast cancer, drops greatly (34%) [7] for those with metastatic disease. Both cancers may be treated with surgery, radiation therapy, chemotherapy, hormone therapy, immunotherapy, targeted therapy, or a combination of two or more, though radiation and chemotherapy will be the focus of this dissertation.

Approximately 50% of all individuals diagnosed with cancer will receive radiation, more than half of whom are treated with curative intent [8]. In addition, radiation is affordable relative to other anti-cancer therapies (only 5% of total cost of cancer care) [9]. Though radiation is primarily used after surgical intervention and tumor removal in patients with breast cancer, its use is important to prevent recurrence and for the treatment of nearby lymph nodes [10]. It is also standard for the treatment of recurrent breast cancer [11]. In prostate cancer, radiation therapy is often the first-line treatment for cancer localized to the prostate [12,13] and is also used to treat advanced and recurrent prostate cancers [14]. However, radiation may be ineffective for some individuals, leading to a higher total radiation dose or reliance on other therapies that have greater potential side effects. Another consideration with radiation is the damage that occurs to other nearby tissues. Though the methods of administering radiation have progressed to decrease

exposure of nearby healthy tissues, the risk of radiation-related toxicities increases with increasing dose [15]. Therefore, optimizing radiosensitivity will improve treatment outcomes and reduce toxicities to other tissues, as well as decrease reliance on other anti-cancer therapies that have the potential for vast systemic side effects (i.e., anti-androgen therapies, anti-VEGF therapies, etc.).

Chemotherapy is also often used to treat breast cancer, either before or after surgery. Doxorubicin is one of the most used and will be the chemotherapy of focus for this dissertation. Doxorubicin belongs to the class of drugs known as anthracyclines and is one of the most effective chemotherapy drugs to treat breast cancer. Doxorubicin works primarily by inhibiting Topoisomerase IIb (TopIIb), which leads to the accumulation of DNA damage, and by producing reactive oxygen species (ROS), which also results in DNA damage [16,17]. While doxorubicin induces irreparable damage in cancer cells, it can unfortunately do the same in off-target tissues, which is of particular concern in the cardiovascular system and can result in cardiotoxicity. The reported incidence of anthracycline cardiotoxicity ranges from 6-48%, occurs in a dose-dependent manner, and is associated with poor patient outcomes and early cessation of treatment [18-20]. While the primary focus of cardiotoxicity research has historically been specific to the heart, emerging evidence suggests an important and understudied role of the vasculature in the manifestations of cardiotoxicity [21-27]. Therefore, strategies to improve treatment efficacy while limiting toxicities are of critical importance to ensuring successful patient outcomes.

Inobrodib, (CCS-1477) a small-molecule inhibitor of p300 and its homologue CBP, is currently in clinical trials for the treatment of several types of cancer and may modulate the effects of anti-cancer therapies. p300 and CBP are transcriptional co-activators that act as histone acetyltransferases, interacting with hundreds of transcription factors. Because p300/CBP is

reported to play a role in DNA damage repair, oxidative stress, and cellular senescence [28-36], it represents a unique treatment that may impact the effects of anti-cancer therapies.

The primary purpose of this dissertation is to explore the role of p300/CBP in the response to radiation therapy and doxorubicin. In Chapter 2, we investigated whether single nucleotide polymorphisms (SNPs) in the p300 or CBP gene encoding regions are associated with the odds of a diagnosis of secondary malignancy in individuals diagnosed with prostate or breast cancer and in those treated explicitly with radiation. We also investigated the role of the highly specific p300/CBP inhibitor CCS-1477 in cancer cell radiosensitivity in prostate and breast cancer cells. In Chapter 3, we investigated whether there is an association between p300/CBP SNPs and the odds of diagnosis of secondary malignancy in individuals who received doxorubicin. Chapter 4 aims to characterize the vascular function of breast tumor arterioles and determine whether cachexia might occur in an orthotopic model of breast cancer. Together, we hope these studies can provide insight into potential therapeutic interventions that improve cancer treatment outcomes and reduce treatment side effects.

References

1 Siegel, R. L., Giaquinto, A. N. & Jemal, A. Cancer statistics, 2024. *CA Cancer J Clin* **74**, 12-49 (2024). https://doi.org:10.3322/caac.21820

2 Hajdu, S. I. A note from history: landmarks in history of cancer, part 1. *Cancer* **117**, 1097-1102 (2011). https://doi.org:10.1002/cncr.25553

3 Halsted, W. S. I. The Results of Radical Operations for the Cure of Carcinoma of the Breast. *Ann Surg* **46**, 1-19 (1907). https://doi.org:10.1097/00000658-190707000-00001

4 Connell, P. P. & Hellman, S. Advances in Radiotherapy and Implications for the Next Century: A Historical Perspective. *Cancer Research* **69**, 383-392 (2009). https://doi.org:10.1158/0008-5472.Can-07-6871

5 DeVita, V. T., Jr. & Chu, E. A History of Cancer Chemotherapy. *Cancer Research* **68**, 8643-8653 (2008). https://doi.org:10.1158/0008-5472.Can-07-6611

6 Survival Rates for Breast Cancer.

7 What Are the Survival Rates for Prostate Cancer?

8 Baskar, R., Lee, K. A., Yeo, R. & Yeoh, K. W. Cancer and radiation therapy: current advances and future directions. *Int J Med Sci* **9**, 193-199 (2012). https://doi.org:10.7150/ijms.3635

9 Norlund, A. Costs of radiotherapy. *Acta Oncol* **42**, 411-415 (2003). https://doi.org:10.1080/02841860310011140

10 Kim, C. S. & Algan, O. Radiation Therapy for Early-Stage Breast Cancer. (2017).

11 Siglin, J., Champ, C. E., Vakhnenko, Y., Anne, P. R. & Simone, N. L. Radiation therapy for locally recurrent breast cancer. *Int J Breast Cancer* **2012**, 571946 (2012). https://doi.org:10.1155/2012/571946

12 Hamdy, F. C. *et al.* 10-Year Outcomes after Monitoring, Surgery, or Radiotherapy for Localized Prostate Cancer. *N Engl J Med* **375**, 1415-1424 (2016). https://doi.org:10.1056/NEJMoa1606220

13 Miller, D. R., Ingersoll, M. A., Teply, B. A. & Lin, M. F. in *Prostate Cancer* (eds S. R. J. Bott & K. L. Ng) (Exon Publications
Copyright: The Authors., 2021).

14 Treating Prostate Cancer That Doesn’t Go Away or Comes Back After Treatment.

15 Wang, K. & Tepper, J. E. Radiation therapy-associated toxicity: Etiology, management, and prevention. *CA Cancer J Clin* **71**, 437-454 (2021). https://doi.org:10.3322/caac.21689

16 Kciuk, M. *et al.* Doxorubicin-An Agent with Multiple Mechanisms of Anticancer Activity. *Cells* **12** (2023). https://doi.org:10.3390/cells12040659

17 Thorn, C. F. *et al.* Doxorubicin pathways: pharmacodynamics and adverse effects. *Pharmacogenet Genomics* **21**, 440-446 (2011). https://doi.org:10.1097/FPC.0b013e32833ffb56

18 Cardinale, D., Iacopo, F. & Cipolla, C. M. Cardiotoxicity of Anthracyclines. *Front Cardiovasc Med* **7**, 26 (2020). https://doi.org:10.3389/fcvm.2020.00026

19 Curigliano, G. *et al.* Cardiotoxicity of anticancer treatments: Epidemiology, detection, and management. *CA Cancer J Clin* **66**, 309-325 (2016). https://doi.org:10.3322/caac.21341

20 Lotrionte, M. *et al.* Review and meta-analysis of incidence and clinical predictors of anthracycline cardiotoxicity. *Am J Cardiol* **112**, 1980-1984 (2013). https://doi.org:10.1016/j.amjcard.2013.08.026

21 Bosman, M. *et al.* Doxorubicin induces arterial stiffness: A comprehensive in vivo and ex vivo evaluation of vascular toxicity in mice. *Toxicol Lett* **346**, 23-33 (2021). https://doi.org:10.1016/j.toxlet.2021.04.015

22 Bosman, M. *et al.* Dexrazoxane does not mitigate early vascular toxicity induced by doxorubicin in mice. *PLoS One* **18**, e0294848 (2023). https://doi.org:10.1371/journal.pone.0294848

23 Bosman, M. *et al.* Doxorubicin Impairs Smooth Muscle Cell Contraction: Novel Insights in Vascular Toxicity. *Int J Mol Sci* **22** (2021). https://doi.org:10.3390/ijms222312812

24 Frye, J. N. *et al.* Vascular and autonomic changes in adult cancer patients receiving anticancer chemotherapy. *J Appl Physiol (1985)* **125**, 198-204 (2018). https://doi.org:10.1152/japplphysiol.00005.2018

25 Parr, S. K. *et al.* Anticancer Therapy-Related Increases in Arterial Stiffness: A Systematic Review and Meta-Analysis. *J Am Heart Assoc* **9**, e015598 (2020). https://doi.org:10.1161/jaha.119.015598

26 Chaosuwannakit, N. *et al.* Aortic stiffness increases upon receipt of anthracycline chemotherapy. *J Clin Oncol* **28**, 166-172 (2010). https://doi.org:10.1200/jco.2009.23.8527

27 Clayton, Z. S. *et al.* Doxorubicin-Induced Oxidative Stress and Endothelial Dysfunction in Conduit Arteries Is Prevented by Mitochondrial-Specific Antioxidant Treatment. *JACC CardioOncol* **2**, 475-488 (2020). https://doi.org:10.1016/j.jaccao.2020.06.010

28 Dutto, I., Scalera, C. & Prosperi, E. CREBBP and p300 lysine acetyl transferases in the DNA damage response. *Cell Mol Life Sci* **75**, 1325-1338 (2018). https://doi.org:10.1007/s00018-017-2717-4

29 Ogiwara, H. & Kohno, T. CBP and p300 Histone Acetyltransferases Contribute to Homologous Recombination by Transcriptionally Activating the *BRCA1* and *RAD51* Genes. *Plos One* **7** (2012). https://doi.org:10.1371/journal.pone.0052810

30 Ogiwara, H. *et al.* Histone acetylation by CBP and p300 at double-strand break sites facilitates SWI/SNF chromatin remodeling and the recruitment of non-homologous end joining factors. *Oncogene* **30**, 2135-2146 (2011). https://doi.org:10.1038/onc.2010.592

31 Wallace, N. A., Robinson, K., Howie, H. L. & Galloway, D. A. β-HPV 5 and 8 E6 Disrupt Homology Dependent Double Strand Break Repair by Attenuating BRCA1 and BRCA2 Expression and Foci Formation. *Plos Pathog* **11** (2015). https://doi.org:10.1371/journal.ppat.1004687

32 Chiu, J., Khan, Z. A., Farhangkhoee, H. & Chakrabarti, S. Curcumin prevents diabetes-associated abnormalities in the kidneys by inhibiting p300 and nuclear factor-kappaB. *Nutrition* **25**, 964-972 (2009). https://doi.org:10.1016/j.nut.2008.12.007

33 Kim, J. Y., Jo, J., Leem, J. & Park, K. K. Inhibition of p300 by Garcinol Protects against Cisplatin-Induced Acute Kidney Injury through Suppression of Oxidative Stress, Inflammation, and Tubular Cell Death in Mice. *Antioxidants (Basel)* **9** (2020). https://doi.org:10.3390/antiox9121271

34 Lan, F., Hu, Y., Tang, D., Cai, J. & Zhang, Q. Transcription coactivator p300 promotes inflammation by enhancing p65 subunit activation in type 2 diabetes nephropathy. *Int J Clin Exp Pathol* **12**, 1826-1834 (2019).

35 Sen, P. *et al.* Histone Acetyltransferase p300 Induces De Novo Super-Enhancers to Drive Cellular Senescence. *Mol Cell* **73**, 684-698.e688 (2019). https://doi.org:10.1016/j.molcel.2019.01.021

36 Zhang, E. *et al.* Metformin and Resveratrol Inhibited High Glucose-Induced Metabolic Memory of Endothelial Senescence through SIRT1/p300/p53/p21 Pathway. *PLoS One* **10**, e0143814 (2015). https://doi.org:10.1371/journal.pone.0143814

Chapter 2 - Role of p300 in prostate and breast cancer radiosensitivity

Abstract

Over 50% of individuals diagnosed with prostate and breast cancer will be treated with radiation therapy at some point during their treatment, but many will experience treatment failure. Understanding potential mediators of treatment failure is critical to improving the efficacy of radiation. Given the role of p300/CBP in DNA damage repair, and because DNA damage is critical for the efficacy of radiation, we hypothesized that p300/CBP may be important in mediating the response to radiation. As such, we hypothesized that there would be an association between p300/CBP single nucleotide polymorphisms and the odds of secondary malignancy after radiation. We also hypothesized that p300/CBP inhibition would enhance the efficacy of radiation *in vitro.* Using a candidate gene association study approach, we found that single nucleotide polymorphisms in the p300 and CBP gene encoding regions are associated with the odds of diagnosing secondary malignancy in individuals who received radiation. We also found that pharmacological inhibition of p300/CBP does not impact the efficacy of radiation in prostate or breast cancer cells *in vitro*. Given that p300/CBP single nucleotides are associated with odds of second malignancy, further investigation into the role of p300/CBPs in mediating or predicting the response to radiation is warranted. In addition, investigating the role of p300/CBP inhibition *in vivo* will provide insight into its role in mediating the efficacy of radiation.

Introduction

Prostate and breast cancers are the most diagnosed cancers in the United States for men and women, respectively, and represent the second leading causes of cancer-related deaths. This translates to approximately 300,000 new diagnoses of each in 2024 alone, and over 10% of all cancer-related deaths for each sex [1]. Over 50% of these individuals will be treated with radiation therapy at some point during their treatment [2], but many will experience treatment failure. In prostate cancer, the relapse rate in men treated with radiation therapy varies greatly, ranging from 6-88%, and depends on cancer stage, prostate specific antigen (PSA) level, and Gleason score [3]. Conversely, in breast cancer, radiation is rarely used as a sole treatment, and thus, estimates of failure rates are difficult to determine. However, even individuals receiving combined therapies with radiation (chemotherapy, surgery, immunotherapy, etc.) experience local, regional, and distant recurrence [4,5]. Despite the wide-ranging estimates for the success of radiation therapy, it remains a critical component of both prostate and breast cancer treatment regimens, and strategies to improve its efficacy are important for improving the outcomes of those diagnosed with cancer.

Several drugs have emerged in recent years as radiosensitizing agents, but the therapeutic advantage remains small, and most do not improve clinical outcomes [6]. As such, there remains a need to develop new strategies to improve radiation efficacy. Briefly, radiation therapy works by causing either direct or indirect damage to the DNA of cancer cells. Direct damage occurs through disruption of the molecular structure of DNA, whereas indirect damage occurs when the molecular structure of DNA is damaged by a reaction with free radicals produced from the interaction of ionizing radiation with other cellular components, like water [7-9]. The most lethal type of radiation damage is the formation of double-stranded breaks (DSBs) [10-13]. DSBs result in

breakage in both strands of the DNA backbone, and cells will not survive without the repair of these breaks. Several DNA damage repair (DDR) mechanisms exist and are important for maintaining the genomic stability of normal cells. However, the ability to repair DNA damage may be a significant contributor to radioresistance of cancer cells. DDR involves an extensive number of repair processes and associated proteins (e.g., Ku70/80, BRCA1, etc.) [13-17]. The two main pathways for DSB repair involving these proteins are non-homologous end joining (NHEJ) and homologous recombination (HR) [9,15,16].

Important for both NHEJ and HR is p300 (as well as its homologue, cREB binding protein (CBP)), a transcriptional co-activator and histone acetyltransferase. p300 is required for the recruitment of Ku70/80 to the sites of DSBs for initiation of NHEJ [18] and is a transcriptional co-activator for the genes encoding the HR proteins BRCA1, BRCA2, and RAD51 [19]. Inhibition of p300/CBP by C646 has been shown to decrease the recruitment of NHEJ-associated proteins to DSB sites [18] and increase radiosensitivity of lung cancer cells [18,20]. Knockdown of p300 has also been shown to decrease mRNA expression of RAD51 and BRCA1 [19], and decrease BRCA1 and BRCA2 protein expression, resulting in inefficient DSB repair in response to radiation-induced damage [21]. There are also various cancer cell lines that demonstrate increased radiosensitivity after inhibition of RAD51 that may be mediated by a decrease in DSB repair [22]. Together, these findings highlight the importance of p300/CBP in mediating the response to radiation via successful repair of DSBs.

Given the growing evidence for the importance of DNA repair proteins in mediating radiosensitivity and potential role of p300/CBP in the expression of these proteins, we investigated the role of p300/CBP in the recurrence of cancer, as well as in the recurrence of cancer in individuals who received radiation. First, we tested the hypothesis that there is an

association between p300/CBP single nucleotide polymorphisms (SNPs) and the odds of second malignancy in individuals diagnosed with prostate or breast cancer by conducting an exploratory candidate gene association study (CGAS) using the NIH *All of Us* database. Second, we tested the hypothesis that pharmacological inhibition of p300/CBP would increase radiosensitivity *in vitro* by assessing the efficacy of radiation in prostate and breast cancer cells exposed to a highly specific small molecule p300/CBP inhibitor (CCS-1477).

Methods

Ethics and Data Availability

The authors declare that all supporting data are available within the present manuscript or its online supplementary files. Registered-tier data (e.g., survey, electronic health record, etc.) and controlled-tier data (i.e., genomic data, specific demographic data) are available through the National Institutes of Health (NIH) *All of Us* Researcher Workbench (https://allofus.nih.gov/).

The *All of Us* database aims to compile data for 1 million participants from diverse ethnic and socioeconomic backgrounds. Currently available data include over 400,000 participants, over 40% of whom identify as racial and ethnic minorities, and over 80% of whom are underrepresented in biomedical research. Informed consent was obtained at the time of participant enrollment, with the enrollment period for the current databank (*Version 7*) occurring from May 1, 2018, to July 1, 2022.

Data were accessed only by authorized users who completed the NIH *All of Us* Responsible Conduct of Research Training and received approval. Data are reported in accordance with the NIH *All of Us* Data and Statistics Dissemination Policy, which prohibits disclosure of any group count less than 20 individuals to protect participant privacy. Data are de-identified and thus, exempt from review by the Kansas State University Institutional Review Board.

Candidate Gene Association Study (CGAS)

Cancer Diagnosis and Treatment

Cancer diagnoses were obtained from electronic health records (EHR) and survey data. EHR data were harmonized using the Observational Medical Outcomes Partnership Common

Data Model (OMOP CDM). The *Personal Medical History* form provided self-reported data on cancer history, cancer type, time of cancer diagnosis, and treatment history. Cancer diagnoses from EHR were determined from Systematized Nomenclature of Medicine (SNOMED) codes, which have previously shown to have high validity [23,24]. Cancers selected for the present study were restricted to prostate and breast cancer, the most common non-skin cancer in men and women, respectively [1]. Participant demographics were derived from the *Basics* survey, which includes age, race and ethnicity, household income, education, and more. Deprivation index is derived from the American Community Survey and serves as a measure of socioeconomic variation in health outcomes. Full survey question content is accessible via the *All of Us* Research Hub.

Variables and Outcomes

Primary cancer diagnosis, diagnosis of second malignancy, and associated cancer treatments were derived from EHR and survey data. Cancer treatments were also recorded from survey and EHR data. *All of Us* concept vocabulary and SNOMED codes were applied to search for the use of radiotherapy (SNOMED Code: 108290001). The primary outcome in the present study was diagnosis of second malignancy (SNOMED Code: 128462008). This was selected as a surrogate indicator of treatment failure after anti-cancer therapy for two reasons: 1) the very low number of recurrent malignancies directly documented in the *All of Us* database health records (n $\leq$ 20), and 2) previous work demonstrating the use of secondary malignancy codes for determining the timing of recurrent or secondary cancer [25]. Those with a diagnosis of second malignancy less than 60 days after primary diagnosis (all treatments combined cohort) or less than 60 days after treatment (i.e., radiotherapy) were excluded from analyses, as were individuals without available genome sequencing. The selection of 60 days is based on international World

Health Organization guidelines previously established for EHR research on infectious disease [26] and frequently adapted for cancer research [27] or cancer management in health systems [28].

Genomic Data

All of Us specimen samples were obtained from participant blood samples. Briefly, DNA extracted from samples was sent to genome centers for whole genome sequencing. For the present study, p300 and CBP were selected as candidate genes, located on chromosome 22q13.2 and 16p13.3, respectively, and all SNPs with a minor allele frequency of 0.01 (MAF $\geq$ 0.01) were considered for analysis. Reference SNP ID (rsID) and respective functional outcomes were obtained from the NIH *National Center for Biotechnology Information* (NCBI) Single Nucleotide Polymorphism database (dbSNP).

Cell Culture Study

Human prostate adenocarcinoma (PC-3) and human breast adenocarcinoma (MDA MB 231) cells were obtained from American Type Culture Collection (ATCC; Manassas, VA). Cells were grown in RPMI-1640 or DMEM medium, respectively, and supplemented with 10% fetal bovine serum (FBS) and 2mM l-glutamine. Cultures were maintained in 75cm^2 flasks at 37º C in a humidified incubator with 5% CO_2/room air balance. Cells were randomized to receive 0 or 2 Gy radiation and vehicle or CCS-1477.

Radiation and p300 inhibition

24 hours prior to radiation, all cells were seeded in 25 cm^2 flasks. Cells were treated with 1uM of the p300/CBP inhibitor CCS-1477 (Chemietek, Indianapolis, IN) dissolved in DMSO or with an equivalent concentration of vehicle (DMSO, less than 1% final media volume) one hour

prior to radiation. Cells were subjected to 0 Gy (sham) or 2 Gy single doses of photon radiation with a linear accelerator (Clinac 2100 CD, Varian Medical Systems, Palo Alto, CA) at room temperature. Cells were re-incubated after radiation until clonogenic survival assays were performed. The experiment was repeated three times on separate days from three different stocks of frozen cells.

Clonogenic Survival

Cells were re-incubated for four hours before preparation for clonogenic survival assays, as the majority of early DNA repair is completed within a few hours [29]. The clonogenic survival assay methods were performed following the methods of Franken, et al., and Feoktistova, et al., [30,31]. Cells were isolated via trypsinization and re-suspended in media. Cells were then counted and seeded into 100 mm culture plates at a density of 200 cells/plate, performed in triplicate. Plates were placed in a humidified incubator maintained at 37º C with 5% CO_2/room air balance. After 9 days, cells were fixed and stained with 20% methanol and 0.5% crystal violet in water (see Figure 2.1A). Cells were observed under a microscope at 10x magnification and colonies >50 cells were counted (see Figure 2.1B). Plating efficiency was determined as the percentage survival of colonies in the control condition. Survival fraction for each group was determined relative to control and expressed as % survival according to the following equation:

$$\%\ survival = \left(\frac{colonies\ formed}{PE * number\ of\ cells\ plated}\right) * 100$$

where PE is the plating efficiency of control cells and % survival is the average of three separate experiments, each performed in technical triplicate.

Data Analysis and Statistics

All statistical analyses for *All of Us* were performed using the *All of Us* integrated cloud based Jupyter Notebook within the *All of Us* Researcher Workbench using Python coding language (version 3.12) and Python package Hail (https://github.com/hail-is/hail/releases/tag/0.2.13). Descriptive statistics of the study population are presented as mean ± standard deviation (SD). Before genetic analyses, SNPs were first filtered according to standard quality control practices. In brief, samples were removed for relatedness between individual participants due to heritability of genetic variants [32], then SNPs were further filtered to include only common variants (MAF ≥ 0.01) and those meeting Hardy-Weinberg equilibrium criteria ($p > 1.0 \times 10^{-10}$) [33]. For subsequent association analyses between SNPs and diagnosis of second malignancy in individuals previously diagnosed with prostate or breast cancer, we performed logistic regression adjusted for the first three principal components representing ancestry. Subgroup analysis was performed including only individuals who received radiation (prostate and breast cancer cohort). Beta (β) values were converted to Odds Ratio (OR) using the equation:

$$OR = \exp(\beta)$$

90% confidence intervals (CI) were constructed from the upper and lower limits from the equation:

$$90\%\ CI = [\exp(\beta) \pm (1.645 * \mathrm{SE})]$$

where SE is the standard error of the mean for β. Due to the exploratory nature of part 1 of the present study, significance was set *a priori* as $p \leq 0.1$.

Statistical analyses for cell culture experiments were performed in Prism (Version 10, GraphPad Software, San Diego, CA) data analysis software. All comparisons were made with two-way analysis of variance (ANOVA), followed by individual comparisons corrected by Holm-Sidak post hoc testing. Data are expressed as % survival, which was determined as percentage of control and presented as mean $\pm$ SEM. The level of significance was set as $p \leq 0.05$.

Figure 2.1. Representative images of clonogenic plates

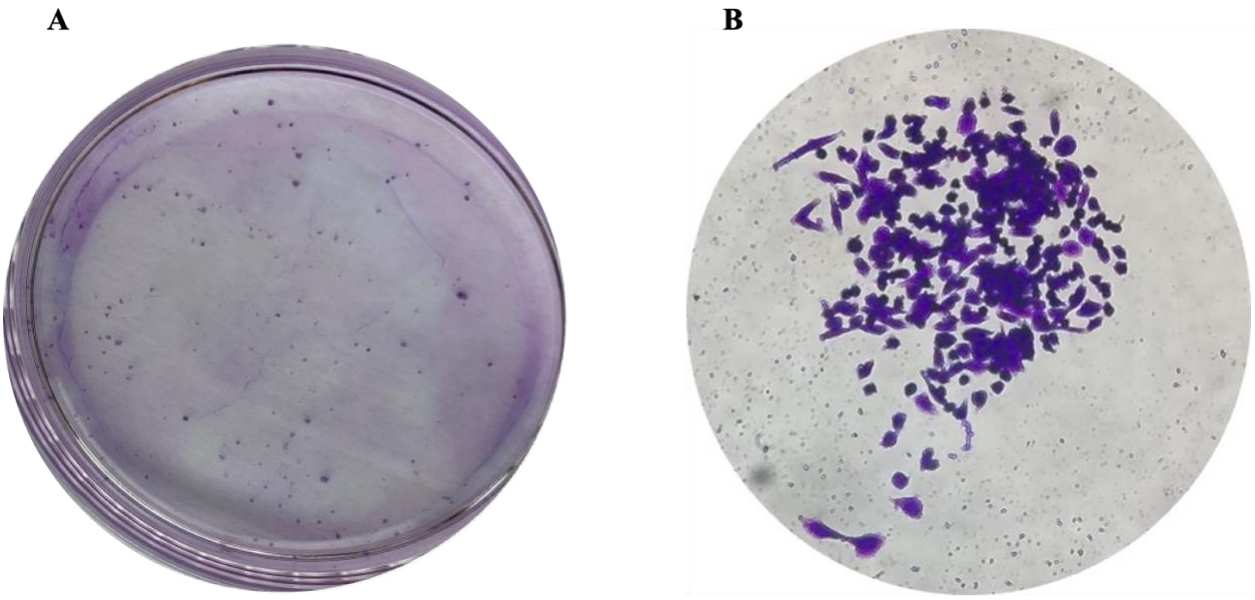

Representative image of clonogenic plate after staining with crystal violet (**A**) and representative image of single colony ≥ 50 cells (**B**).

Results

NIH *All of Us* Genomic Data

Our initial database search identified 4,371 individuals diagnosed with prostate cancer for whom genomic data was available. Of these, 522 (11.9%) received a diagnosis of second malignancy. 46 (8.8%) of the individuals diagnosed with secondary malignancy received radiation therapy, and 96 (2.5%) of those not diagnosed with second malignancy received radiation therapy. Our initial database search also identified 6,584 individuals diagnosed with breast cancer for whom genomic data was available. Of these, 1,085 individuals (16.5%) received a diagnosis of second malignancy. 80 (7.4%) of these individuals received radiation therapy, and 207 (3.8%) of those who were not diagnosed with second malignancy received radiation therapy. Patient characteristics are summarized in Tables 2.1 (prostate cancer cohort) and 2.2 (breast cancer cohort). In the prostate cancer cohort, there was no significant difference in age between those who were diagnosed with second malignancy and those who were not (75.7 ± 9.4 vs. 75.7 ± 8.5 yrs, respectively; $p > 0.05$). There was a significantly higher median income ($72,268 ± $20,217 vs. $69,707 ± $19,265) and lower deprivation index (0.3 ± 0.07 vs. 0.31 ± 0.07) for individuals diagnosed with secondary malignancy compared those who were not ($p \leq 0.05$). In the breast cancer cohort, age and median income were significantly lower (64.8 ± 12.5 vs. 69.1 ± 11.6 yrs and $67,144 ± $16,937 vs. $68,315 ± $18,051) and deprivation index higher (0.32 ± 0.07 vs. 0.31 ± 0.07) for those diagnosed with secondary malignancy compared to those who were not (all $p \leq 0.05$). Due to NIH *All of Us* Data and Statistics Dissemination Policy, disclosure of group counts ≤ 20 is prohibited. As such, statistical comparisons cannot be made for all demographic information.

All SNPs with a significant odds ratio (OR) identified from the CBP or p300 gene encoding regions are summarized in Tables 2.3 and 2.4, with rsIDs and functional outcomes of given SNPs reported, if known. In the prostate cancer cohort, there were two CBP (Figure 2.2) and seven p300 (Figure 2.3) SNPs associated with the odds of diagnosis of second malignancy, regardless of treatment. One CBP polymorphism was associated with lower odds (locus chr16:3725985, OR, 0.346 [90% CI, 0.145 – 0.827])) and one CBP polymorphism was associated with higher odds (locus chr16:3880667, OR, 2.8 [90% CI, 1.170 – 6.723]) of diagnosis of second malignancy. Four p300 polymorphisms were associated with lower odds (loci chr22:41149746, OR, 0.341 [90% CI, 0.130 – 0.894]; chr22:41157255, OR, 0.342 [90% CI, 0.131 – 0.894]; chr22:41179879, OR, 0.271 [90% CI, 0.079 – 0.923]; and chr22:41179880, OR, 0.558 [90% CI, 0.346 – 0.900]) and three were associated with higher odds (loci chr22:41178965, OR, 1.513 [90% CI, 1.080 – 2.120]; chr22:41179533, OR, 1.433 [90% CI, 1.036 – 1.982]; and chr22:41179880, OR, 1.495 [90% CI, 1.051 – 2.126]) of diagnosis of second malignancy. Of note, there were two different polymorphisms at locus chr22:41179880, one associated with increased odds, and one associated with decreased odds of second malignancy. There were no CBP (Figure 2.4) and two p300 (Figure 2.5) SNPs associated with odds of diagnosis of second malignancy in those who received radiation therapy, one of which was associated with decreased odds (locus chr22:41179879, OR, 0.091 [90% CI, 0.10 – 0.834]) and one of which was associated with increased odds (locus chr22:41178965, OR,1.808 [90% CI, 1.084 – 2.017]) of diagnosis of second malignancy, which were also significantly associated with second malignancy in the overall cohort.

In the breast cancer cohort, there were two CBP (Figure 2.6) and no p300 (Figure 2.7) SNPs associated with odds of diagnosis of second malignancy, regardless of treatment. One CBP

polymorphism was associated with decreased odds (locus chr16:3731951, OR, 0.497 [90% CI, 0.314 – 0.787]) and one was associated with increased odds (locus chr16:3727491, OR, 6.687 [90% CI, 1.061 – 42.156]) of diagnosis of second malignancy. There were one CBP (Figure 2.8) and two p300 (Figure 2.9) SNPs associated with odds of diagnosis of second malignancy in those who received radiation therapy. The CBP polymorphism and one p300 polymorphism were associated with decreased odds (locus chr16:3726239, OR, 0.239 [90% CI, 0.098 – 0.583]; and locus chr22:41155035, OR, 0.704 [90% CI, 0.499 – 0.993]) and the other p300 polymorphism was associated with increased odds (locus chr22:41179880, OR, 2.218 [90% CI, 1.162 – 4.236]) of diagnosis of second malignancy.

Cell Culture Experiments

p300 inhibition and radiation: prostate cancer

The % survival of PC-3 cells was determined after correcting for the plating efficiency of control cells, as even untreated cells do not form colonies from each plated cell. There was no significant interaction effect between radiation dose and treatment ($p = 0.410$). There was a significant main effect for radiation dose (0 vs. 2 Gy, $p = 0.0005$) but not for treatment (vehicle vs. CCS-1477, $p = 0.978$). Relative to plating-efficiency corrected survival of vehicle treated and non-radiated cells (100%), survival was $108.86 \pm 15\%$ in CCS-1477 treated, non-radiated cells, $61.33 \pm 16\%$ in vehicle, radiated cells, and $51.86 \pm 5.7\%$ in CCS-1477 treated, radiated cells (Figure 2.10). The significant effect of radiation was present in both vehicle and CCS-1477 treated cells ($p = 0.027$ and $p = 0.003$, respectively). These results suggest that there is no effect of CCS-1477 on radiosensitivity and that CCS-1477 did not affect the efficacy of radiation.

p300 inhibition and radiation: breast cancer

As with PC-3 cells, % survival of MDA MB 231 cells was determined after correcting for the plating efficiency of control cells. There was no significant interaction effect between radiation dose and treatment ($p = 0.327$). There was a significant main effect for both radiation dose (0 vs. 2 Gy, $p = 0.002$) and treatment (vehicle vs. CCS-1477, $p = 0.012$). Compared to the plating-efficiency corrected survival of vehicle, non-radiated cells (100%), survival was $63.9 \pm 4.7\%$ in CCS-1477 treated, non-radiated cells, $54.1 \pm 14\%$ in vehicle, radiated cells, and $36.6 \pm 10.5\%$ in CCS-1477 treated, radiated cells (Figure 2.11). The significant effect of radiation was present in vehicle treated, but not CCS-1477 treated cells ($p = 0.008$ and $p = 0.055$, respectively). The significant effect of treatment was present within non-radiated but not radiated cells ($p = 0.032$ and $p = 0.199$, respectively). These results suggest CCS-1477 may have some effect on MDA MB 231 cell survival independent of radiation but does not enhance the efficacy of radiation.

Table 2.1. Prostate cancer cohort characteristics

	+ diagnosis of secondary malignancy (n = 522)	- diagnosis of secondary malignancy (n = 3849)
Age (yrs)	75.7 ± 9.4	75.7 ± 8.5
Median income ($)	72,269 *	69,707
Deprivation index	0.30 ± 0.07 *	0.31 ± 0.07
White	393 (75.3%)	2793 (72.6%)
Black or African American	55 (10.5%)	527 (13.7%)
Asian	≤ 20	38 (1%)
Multiple	≤ 20	31 (0.8%)
Middle Eastern or North African	≤ 20	≤ 20
Prefer not to answer/other	62 (11.9%)	445 (11.6%)
Not Hispanic	458 (87.7%)	3374 (87.7%)
Hispanic or Latino	43 (8.2%)	293 (7.6%)
Prefer not to answer/other	21 (4.0%)	182 (4.7%)
Received radiation	46 (8.8%)	96 (2.5%)

*significant vs. -diagnosis of secondary malignancy

Table 2.2. Breast cancer cohort characteristics

	+ diagnosis of secondary malignancy (n = 1085)	- diagnosis of secondary malignancy (n = 5499)
Age (yrs)	64.8 ± 12.5 *	69.1 ± 11.6
Median income ($)	67,144 *	68,315
Deprivation index	0.32 ± 0.07 *	0.31 ± 0.07
Female	1039 (95.8%)	5311 (96.6%)
Male	22 (2%)	58 (1.1%)
Other/no response	24 (2.2%)	130 (2.4%)
White	703 (64.8%)	3824 (69.5%)
Black or African American	126 (11.6%)	659 (12%)
Asian	33 (3%)	119 (2.2%)
Multiple	≤ 20	68 (1.2%)
Middle Eastern or North African	≤ 20	26 (0.5%)
Prefer not to answer/other	198 (18.2%)	803 (14.6%)
Not Hispanic	879 (81%)	4623 (84.1%)
Hispanic or Latino	163 (15%)	656 (11.9%)
Prefer not to answer/other	43 (4%)	220 (4%)
Received radiation	80 (7.4%)	207 (3.8%)

*significant vs. -diagnosis of secondary malignancy

Table 2.3. Summary of significant SNPs, prostate cancer cohort

SNP location	rsID	OR [90% CI]	outcome
Prostate cancer, all			
chr16:3725985	rs149345743	0.346 [0.145, 0.827]	3' UTR variant
chr16:3880667	rs539913897	2.805 [1.170, 6.723]	5' UTR variant
chr22:41149746	rs17002316	0.341 [0.130, 0.891]	Intron variant
chr22:41157255	rs20554	0.342 [0.131, 0.894]	Coding sequence variant-synonymous
chr22:41178965	n/a	1.513 [1.080, 2.120]	unknown
chr22:41179533	rs60283061	1.433 [1.036, 1.982]	3' UTR variant
chr22:41179879	n/a	0.271 [0.079, 0.923]	unknown
chr22:41179880	rs1555912621	0.558 [0.346, 0.900]	3' UTR variant
chr22:41179880	rs747975866	1.495 [1.051, 2.126]	3' UTR variant
Prostate cancer, with radiation			
chr22:41178965	n/a	1.808 [1.084, 3.017]	unknown
chr22:4117879	n/a	0.091 [0.010, 0.834]	unknown

Table 2.4. Summary of significant SNPs, breast cancer cohort

SNP location	rsID	OR [90% CI]	outcome
Breast cancer, all			
chr16:3727491	rs1280949298	6.687 [1.061, 42.156]	3' UTR variant
chr16:3731951	rs539913897	0.497 [0.314, 0.787]	Intron variant
Breast cancer, with radiation			
chr16:3726239	rs1555470188	0.239 [0.098, 0.583]	3’ UTR variant
chr22:41155035	rs20552	0.704 [0.499, 0.993]	Coding sequence variant
chr22:41179880	rs1555912621	2.218 [1.162, 4.236]	3’ UTR variant

Figure 2.2. CBP SNPs, prostate cancer, any treatment

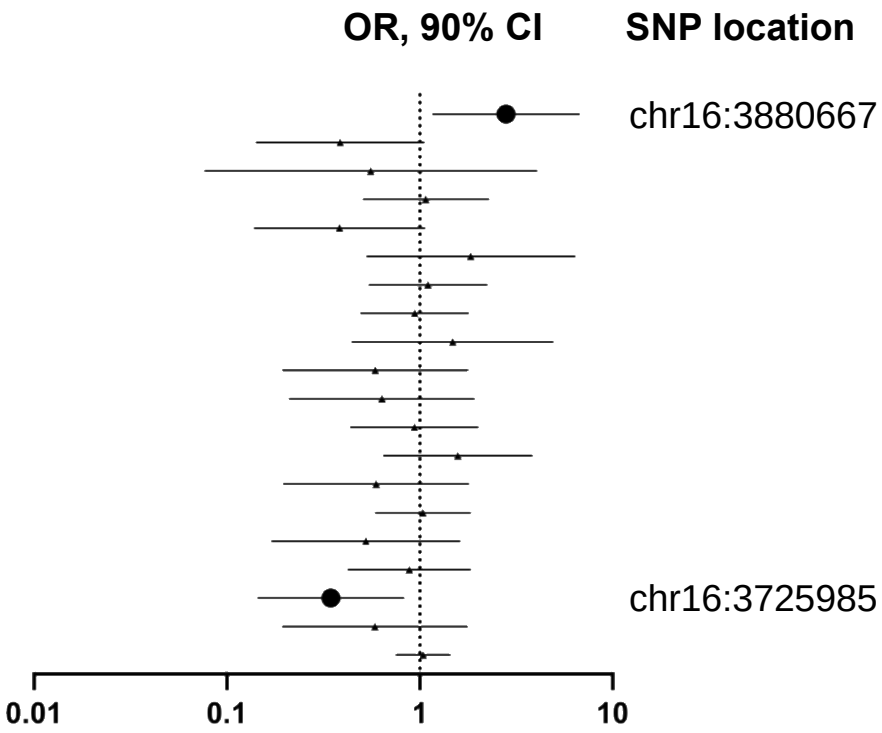

Figure 2.3. p300 SNPs, prostate cancer, any treatment

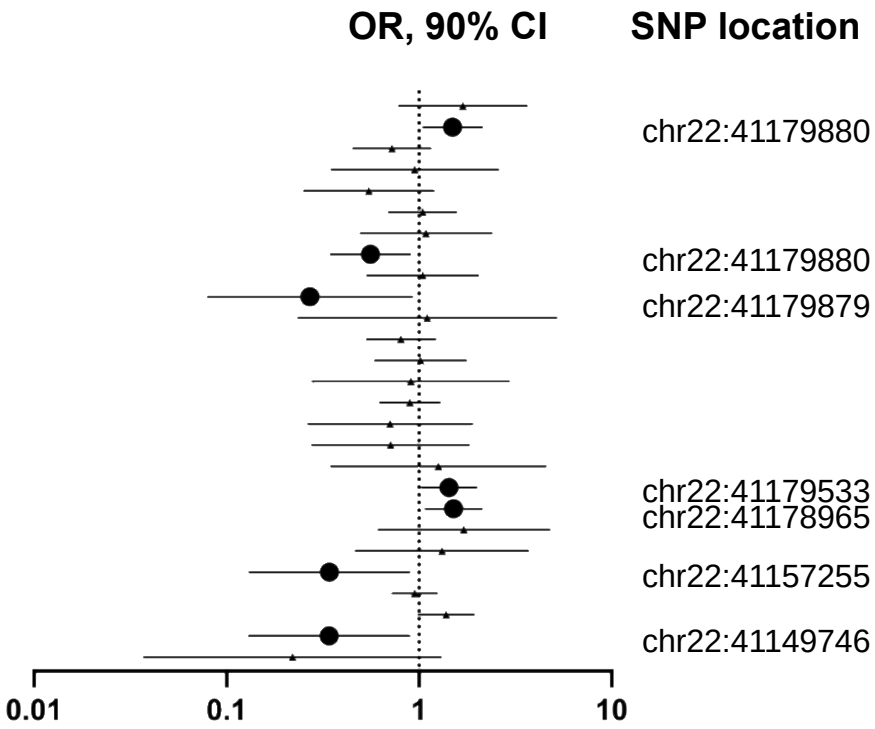

Figure 2.4. CBP SNPs, prostate cancer, received radiation

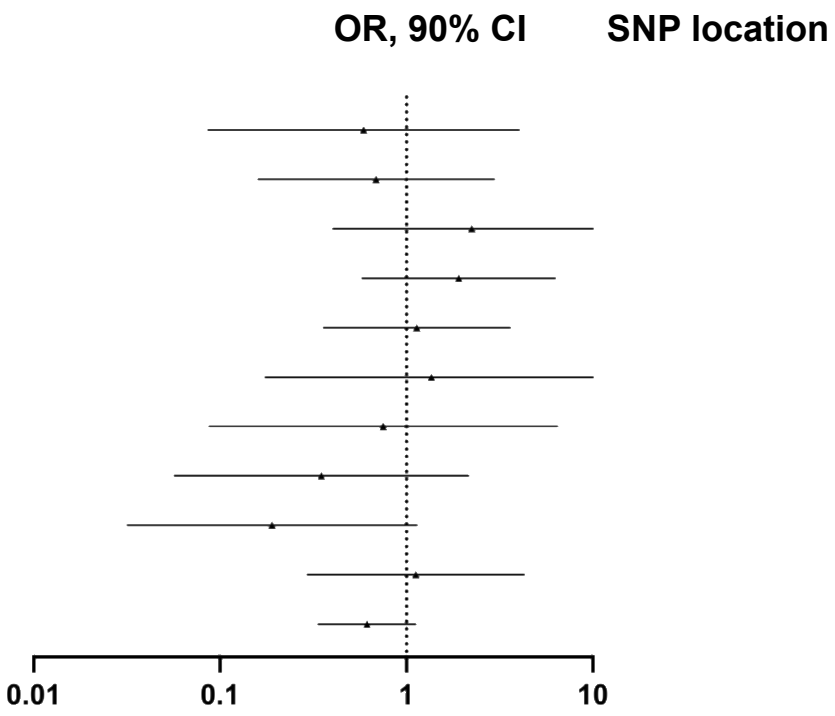

Figure 2.5. p300 SNPs, prostate cancer, received radiation

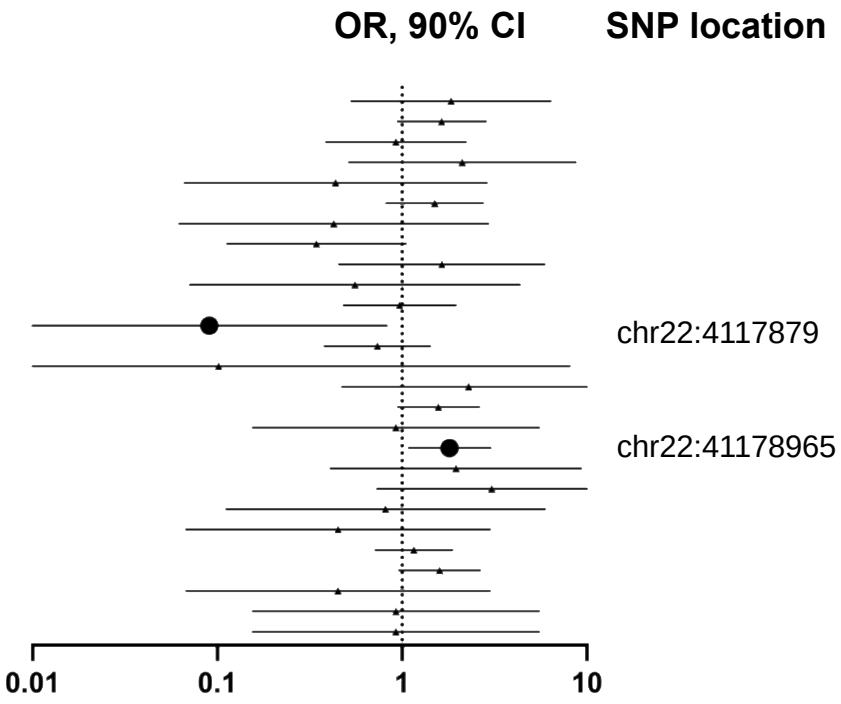

Figure 2.6. CBP SNPs, breast cancer, any treatment

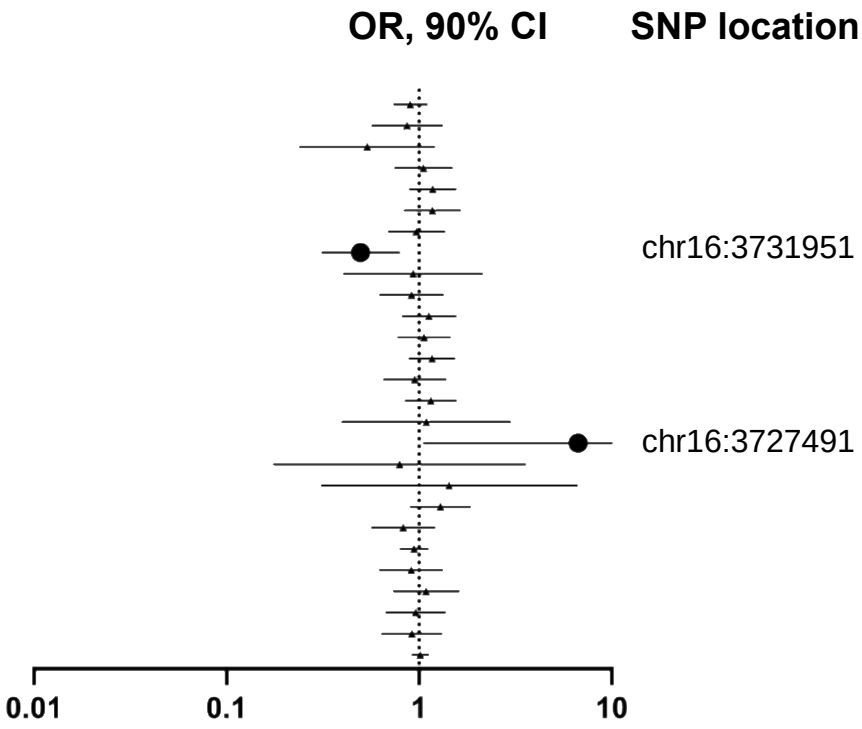

Figure 2.7. p300 SNPs, breast cancer, any treatment

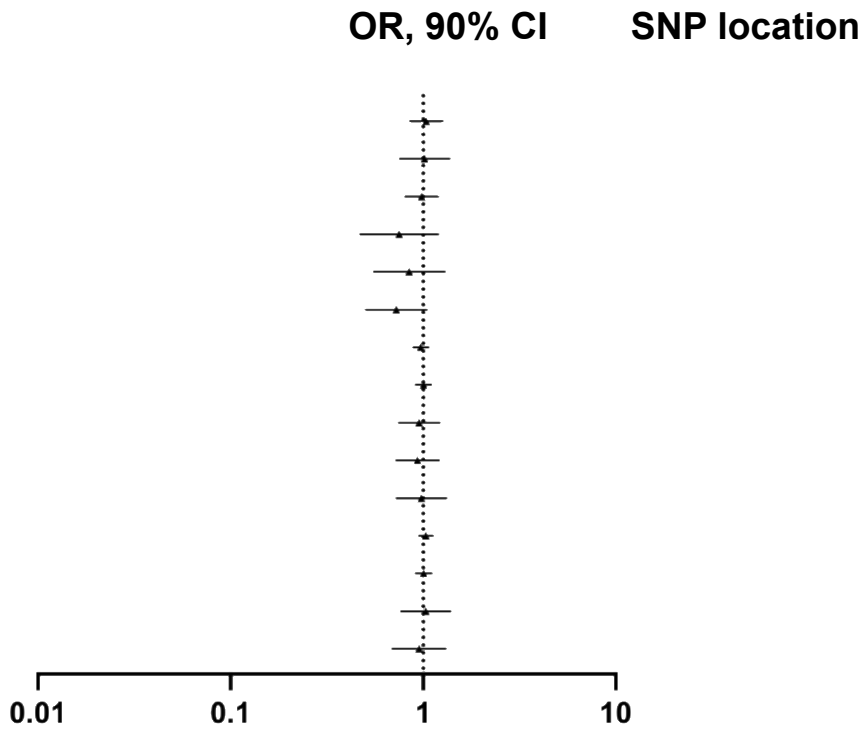

Figure 2.8. CBP SNPs, breast cancer, received radiation

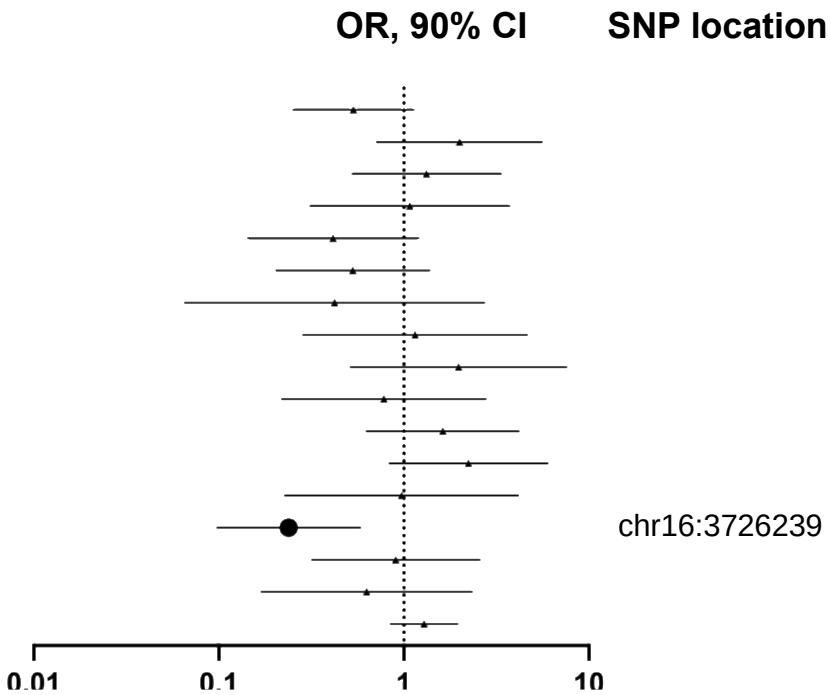

Figure 2.9. p300 SNPs, breast cancer, received radiation

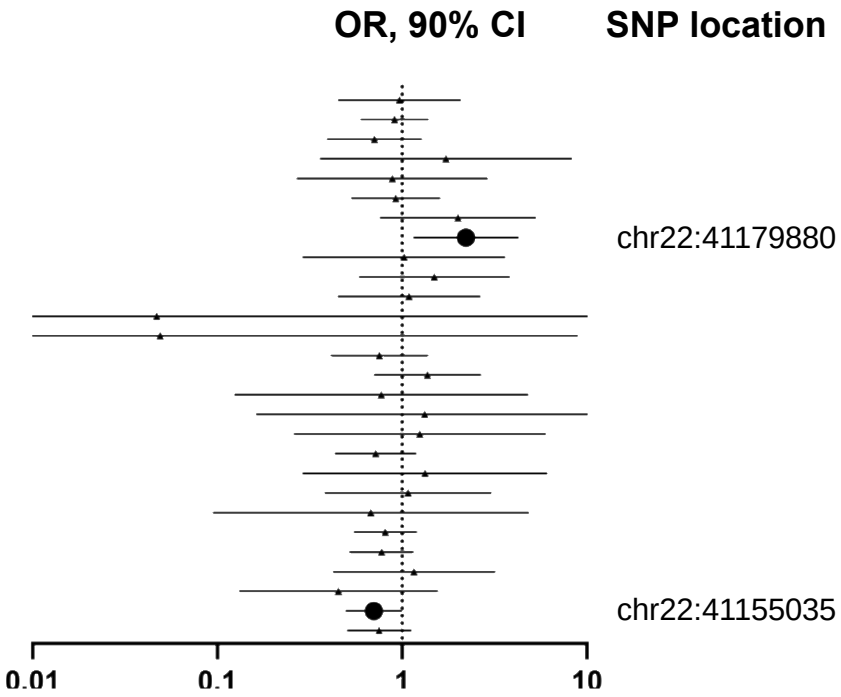

Figure 2.10. PC-3 clonogenic survival

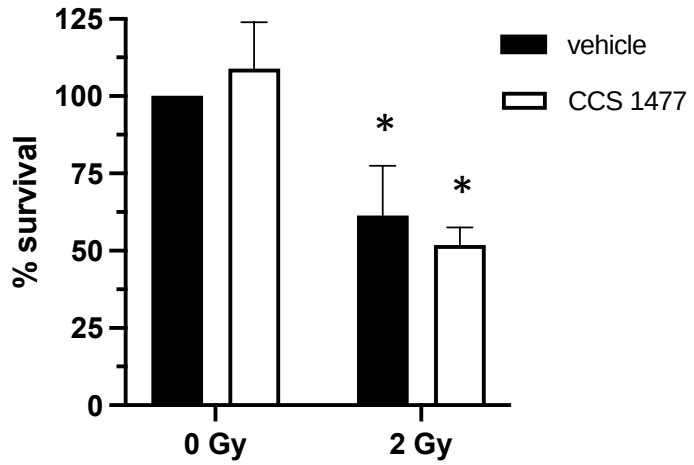

Data are mean ± SEM. *significant vs. 0 Gy within group (vehicle or CCS 1477; $p \leq 0.05$). Results are the average of at least 3 independent experiments.

Figure 2.11. MDA MB 231 clonogenic survival

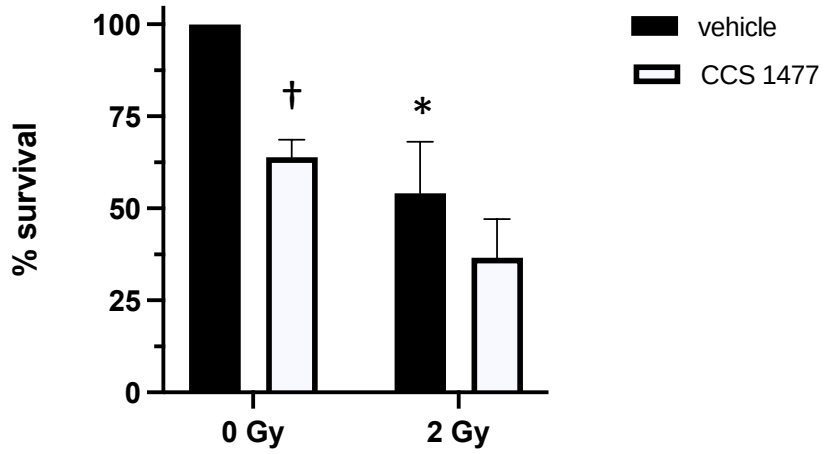

Data are mean ± SEM. *significant vs. 0 Gy within group (vehicle or CCS 1477; $p \leq 0.05$).

†significant vs. vehicle within group (0 Gy or 2 Gy; $p \leq 0.05$).

Results are the average of at least 3 independent experiments.

Discussion

In the present study, we utilized an exploratory investigation of a publicly available large dataset, alongside cell culture experiments, to determine the role of p300/CBP in mediating the efficacy of anti-cancer therapies, and specifically, radiation, for the treatment of prostate and breast cancers. Our findings from the NIH *All of Us* genomic data suggest a potential role for p300/CBP in mediating or predicting the response to cancer treatment, including radiation, but our *in vitro* investigation does not support a direct role of p300/CBP in mediating the efficacy of radiation.

Candidate Gene Association

Utilizing a CGAS to investigate SNPs with known functional outcomes can be used to predict how individuals might respond to a certain drug or their risk of disease development [34]. In our study, we sought to determine if p300/CBP SNPs share an association with odds of second malignancy in individuals diagnosed with prostate and breast cancers. We then explored the relationship between p300/CBP SNPs and odds of second malignancy specific to those who received radiation therapy. Interestingly, in all study cohorts, there were p300 and/or CBP SNPs associated with both increased and decreased odds of diagnosis of secondary malignancy (Tables 2.3 and 2.4). Because the SNPs we identified are not associated with altered protein products or not yet reported in the literature, it is difficult to determine what effect they may have, but SNPs that do not impact the protein product (e.g. do not result in an amino acid substitution, early stop codon, etc.) can still impact gene or protein function, and the majority of SNPs with significant associations with disease risk are from non-coding regions [35,36]. Non-coding SNPs can result in changes in mRNA stability/translation/localization, miRNA binding, and protein folding, which

can have a profound effect on protein expression and function [37-41]. Because we found that p300/CBP SNPs are associated with both increased and decreased odds of secondary malignancy after radiation and with all treatments combined, p300 or CBP SNPs likely influence gene or protein function via multiple mechanisms. For example, if p300 SNPs are associated with decreased mRNA stability, it could result in a lower expression of the p300 protein [42], resulting in a decreased amount of functional p300. Because p300 is critical for DNA repair [18,19,21,43], the efficacy of radiation may be increased by a reduction in p300, thus resulting in a lower odds of secondary malignancy. Likewise, p300 SNPs associated with increased mRNA stability could lead to p300 protein overexpression [42], resulting in greater repair of radiation-induced DNA damage and a decreased efficacy of radiation therapy. Though the exact mechanisms are not able to be inferred from our study, our findings suggest some role of p300/CBP in mediating the response to radiation and other therapies, which warrants further investigation. Secondly, several SNPs were associated with the odds of second malignancy in the cohort including all possible therapies. As such, the second part of this study was undertaken to further explore this relationship without the influence of the other factors that may have an impact on our results, such as exposure to other anti-cancer therapies or initial cancer staging.

p300/CBP inhibition and radiosensitivity

Radiation induces DSBs [7-9] and these DSBs are primarily repaired by NHEJ or HR [9,15,16]. Prior studies suggest that p300 is critical for NHEJ- and HR-associated protein expression [18,19,21] and that impaired DSB repair may sensitize cells to radiation [44-48]. In addition, part one of this study suggested there may be some association of p300/CBP on the response to radiation. As such, in part two of this study, we hypothesized that p300/CBP inhibition would sensitize cancer

cells to radiation *in vitro*. Our findings did not support this hypothesis, as p300/CBP inhibition did not impact prostate or breast cancer cell survival after radiation (Figures 2.10 and 2.11). However, p300/CBP inhibition reduced breast cancer cell survival in the absence of radiation. There are several potential explanations for our findings. First, the dose or duration of CCS-1477 exposure may not have been adequate to fully inhibit p300/CBP. Importantly, we did not validate p300/CBP inhibition, but preliminary studies in our lab indicated the present dosing protocol of CCS-1477 was sufficient to impact cell survival (data not shown). Second, several forms of redundancy exist in DNA repair pathways [49,50]. As such, it is possible that cells were able to utilize other repair pathways to offset the effect of p300/CBP inhibition and repair DNA damage. However, because many cancers arise due to defects in DNA repair pathways [51], we expected that cancer cells would lack redundancy in DNA repair. Nonetheless, it is possible that some of the alternative repair pathways were able to be utilized. Third, the dose of radiation utilized in our study is relatively low. In the literature, the effects of p300/CBP inhibition on cancer cell survival are more prominent at higher doses of radiation than what was used in our study [18-20] and have primarily been demonstrated in lung cancer cells. However, 2 Gy radiation represents a single fraction of radiation for patients on a conventional fractionation regimen. As such, we sought to utilize the clinically relevant dose for better translatability. Nonetheless, an effect of p300/CBP inhibition may not be present at low doses of radiation. In addition, p300/CBP are known to interact with hundreds of other genes [43,52-54], and there could be an effect of p300/CBP inhibition on other pathways that impact cell survival. Namely, p300 is a known co-activator of p53 [55-58]. p53 is important for cell cycle regulation and is the most commonly mutated gene in cancers [59,60]. PC-3 cells are reported to be $p53^{null}$ [61], which suggests that any interaction between p300/CBP and p53 may not be relevant in this cell line. MDA MB 231 cells, however, are

reported to have a p53 mutation [62]. Mutant p53 is reported to have variable effects on radiosensitivity [63]; as such, the interaction between p300/CBP and p53 on the radiosensitivity of breast cancer cells warrants further investigation. The impact of p300/CBP inhibition on breast cancer cell survival in the absence of radiation suggests that p300/CBP play a role in cancer cell growth or survival. In support of this, Tanaka et al. found that p300/CBP knockdown resulted in a significant reduction in cell growth/survival of MDA MB 231 cells, concomitant with G2/M cell cycle arrest and the induction of apoptosis [64]. This effect appeared to be mediated through a significant reduction in survivin (a member of the inhibitor of apoptosis family) that may be overexpressed in triple negative breast cancer. Taken together with our findings that p300/CBP may relate to the odds of diagnosis of secondary malignancy, and that pharmacological inhibition of p300/CBP also resulted in reduced MDA MB 231 survival, this represents an exciting avenue for future research.

Limitations

Our study is not without limitations. First, the NIH *All of Us* database includes many people who are considered underrepresented in biomedical research. However, our cohorts were composed primarily of individuals who identify as non-Hispanic white. The presence of several SNPs in our study are reported at varying frequencies among different ethnic backgrounds. In addition, cancer cells studied *in vitro* are generally derived from a single individual and are considered highly homogenous. As such, our findings may not adequately represent the associations between p300/CBP and radiosensitivity among populations with disproportionately greater frequencies of p300 or CBP SNPs. Secondly, the cohorts exposed to radiation likely received other anti-cancer therapies; radiation therapy was an inclusion criterion, and we did not

exclude those receiving other treatments. Though there may be an effect of other treatments, most individuals do receive more than one anti-cancer therapy, and evaluating the response to radiation in combination with other therapies is representative of the patient population. As mentioned, the dose of CCS-1477 could be too low to elicit adequate inhibition of p300/CBP. Therefore, functional p300 and CBP may still be present in great enough concentrations for sufficient DNA damage repair to occur after radiation. Lastly, we did not perform any measure to detect actual DNA damage. Doing so is a logical next step to understand whether this dose of CCS-1477 is sufficient to increase DNA damage, which would provide valuable insight to our findings.

Conclusions

Our findings suggest that p300/CBP SNPs are associated with the odds of diagnosis of secondary malignancy. The exact consequences of these SNPs are unknown, but the SNPs we identified are primarily associated with non-coding regions, suggesting that they may alter mRNA stability, miRNA binding, or protein folding. Future investigations to explore the impact/outcome of these SNPs should be performed and may provide valuable insight into new treatment targets. Though we did not observe an effect of p300/CBP inhibition on prostate or breast cancer cell survival after radiation, *in vivo* investigations utilizing pre-clinical cancer models may provide important information regarding the impact of p300/CBP inhibition in combination with radiation.

References

1 Siegel, R. L., Giaquinto, A. N. & Jemal, A. Cancer statistics, 2024. *CA Cancer J Clin* **74**, 12-49 (2024). https://doi.org:10.3322/caac.21820

2 Baskar, R., Lee, K. A., Yeo, R. & Yeoh, K. W. Cancer and radiation therapy: current advances and future directions. *Int J Med Sci* **9**, 193-199 (2012). https://doi.org:10.7150/ijms.3635

3 Zagars, G. K., Pollack, A., Kavadi, V. S. & von Eschenbach, A. C. Prostate-specific antigen and radiation therapy for clinically localized prostate cancer. *Int J Radiat Oncol Biol Phys* **32**, 293-306 (1995). https://doi.org:10.1016/0360-3016(95)00077-c

4 Colleoni, M. *et al.* Annual Hazard Rates of Recurrence for Breast Cancer During 24 Years of Follow-Up: Results From the International Breast Cancer Study Group Trials I to V. *J Clin Oncol* **34**, 927-935 (2016). https://doi.org:10.1200/jco.2015.62.3504

5 Pedersen, R. N. *et al.* The Incidence of Breast Cancer Recurrence 10-32 Years After Primary Diagnosis. *J Natl Cancer Inst* **114**, 391-399 (2022). https://doi.org:10.1093/jnci/djab202

6 Gong, L., Zhang, Y., Liu, C., Zhang, M. & Han, S. Application of Radiosensitizers in Cancer Radiotherapy. *Int J Nanomedicine* **16**, 1083-1102 (2021). https://doi.org:10.2147/ijn.S290438

7 Desouky, O., Ding, N. & Zhou, G. Targeted and non-targeted effects of ionizing radiation. *Journal of Radiation Research and Applied Sciences* **8**, 247-254 (2015). https://doi.org:https://doi.org/10.1016/j.jrras.2015.03.003

8 Ward, J. F. DNA damage produced by ionizing radiation in mammalian cells: identities, mechanisms of formation, and reparability. *Prog Nucleic Acid Res Mol Biol* **35**, 95-125 (1988). https://doi.org:10.1016/s0079-6603(08)60611-x

9 van Gent, D. C., Hoeijmakers, J. H. & Kanaar, R. Chromosomal stability and the DNA double-stranded break connection. *Nat Rev Genet* **2**, 196-206 (2001). https://doi.org:10.1038/35056049

10 Jeggo, P. A., Geuting, V. & Lobrich, M. The role of homologous recombination in radiation-induced double-strand break repair. *Radiother Oncol* **101**, 7-12 (2011). https://doi.org:10.1016/j.radonc.2011.06.019

11 Santivasi, W. L. & Xia, F. Ionizing Radiation-Induced DNA Damage, Response, and Repair. *Antioxidants & Redox Signaling* **21**, 251-259 (2013). https://doi.org:10.1089/ars.2013.5668

12 Willers, H., Dahm-Daphi, J. & Powell, S. N. Repair of radiation damage to DNA. *British Journal of Cancer* **90**, 1297-1301 (2004). https://doi.org:10.1038/sj.bjc.6601729

13 Davis, A. J. & Chen, D. J. DNA double strand break repair via non-homologous end-joining. *Transl Cancer Res* **2**, 130-143 (2013). https://doi.org:10.3978/j.issn.2218-676X.2013.04.02

14 Dexheimer, T. S. in *DNA Repair of Cancer Stem Cells* (eds Lesley A. Mathews, Stephanie M. Cabarcas, & Elaine M. Hurt) 19-32 (Springer Netherlands, 2013).

15 Lieber, M. R. The Mechanism of Double-Strand DNA Break Repair by the Nonhomologous DNA End-Joining Pathway. *Annu Rev Biochem* **79**, 181-211 (2010). https://doi.org:10.1146/annurev.biochem.052308.093131

16 Rothkamm, K., Kruger, I., Thompson, L. H. & Lobrich, M. Pathways of DNA double-strand break repair during the mammalian cell cycle. *Mol Cell Biol* **23**, 5706-5715 (2003). https://doi.org:10.1128/MCB.23.16.5706-5715.2003

17 Yoshida, K. & Miki, Y. Role of BRCA1 and BRCA2 as regulators of DNA repair, transcription, and cell cycle in response to DNA damage. *Cancer Sci* **95**, 866-871 (2004). https://doi.org:10.1111/j.1349-7006.2004.tb02195.x

18 Ogiwara, H. *et al.* Histone acetylation by CBP and p300 at double-strand break sites facilitates SWI/SNF chromatin remodeling and the recruitment of non-homologous end joining factors. *Oncogene* **30**, 2135-2146 (2011). https://doi.org:10.1038/onc.2010.592

19 Ogiwara, H. & Kohno, T. CBP and p300 Histone Acetyltransferases Contribute to Homologous Recombination by Transcriptionally Activating the *BRCA1* and *RAD51* Genes. *Plos One* **7** (2012). https://doi.org:10.1371/journal.pone.0052810

20 Oike, T. *et al.* C646, a selective small molecule inhibitor of histone acetyltransferase p300, radiosensitizes lung cancer cells by enhancing mitotic catastrophe. *Radiother Oncol* **111**, 222-227 (2014). https://doi.org:10.1016/j.radonc.2014.03.015

21 Wallace, N. A., Robinson, K., Howie, H. L. & Galloway, D. A. β-HPV 5 and 8 E6 Disrupt Homology Dependent Double Strand Break Repair by Attenuating BRCA1 and

BRCA2 Expression and Foci Formation. *Plos Pathog* **11** (2015). https://doi.org:10.1371/journal.ppat.1004687

22 Choudhury, A. *et al.* Targeting homologous recombination using imatinib results in enhanced tumor cell chemosensitivity and radiosensitivity. *Mol Cancer Ther* **8**, 203-213 (2009). https://doi.org:10.1158/1535-7163.Mct-08-0959

23 Asgari, M. M., Eide, M. J., Warton, E. M. & Fletcher, S. W. Validation of a large basal cell carcinoma registry. *J Registry Manag* **40**, 65-69 (2013).

24 Senior, R. *et al.* Evaluation of SNOMED CT Grouper Accuracy and Coverage in Organizing the Electronic Health Record Problem List by Clinical System: Observational Study. *JMIR Med Inform* **12**, e51274 (2024). https://doi.org:10.2196/51274

25 Uno, H. *et al.* Determining the Time of Cancer Recurrence Using Claims or Electronic Medical Record Data. *JCO Clin Cancer Inform* **2**, 1-10 (2018). https://doi.org:10.1200/cci.17.00163

26 infection, W. W. G. o. t. C. C. a. M. o. C.-. A minimal common outcome measure set for COVID-19 clinical research. *Lancet Infect Dis* **20**, e192-e197 (2020). https://doi.org:10.1016/s1473-3099(20)30483-7

27 Yuan, Q. *et al.* Performance of a Machine Learning Algorithm Using Electronic Health Record Data to Identify and Estimate Survival in a Longitudinal Cohort of Patients With Lung Cancer. *JAMA Netw Open* **4**, e2114723 (2021). https://doi.org:10.1001/jamanetworkopen.2021.14723

28 Hassett, M. J. *et al.* eSyM: An Electronic Health Record-Integrated Patient-Reported Outcomes-Based Cancer Symptom Management Program Used by Six Diverse Health Systems. *JCO Clin Cancer Inform* **6**, e2100137 (2022). https://doi.org:10.1200/cci.21.00137

29 Penninckx, S., Pariset, E., Cekanaviciute, E. & Costes, S. V. Quantification of radiation-induced DNA double strand break repair foci to evaluate and predict biological responses to ionizing radiation. *NAR Cancer* **3**, zcab046 (2021). https://doi.org:10.1093/narcan/zcab046

30 Franken, N. A., Rodermond, H. M., Stap, J., Haveman, J. & van Bree, C. Clonogenic assay of cells in vitro. *Nat Protoc* **1**, 2315-2319 (2006). https://doi.org:10.1038/nprot.2006.339

31 Feoktistova, M., Geserick, P. & Leverkus, M. Crystal Violet Assay for Determining Viability of Cultured Cells. *Cold Spring Harb Protoc* **2016**, pdb.prot087379 (2016). https://doi.org:10.1101/pdb.prot087379

32 Gross, A., Tönjes, A. & Scholz, M. On the impact of relatedness on SNP association analysis. *BMC Genet* **18**, 104 (2017). https://doi.org:10.1186/s12863-017-0571-x

33 Graffelman, J., Jain, D. & Weir, B. A genome-wide study of Hardy-Weinberg equilibrium with next generation sequence data. *Hum Genet* **136**, 727-741 (2017). https://doi.org:10.1007/s00439-017-1786-7

34 David, S. A current guide to candidate gene association studies. *Trends Genet* **37**, 1056-1059 (2021). https://doi.org:10.1016/j.tig.2021.07.009

35 Zhang, F. & Lupski, J. R. Non-coding genetic variants in human disease. *Hum Mol Genet* **24**, R102-110 (2015). https://doi.org:10.1093/hmg/ddv259

36 Hrdlickova, B., de Almeida, R. C., Borek, Z. & Withoff, S. Genetic variation in the non-coding genome: Involvement of micro-RNAs and long non-coding RNAs in disease. *Biochim Biophys Acta* **1842**, 1910-1922 (2014). https://doi.org:10.1016/j.bbadis.2014.03.011

37 Hong, D. & Jeong, S. 3'UTR Diversity: Expanding Repertoire of RNA Alterations in Human mRNAs. *Mol Cells* **46**, 48-56 (2023). https://doi.org:10.14348/molcells.2023.0003

38 Mayr, C. What Are 3' UTRs Doing? *Cold Spring Harb Perspect Biol* **11** (2019). https://doi.org:10.1101/cshperspect.a034728

39 Rykova, E., Ershov, N., Damarov, I. & Merkulova, T. SNPs in 3'UTR miRNA Target Sequences Associated with Individual Drug Susceptibility. *Int J Mol Sci* **23** (2022). https://doi.org:10.3390/ijms232213725

40 Steri, M., Idda, M. L., Whalen, M. B. & Orrù, V. Genetic variants in mRNA untranslated regions. *Wiley Interdiscip Rev RNA* **9**, e1474 (2018). https://doi.org:10.1002/wrna.1474

41 Zhang, N. *et al.* Genome-Wide 3'-UTR Single Nucleotide Polymorphism Association Study Identifies Significant Prostate Cancer Risk-Associated Functional Loci at 8p21.2 in Chinese Population. *Adv Sci (Weinh)* **9**, e2201420 (2022). https://doi.org:10.1002/advs.202201420

42 Mauger, D. M. *et al.* mRNA structure regulates protein expression through changes in functional half-life. *Proc Natl Acad Sci U S A* **116**, 24075-24083 (2019). https://doi.org:10.1073/pnas.1908052116

43 Dutto, I., Scalera, C. & Prosperi, E. CREBBP and p300 lysine acetyl transferases in the DNA damage response. *Cell Mol Life Sci* **75**, 1325-1338 (2018). https://doi.org:10.1007/s00018-017-2717-4

44 Ciszewski, W. M., Tavecchio, M., Dastych, J. & Curtin, N. J. DNA-PK inhibition by NU7441 sensitizes breast cancer cells to ionizing radiation and doxorubicin. *Breast Cancer Res Tr* **143**, 47-55 (2014). https://doi.org:10.1007/s10549-013-2785-6

45 Ismail, I. H. *et al.* SU11752 inhibits the DNA-dependent protein kinase and DNA double-strand break repair resulting in ionizing radiation sensitization. *Oncogene* **23**, 873-882 (2004). https://doi.org:10.1038/sj.onc.1207303

46 Rosenzweig, K. E., Youmell, M. B., Palayoor, S. T. & Price, B. D. Radiosensitization of human tumor cells by the phosphatidylinositol3-kinase inhibitors wortmannin and LY294002 correlates with inhibition of DNA-dependent protein kinase and prolonged G2-M delay. *Clin Cancer Res* **3**, 1149-1156 (1997).

47 Boulton, S., Kyle, S., Yalcintepe, L. & Durkacz, B. W. Wortmannin is a potent inhibitor of DNA double strand break but not single strand break repair in Chinese hamster ovary cells. *Carcinogenesis* **17**, 2285-2290 (1996). https://doi.org:10.1093/carcin/17.11.2285

48 Chernikova, S. B., Wells, R. L. & Elkind, M. M. Wortmannin sensitizes mammalian cells to radiation by inhibiting the DNA-dependent protein kinase-mediated rejoining of double-strand breaks. *Radiat Res* **151**, 159-166 (1999).

49 Gartner, A. & Engebrecht, J. DNA repair, recombination, and damage signaling. *Genetics* **220** (2022). https://doi.org:10.1093/genetics/iyab178

50 Alberts, B. *et al.* Ch. DNA Repair, (Garland Science, 2002).

51 Curtin, N. J. DNA repair dysregulation from cancer driver to therapeutic target. *Nat Rev Cancer* **12**, 801-817 (2012). https://doi.org:10.1038/nrc3399

52 Vo, N. & Goodman, R. H. CREB-binding protein and p300 in transcriptional regulation. *J Biol Chem* **276**, 13505-13508 (2001). https://doi.org:10.1074/jbc.R000025200

53 Giordano, A. & Avantaggiati, M. L. p300 and CBP: partners for life and death. *J Cell Physiol* **181**, 218-230 (1999). https://doi.org:10.1002/(sici)1097-4652(199911)181:2<218::Aid-jcp4>3.0.Co;2-5

54 Shiama, N. The p300/CBP family: integrating signals with transcription factors and chromatin. *Trends Cell Biol* **7**, 230-236 (1997). https://doi.org:10.1016/s0962-8924(97)01048-9

55 Grossman, S. R. p300/CBP/p53 interaction and regulation of the p53 response. *Eur J Biochem* **268**, 2773-2778 (2001). https://doi.org:10.1046/j.1432-1327.2001.02226.x

56 Lill, N. L., Grossman, S. R., Ginsberg, D., DeCaprio, J. & Livingston, D. M. Binding and modulation of p53 by p300/CBP coactivators. *Nature* **387**, 823-827 (1997). https://doi.org:10.1038/42981

57 Gu, W., Shi, X. L. & Roeder, R. G. Synergistic activation of transcription by CBP and p53. *Nature* **387**, 819-823 (1997). https://doi.org:10.1038/42972

58 Kaypee, S. *et al.* Mutant and Wild-Type Tumor Suppressor p53 Induces p300 Autoacetylation. *iScience* **4**, 260-272 (2018). https://doi.org:10.1016/j.isci.2018.06.002

59 Chen, X. *et al.* Mutant p53 in cancer: from molecular mechanism to therapeutic modulation. *Cell Death Dis* **13**, 974 (2022). https://doi.org:10.1038/s41419-022-05408-1

60 Hernández Borrero, L. J. & El-Deiry, W. S. Tumor suppressor p53: Biology, signaling pathways, and therapeutic targeting. *Biochim Biophys Acta Rev Cancer* **1876**, 188556 (2021). https://doi.org:10.1016/j.bbcan.2021.188556

61 Chappell, W. H. *et al.* p53 expression controls prostate cancer sensitivity to chemotherapy and the MDM2 inhibitor Nutlin-3. *Cell Cycle* **11**, 4579-4588 (2012). https://doi.org:10.4161/cc.22852

62 Li, S. J. *et al.* Low-dose irradiation promotes proliferation of the human breast cancer MDA-MB-231 cells through accumulation of mutant P53. *Int J Oncol* **50**, 290-296 (2017). https://doi.org:10.3892/ijo.2016.3795

63 Chiarugi, V., Magnelli, L. & Cinelli, M. Role of p53 mutations in the radiosensitivity status of tumor cells. *Tumori* **84**, 517-520 (1998). https://doi.org:10.1177/030089169808400501

64 Tanaka, S. *et al.* Abstract P3-06-06: The importance of p300/CBP (CREBBP)-survivin (BIRC5) for cell cycle and apoptosis in triple negative breast cancer. *Cancer Research* **80**, P3-06-06-P03-06-06 (2020). https://doi.org:10.1158/1538-7445.Sabcs19-p3-06-06

Chapter 3 - Doxorubicin and p300: dual impact on breast cancer cell survival and vascular function

Abstract

Doxorubicin is the most common anthracycline used to treat individuals with breast cancer. In addition to damaging cancer cells, doxorubicin also causes damage to healthy cells in the cardiovascular system, leading to cardiotoxicity. Given the growing evidence for the incidence of cardiotoxicity, many efforts have been employed to monitor cardiovascular parameters during and after treatment with doxorubicin. However, less attention is placed on vascular damage induced by doxorubicin, which is also implicated in doxorubicin cardiotoxicity. Though doxorubicin is quite effective as a cancer treatment, improving its efficacy further could limit the dose of doxorubicin required for treatment and lessen the risk of cardiac and vascular toxicities. Given its role in DNA damage repair, one potential mediator of doxorubicin efficacy is p300/CBP. As such, we assessed whether p300/CBP is associated with the odds of a diagnosis of second malignancy in individuals with breast cancer who received doxorubicin. We also investigated whether p300/CBP inhibition would increase the efficacy of doxorubicin *in vitro,* and whether it would modulate the effects of doxorubicin on aortic vascular function. We found that single nucleotide polymorphisms in the CBP gene encoding region are associated with the odds of diagnosis of second malignancy in breast cancer patients who received doxorubicin. However, *in vitro,* p300/CBP inhibition did not enhance the efficacy of doxorubicin in breast cancer cells. Doxorubicin and p300/CBP inhibition also did not impact aortic vascular function *ex vivo.* Further investigation into the role of CBP single nucleotide polymorphisms on the response to doxorubicin may provide valuable insight into potential therapeutic targets in breast cancer. In addition, although we did not demonstrate any effect of p300/CBP inhibition on breast

cancer cells exposed to doxorubicin *in vitro* or of doxorubicin and p300/CBP inhibition on aortic vascular function *ex vivo,* evaluating their roles *in vivo* may provide important insight.

Introduction

Breast cancer is the most diagnosed non-skin cancer in women in the United States, with a lifetime risk of diagnosis of 13.1%. This represents over 300,000 new cancer diagnoses and over 40,000 deaths in 2024 alone [1]. While quite effective at limiting tumor growth, the DNA damaging effects of anthracycline chemotherapies, and specifically of doxorubicin (DOX), are not exclusive to cancer cells and often lead to damage in healthy cells of other tissues, especially those of the cardiovascular system, and can lead to cardiotoxicity. Despite the recognition of cardiotoxicity during the early development and clinical use of anthracyclines, it wouldn't be until decades later that the field of cardio-oncology was introduced. Since then, many large studies have sought to better understand the incidence and therapeutic targets for anthracycline cardiotoxicity. With current estimates of anthracycline-induced clinical cardiotoxicity ranging from 6% [2] to as high as 48% in those receiving more than 700 mg/m^2 of anthracycline [3,4], there is a critical need to identify molecular targets for mitigating these adverse effects. Moreover, sub-clinical cardiotoxicity is reported to occur in another 18% of patients, with cumulative anthracycline dose reported as the most common predictor of cardiotoxicity [2].

Onset of cardiotoxicity during treatment may result in the withdrawal of doxorubicin from a patient's treatment regimen, resulting in reliance on less efficacious treatments and adversely impacting cancer-specific outcomes. Many patients also experience the cardiotoxic effects of doxorubicin years after treatment [5,6]. As such, there are strong guidelines for monitoring both acute and chronic left ventricular cardiotoxicity [7,8], but less emphasis is placed on vascular toxicity, despite evidence from several groups suggesting anthracycline exposure results in vascular dysfunction of the aorta in both patients and in pre-clinical models [9-15], as well as evidence to suggest that vascular dysfunction predicts future CVD risk [16,17].

DOX primarily functions through the inhibition of topoisomerase IIb (TopIIb) and the production of reactive oxygen species (ROS) [18,19], which results in oxidative stress and DNA damage, limiting the reproductive potential of cancer cells. While not traditionally considered a primary means of tumor control, evidence suggests that anti-cancer therapies, including chemotherapies like doxorubicin, also reduce the replicative abilities of cancer cells by inducing senescence [20,21]. Though the pathophysiology of DOX-induced cardiotoxicity is complex, these same mechanisms—DNA damage, oxidative stress, and senescence—are all suggested as potential mechanisms of DOX-induced cardiac and/or vascular damage [13,22-32]. One potential mechanism to modulate these pathways is through inhibition of the histone acetyltransferase, p300 (and its homologue CBP). p300/CBP has been suggested to play an important role in DNA damage repair [33-36], oxidative stress [37-39], and senescence [40,41] through histone modification and direct binding to transcription factors. Thus, p300/CBP inhibition may modulate the efficacy of anti-cancer therapy, like DOX, against cancer cells, as well as impact its effects on the vasculature. Enhancing the efficacy of DOX may reduce the doses required for treatment, thereby reducing the risk of cardiotoxicity.

We sought to determine whether p300/CBP plays a role in the response to DOX by 1) Investigating whether there is an association between p300 or CBP and response to DOX in individuals diagnosed with breast cancer and 2) Investigating the role of p300/CBP inhibition in breast cancer cell culture DOX sensitivity. Finally, we sought to determine whether acute DOX exposure induces aortic vascular dysfunction and whether pharmacological inhibition of p300/CBP would modulate the effect of DOX on the vasculature.

Methods

Ethics and Data Availability

The authors declare that all supporting data are available within the present manuscript or its online supplementary files. Registered-tier data (e.g., survey, electronic health record, etc.) and controlled-tier data (i.e., genomic data, specific demographic data) are available through the National Institutes of Health (NIH) *All of Us* Researcher Workbench (https://allofus.nih.gov/).

The *All of Us* database aims to compile data for 1 million participants from diverse ethnic and socioeconomic backgrounds. Currently available data include over 400,000 participants, over 40% of whom identify as racial and ethnic minorities, and over 80% of whom are underrepresented in biomedical research. Informed consent was obtained at the time of participant enrollment, with the enrollment period for the current databank (*Version 7*) occurring from May 1, 2018, to July 1, 2022.

Data were accessed only by authorized users who completed the NIH *All of Us* Responsible Conduct of Research Training and received approval. Data are reported in accordance with the NIH *All of Us* Data and Statistics Dissemination Policy which prohibits disclosure of any group count less than 20 individuals to protect participant privacy. Data are de-identified and thus, exempt from review by the Kansas State University Institutional Review Board.

Candidate Gene Association Study (CGAS)

Cancer Diagnosis and Treatment

Cancer diagnoses were obtained from electronic health records (EHR) and survey data. EHR data were harmonized using the Observational Medical Outcomes Partnership Common

Data Model (OMOP CDM). The *Personal Medical History* form provided self-reported data on cancer history, cancer type, time of cancer diagnosis, and treatment history. Cancer diagnoses from EHR were determined from Systematized Nomenclature of Medicine (SNOMED) codes, which have previously shown to have high validity [42,43]. Cancer selected for the present study was restricted to breast cancer, the most common non-skin cancer in women [1]. Participant demographics were derived from the *Basics* survey, which includes age, race and ethnicity, household income, education, and more. Deprivation index is derived from the American Community Survey and serves as a measure of socioeconomic variation in health outcomes. Full survey question content is accessible via the *All of Us* Research Hub.

Variables and Outcomes

Primary cancer diagnosis and diagnosis of second malignancy were derived from EHR and survey data. Cancer treatments were also recorded from survey and EHR data. *All of Us* concept vocabulary and SNOMED codes were applied to search for the use of antineoplastic agents (Doxorubicin, Concept ID: 1338512). The primary outcome in the present study was the diagnosis of second malignancy (SNOMED Code: 128462008). This was selected as a surrogate indicator of treatment failure after anti-cancer therapy for two reasons: 1) the very low number of recurrent malignancies directly documented in the All of Us database health records ($n \leq 20$), and 2) previous work demonstrating the use of secondary malignancy codes for determining the timing of recurrent or secondary cancer [44]. Those with a diagnosis of second malignancy less than 60 days after primary diagnosis (all treatments combined cohort) or less than 60 days after treatment (i.e., doxorubicin) were excluded from analyses, as were individuals without available

genome sequencing. The selection of 60 days is based on international World Health Organization guidelines previously established for EHR research on infectious disease [45] and frequently adapted for cancer research [46] or cancer management in health systems [47].

Genomic Data

All of Us specimen samples were obtained from participant blood samples. Briefly, DNA extracted from samples was sent to genome centers for whole genome sequencing. For the present study, p300 and CBP were selected as candidate genes, located on chromosome 22q13.2 and 16p13.3, respectively, and all single nucleotide polymorphisms (SNPs) with a minor allele frequency of 0.01 (MAF $\geq$ 0.01) were considered for analysis. Reference SNP ID (rsID) and respective functional outcomes were obtained from the NIH *National Center for Biotechnology Information* (NCBI) Single Nucleotide Polymorphism database (dbSNP).

Cell Culture

Human breast adenocarcinoma (MDA MB 231) cells were obtained from American Type Culture Collection (ATCC; Manassas, VA). Cells were grown in DMEM medium, supplemented with 10% fetal bovine serum (FBS) and 2mM l-glutamine. Cultures were maintained in 75 cm^2 flasks at 37º C in a humidified incubator with 5% CO_2/room air balance. Cells were randomized to receive vehicle, 1 µM doxorubicin, or 2 µM doxorubicin and vehicle or 1 µM CCS-1477.

Doxorubicin and p300 inhibition

48 hours prior to DOX administration, cells were seeded into 6-well plates. Cells were treated with 1 µM CCS-1477 (Chemietek, Indianapolis, IN) dissolved in DMSO or with an equivalent concentration of vehicle (DMSO, less than 1% final media volume) 24 hours prior to

clonogenic plating. Either 1 or 2 µM doxorubicin (Fisher Scientific, Hampton, NH) dissolved in sterile water, or sterile water as vehicle, was administered to cells for 2 hours prior to clonogenic plating.

Clonogenic Survival

The clonogenic survival assay was performed according to the methods of Franken, et al., and Feoktistova, et al., [48,49]. Cells were isolated with trypsin, centrifuged, and re-suspended in fresh media, then stained with trypan blue and counted using a hemacytometer. Cells were then seeded into 100 mm culture plates at a density of 200 cells/plate, performed in triplicate. Plates were returned to a humidified incubator at 37 C and 5% CO_2/room air balance and undisturbed for 9 days. Cells were then fixed and stained with 20% methanol and 0.5% crystal violet in water (see Figure 3.1A), and observed under a microscope at 10x magnification, with colonies >50 cells counted (see Figure 3.1B). Plating efficiency was determined as the percentage of control cells surviving after 9 days and used to normalize the % survival for all other treatment conditions. % survival was determined according to the following equation:

$$\%\ survival = \left(\frac{colonies\ formed}{PE * number\ of\ cells\ plated}\right) * 100$$

where PE is the plating efficiency of control cells and % survival is the average of three separate experiments, each performed in technical triplicate.

Animal Handling and Tissue Acquisition

All procedures were approved by the Kansas State University Institutional Animal Care and Use Committee and carried out in accordance with the National Institutes of Health Guide for the Care and Use of Laboratory Animals. Healthy retired breeder female Fischer 344 rats (n = 10) obtained from Charles River Laboratories were housed and maintained in a temperature controlled (23 ± 2°C) room with a 12:12-h light-dark cycle, with water and standard rat chow provided *ad libitum*.

Tissue Preparation and Wire Myography

After a minimum 2-week acclimation period, rats were anesthetized with 5% isoflurane/O_2 balance and euthanized. The aorta was removed, and thoracic aortic segments were isolated, cleaned of perivascular adipose tissue, sectioned into 1-2 mm segments, and placed into a modified physiological saline solution (PSS; 130.0 mM NaCl, 4.7 mM KCl, 1.6 mM $CaCl_2$, 1.2 mM $MgSO_4$, 3.0 mM MOPS, 1.2 mM H_2NaPO_4, 5.0 mM glucose, 2.0 mM $C_3H_3NaO_3$, 0.02 mM EDTA) [50]. Four equally sized segments from each vessel were randomized to receive 1 µM CCS-1477 (dissolved in DMSO) or vehicle (DMSO) and incubated overnight (20-24 h) in PSS at 4° C. Vessel segments were also randomized to receive Doxorubicin (1 or 2 µM) or vehicle (sterile deionized water) overnight for 20-24 hours. Vessels were then mounted onto stainless steel pins in the chamber of a wire myograph (Danish Myo Technology, Hinnerup, Denmark) and allowed to equilibrate for at least 30 minutes in PSS gassed with 16% O_2 and 4% CO_2 at 37° C. Vessel baths were washed with fresh PSS every 15 minutes throughout equilibration. Tension was set at 12 mN of force (as determined in our laboratory by preliminary experiments following

the DMT Normalization Guide, which establishes the baseline tension to maximize actin-myosin interaction for optimal contractile responses) and tension was continuously recorded throughout both equilibration and subsequent experiments. Vessel viability was assessed by addition of high-potassium PSS (KPSS), which contains an equimolar substitution of potassium for sodium and elicits a contractile response in viable vessels.

After pre-constriction with phenylephrine (PE), endothelium-dependent vasodilation was assessed via cumulative dose-response to acetylcholine (Ach; 10^{-10} to 10^{-5} M), and endothelium-independent vasodilation was assessed via cumulative dose-response to sodium nitroprusside (10^{-10} to 10^{-5} M). Concentration-response curves were also preformed using the α-adrenergic agonist norepinephrine (NE; 10^{-10} to 10^{-5} M). Vessels were allowed to reach a steady state tension over 3 minutes between each drug addition. Between each dose-response curve, vessels were allowed to return to baseline tension following two 5-minutes washes with PSS.

Materials

CCS-1477 was obtained from Chemietek (Indianapolis, IN) and prepared in DMSO. All other chemicals were obtained from Fisher Scientific or Sigma Aldrich and prepared in sterile water or PSS.

Data Analysis

All statistical analyses for *All of Us* were performed using the *All of Us* integrated cloud based Jupyter Notebook within the *All of Us* Researcher Workbench using Python coding language (version 3.12) and Python package Hail (https://github.com/hail-

is/hail/releases/tag/0.2.13). Descriptive statistics of the study population are presented as mean ± standard deviation (SD). Before genetic analyses, SNPs were first filtered according to standard quality control practices. In brief, samples were removed for relatedness between individual participants due to heritability of genetic variants [51], then SNPs were further filtered to include only common variants (MAF ≥ 0.01) and those meeting Hardy-Weinberg equilibrium criteria (p > 1.0 x 10-10) [52]. For association analyses between SNPs and diagnosis of second malignancy in individuals previously diagnosed with breast cancer, we performed logistic regression adjusted for the first three principal components representing ancestry. Subgroup analysis was performed including only individuals who received doxorubicin. Beta (β) values were converted to Odds Ratio (OR) using the equation:

$$OR = \exp(\beta)$$

90% confidence intervals (CI) were constructed from the upper and lower limits from the equation:

$$90\%\ CI = [\exp(\beta) \pm (1.645 * \mathrm{SE})]$$

where SE is the standard error of the mean for β. Due to the exploratory nature of part 1 of the present study, significance was set as *a priori* $p \leq 0.1$.

Statistical analyses for cell culture and wire myography experiments were performed in Prism (Version 10, GraphPad Software, San Diego, CA) data analysis software. Cell survival was compared with two-way analysis of variance (ANOVA), followed by Holm-Sidak post hoc testing to correct for multiple comparisons. Data are expressed as % survival, determined as a

percentage of control and presented as mean ± SEM. The level of significance was set as $p \leq 0.05$. Responses to ACh and sodium nitroprusside were recorded as tension and normalized to the sustained phenylephrine-induced contraction according to the following equation [53,54]:

$$\% \text{ relaxation} = ((T_{max}-T_s)/(T_{max}-T_b) * 100$$

where T_{max} is the maximum tension after constriction to PE, T_s is the steady state tension after addition of drug, and T_b is the baseline tension prior to constriction with PE.

Responses to NE were recorded as tension and normalized to the maximum KPSS-induced contraction according to the following equation [54]:

$$\% \text{ KPSS constriction} = ((T_{sN}-T_{bN})/(T_{KPSS}-T_{bK})) * 100$$

where T_{sN} is the steady state tension after addition of NE, T_{bN} is the baseline tension prior to addition of NE, T_{KPSS} is the maximum tension to KPSS, and T_{bK} is the baseline tension prior to addition of KPSS. All data are expressed as mean ± SEM and results were analyzed using a two-way ANOVA with repeated measures to compare between groups, with post hoc analyses performed using Holm-Sidak test to correct for multiple comparisons. Significance was set as $p \leq 0.05$.

Figure 3.1. Representative images of clonogenic plates

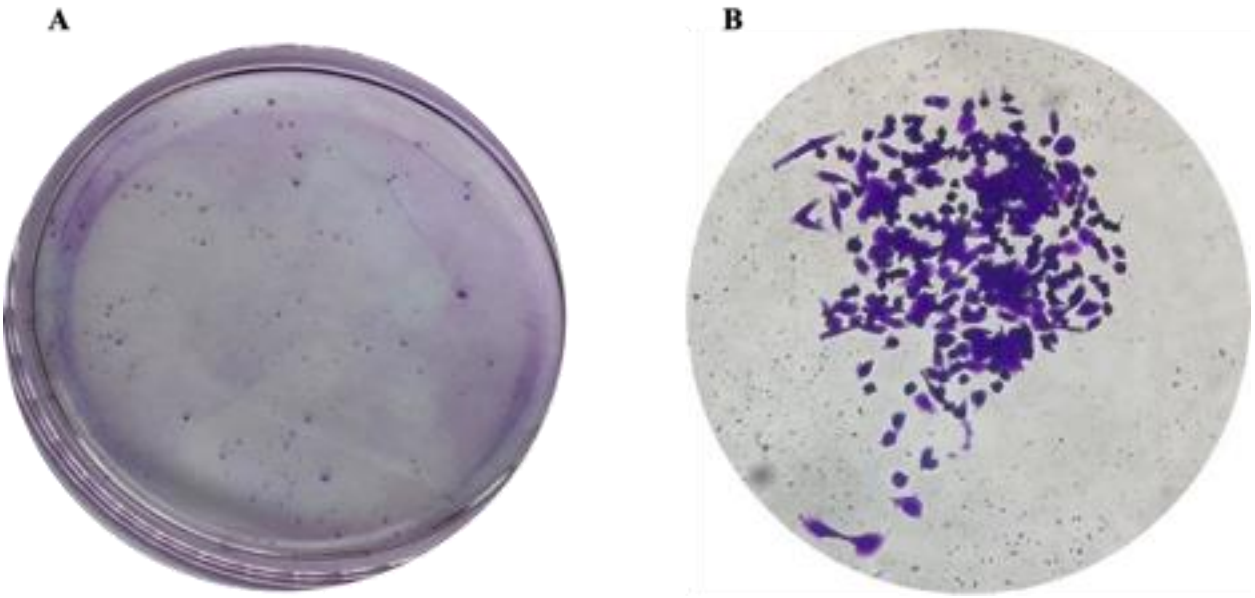

Representative image of clonogenic plate after staining with crystal violet (**A**) and representative image of an individual colony ≥ 50 cells (**B**).

Results

NIH *All of Us* Genomic Data

Our initial database search identified 6,584 individuals diagnosed with breast cancer for whom genomic data was available. Of these, 1,085 individuals (16.5%) received a diagnosis of second malignancy. 197 (18.2%) of these individuals received doxorubicin, and 188 (3.4%) of those who were not diagnosed with second malignancy received doxorubicin. Patient characteristics are summarized in Table 3.1. There was a significant difference in age between those who were diagnosed with second malignancy and those who were not (64.8 ± 12.5 vs. 69.1 ± 11.6 yrs, respectively; $p < 0.0001$). Those diagnosed with secondary malignancy also had a significantly lower income and greater deprivation index compared to those not diagnosed with secondary malignancy ($p = 0.049$ and $p < 0.0001$, respectively). Due to NIH *All of Us* Data and Statistics Dissemination Policy, disclosure of group counts ≤ 20 is prohibited. As such, statistical comparisons cannot be made for all demographic information.

All SNPs with a significant odds ratio (OR) identified from the CBP or p300 gene encoding regions are summarized in Table 3.2, with rsIDs and outcomes of given SNPs reported, if known. There were four CBP (Figure 3.2) and no p300 (Figure 3.3) SNPs associated with the odds of diagnosis of second malignancy in those treated with doxorubicin. All four CBP SNPs were associated with a decreased odds (loci chr16:3725961, OR, 0.269 [90% CI, 0.075 – 0.962]; chr16:3726197, OR, 0.169 [90% CI, 0.031 – 0.925]; chr16:3729059, OR, 0.161 [90% CI, 0.028 – 0.915]; and chr16:3745362, OR, 0.599 [90% CI, 0.367 – 0.978]) of diagnosis of second malignancy after receiving doxorubicin.

Cell Culture Experiments

p300 inhibition and doxorubicin

The % survival of MDA MB 231 cells was determined after correcting for the plating efficiency of control cells. Untreated cells will not exhibit 100% survival and raw counts must be corrected to set control as 100%. This plating efficiency is then applied to all treatment groups. There was no significant interaction between DOX dose and inhibitor treatment ($p = 0.710$). There was a significant main effect for DOX dose (0 vs. 1 vs. 2 µM, $p < 0.0001$) but not for inhibitor treatment (vehicle vs. CCS-1477, $p = 0.312$). Relative to the survival of 0 µM DOX/vehicle treated cells (100%), survival was 11.3 ± 1.9% in 1 µM DOX/vehicle, 3.1 ± 1.8% in 2 µM DOX/vehicle, 84.7 ± 21% in 0 µM DOX/CCS-1477, 4.75 ± 0.5% in 1 µM DOX/CCS-1477, and 2.35 ± 0.6% in 2 µM DOX/CCS-1477 (Figure 3.4). The significant effect of DOX dose was present in 0 vs. 1 µM DOX and 0 vs. 2 µM DOX in vehicle treated cells ($p < 0.0001$ for both comparisons), and in 0 vs. 1 µM DOX and 0 vs. 2 µM DOX in CCS-14770 treated cells ($p < 0.0001$ for both comparisons). There was no significant effect of DOX dose between 1 and 2 µM DOX in vehicle treated cells ($p = 0.788$) or CCS-1477 treated cells ($p = 0.980$). These results suggest that p300/CBP inhibition dose not impact the efficacy of DOX in breast cancer cells.

Wire Myography

Vasodilatory Responses

In the 1 µM DOX group, there were no differences between any group in vasodilatory response ($p > 0.05$) or sensitivity ($\log EC_{50;}$ $p > 0.05$) to the endothelium-dependent dilator ACh

(Figure 3.5). In the 2 µM DOX group, the sensitivity to ACh was significantly lower in CCS-1477-treated vessels ($p = 0.0097$), but there were no other differences in vasodilatory responses to ACh ($p > 0.05$; Figure 3.6). In both the 1 µM DOX and 2 µM groups, there were no differences in vasodilatory response or sensitivity to the exogenous NO donor sodium nitroprusside (all $p > 0.05$; Figures 3.7 and 3.8).

Vasoconstrictor Responses

In the 1 µM DOX group, there were no differences between any group in vasoconstriction response or sensitivity to α-adrenoreceptor agonist NE (all $p > 0.05$; Figure 3.9). In the 2 µM DOX group, there were no differences between any group in vasoconstriction or sensitivity to NE (all $p > 0.05$; Figure 3.10).

Table 3.1. Cohort characteristics

	+ diagnosis of secondary malignancy (n = 1085)	- diagnosis of secondary malignancy (n = 5499)
Age (yrs)	64.8 ± 12.5 *	69.1 ± 11.6
Median income ($)	67,144 *	68,315
Deprivation index	0.32 ± 0.07 *	0.31 ± 0.07
Female	1039 (95.8%)	5311 (96.6%)
Male	22 (2%)	58 (1.1%)
Other/no response	24 (2.2%)	130 (2.4%)
White	703 (64.8%)	3824 (69.5%)
Black or African American	126 (11.6%)	659 (12%)
Asian	33 (3%)	119 (2.2%)
Multiple	≤ 20	68 (1.2%)
Middle Eastern or North African	≤ 20	26 (0.5%)
Prefer not to answer/other	198 (18.2%)	803 (14.6%)
Not Hispanic	879 (81%)	4623 (84.1%)
Hispanic or Latino	163 (15%)	656 (11.9%)
Prefer not to answer/other	43 (4%)	220 (4%)
Received doxorubicin	197 (18.2%)	188 (3.4%)

*significant vs. -diagnosis of secondary malignancy

Table 3.2. Summary of significant SNPs

SNPs location	rsID	OR [90% CI]	outcome
Breast cancer, with DOX			
chr16:3725961	rs150224533	0.269 [0.075, 0.962]	3' UTR variant
chr16:3726197	n/a	0.169 [0.031, 0.925]	unknown
chr16:3729059	rs181646656	0.161 [0.028, 0.915]	Synonymous variant
chr16:3745362	rs3025684	0.599 [0.367, 0.978]	Intron variant

Figure 3.2. CBP SNPs in breast cancer patients who received doxorubicin

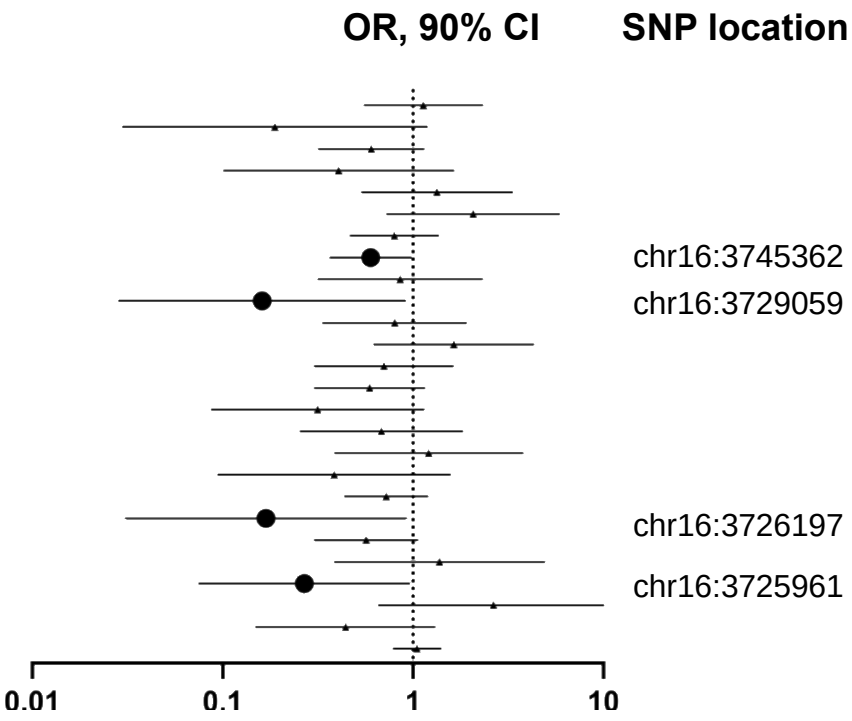

Figure 3.3. p300 SNPs in breast cancer patients who received doxorubicin

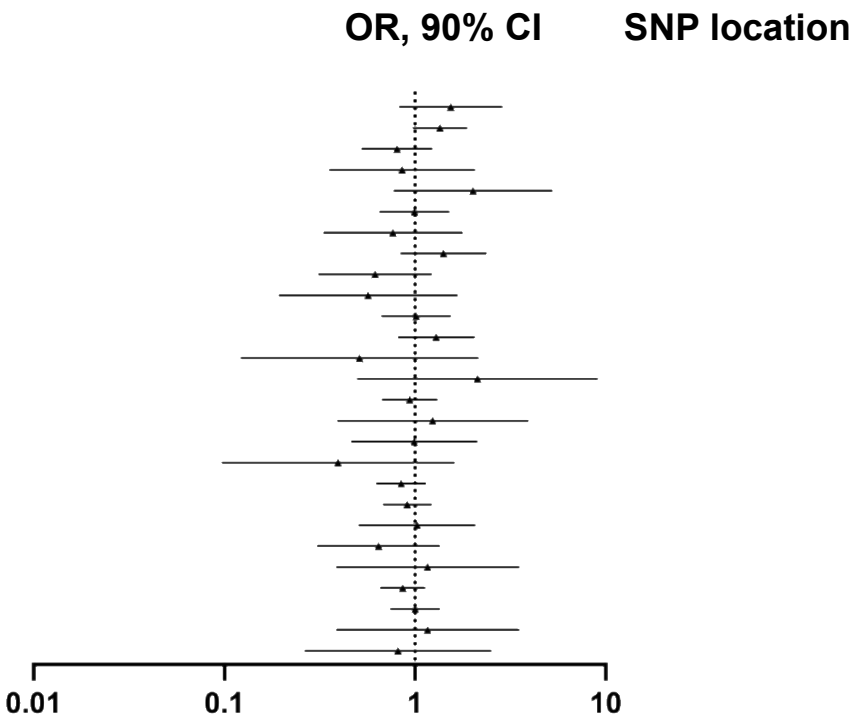

Figure 3.4. MDA MB 231 clonogenic survival

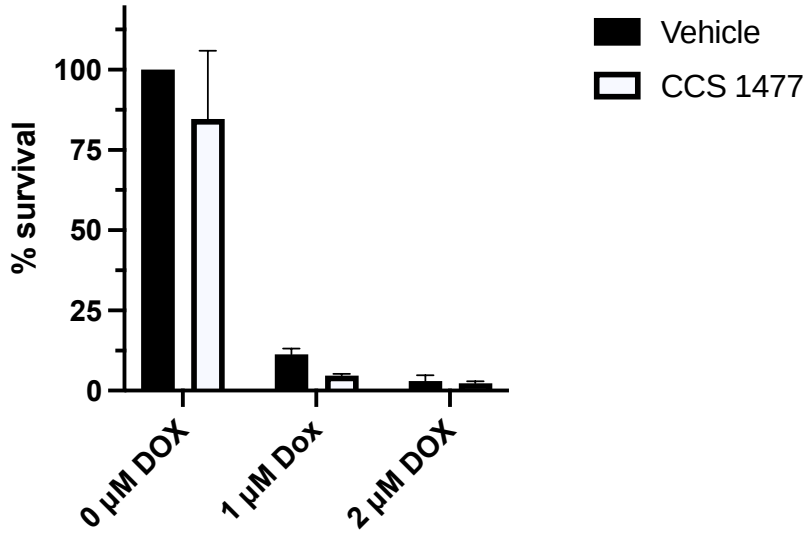

Data are mean ± SEM. *significant vs. 0 µM DOX within group (vehicle or CCS 1477; $p \leq 0.05$).

Results are the average of 3 independent experiments.

Figure 3.5. Dose response to ACh (1 µM DOX group)

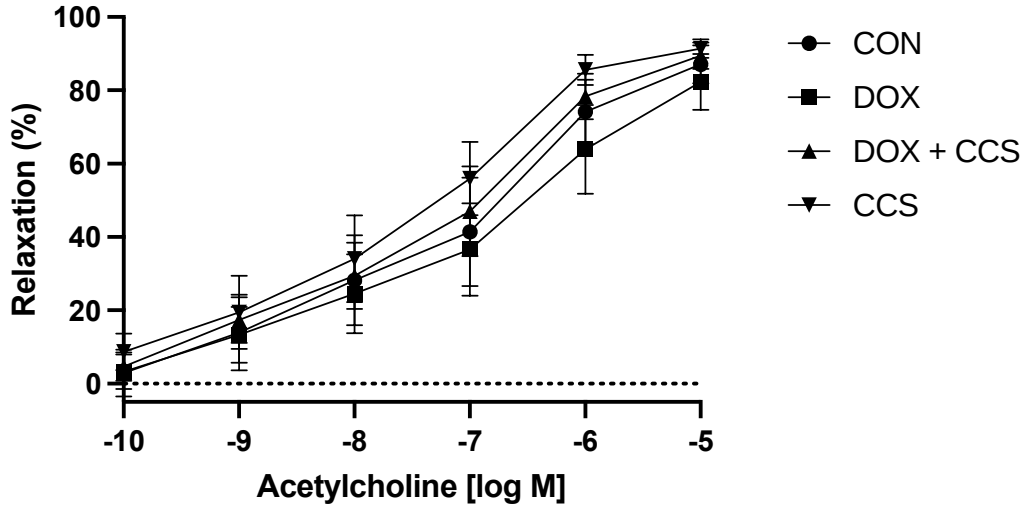

Concentration dose response to ACh in aortic segments treated with vehicle (CON; n = 5), 1 µM doxorubicin (DOX; n = 5), 1 µM doxorubicin and 1 µM CCS-1477 (DOX + CCS; n = 5), or 1 µM CCS-1477 (CCS; n = 5). Data are mean ± SEM. $p > 0.05$.

Figure 3.6. Dose response to ACh (2 µM DOX group)

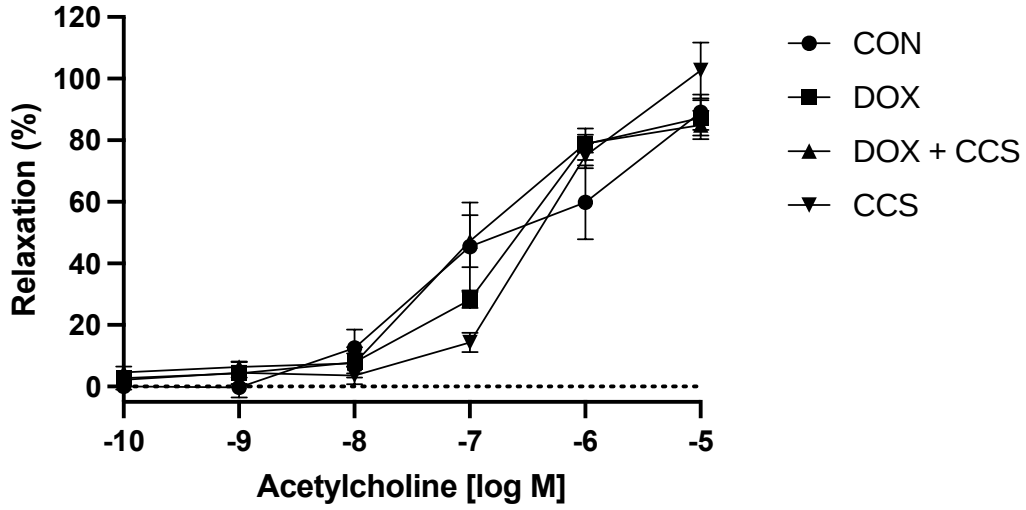

Concentration dose response to ACh in aortic segments treated with vehicle (CON; n = 4), 2 µM doxorubicin (DOX; n = 4), 2 µM doxorubicin and 1 µM CCS-1477 (DOX + CCS; n = 5), or 1 µM CCS-1477 (CCS; n = 3). Data are mean ± SEM. $p > 0.05$.

The sensitivity (logEC50) to ACh is significantly decreased in CCS vs. CON ($p \leq 0.05$).

Figure 3.7. Dose response to sodium nitroprusside (1 µM DOX group)

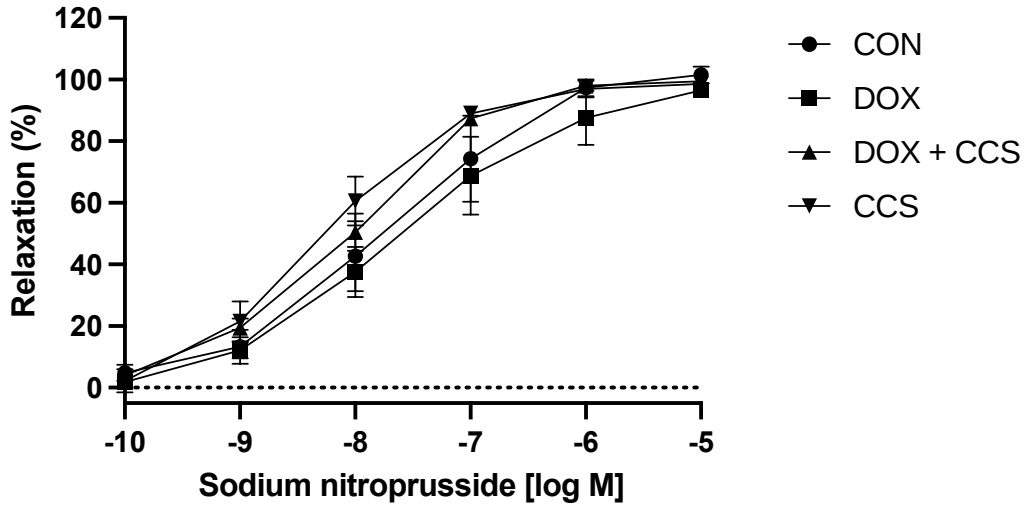

Concentration dose response to sodium nitroprusside in aortic segments treated with vehicle (CON; n = 5), 1 µM doxorubicin (DOX; n = 5), 1 µM doxorubicin and 1 µM CCS-1477 (DOX + CCS; n = 5), or 1 µM CCS-1477 (CCS; n = 5). Data are mean ± SEM. $p > 0.05$.

Figure 3.8. Dose response to sodium nitroprusside (2 µM DOX group)

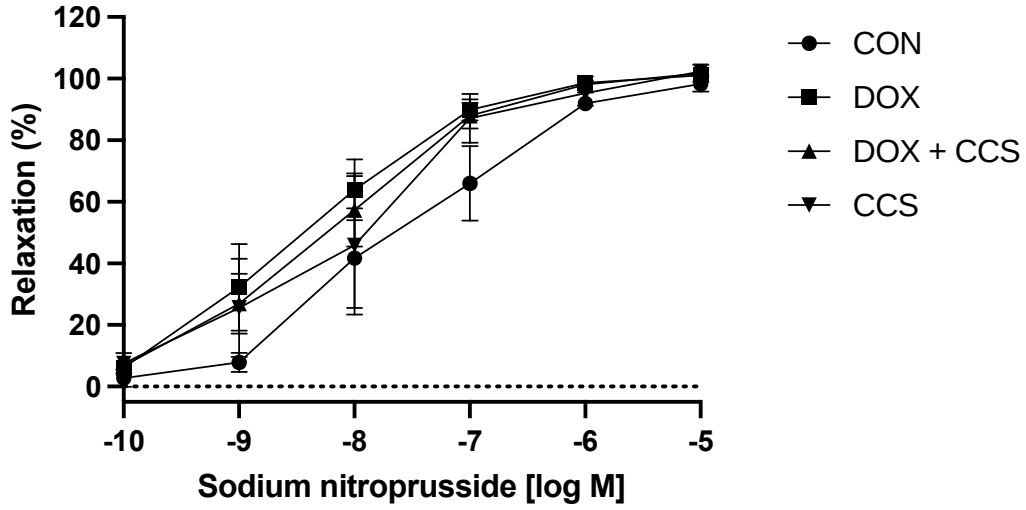

Concentration dose response to sodium nitroprusside in aortic segments treated with vehicle (CON; n = 3), 2 µM doxorubicin (DOX; n = 4), 2 µM doxorubicin and 1 µM CCS-1477 (DOX + CCS; n = 4), or 1 µM CCS-1477 (CCS; n = 3). Data are mean ± SEM. $p > 0.05$.

Figure 3.9. Dose response to NE (1 µM DOX group)

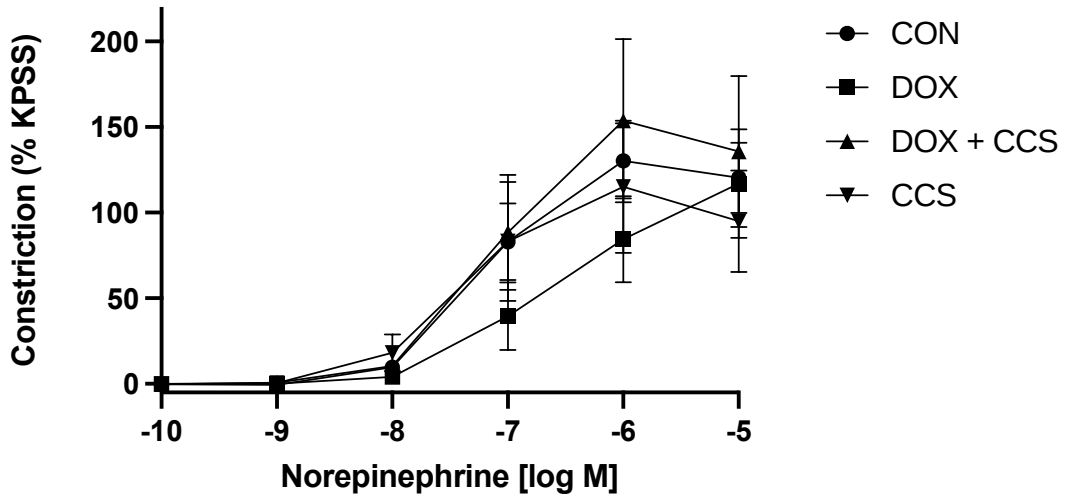

Concentration dose response to NE in aortic segments treated with vehicle (CON; n = 5), 1 µM doxorubicin (DOX; n = 5), 1 µM doxorubicin and 1 µM CCS-1477 (DOX + CCS; n = 5), or 1 µM CCS-1477 (CCS; n = 5). Data are mean ± SEM. $p > 0.05$.

Figure 3.10. Dose response to NE (2 µM DOX group)

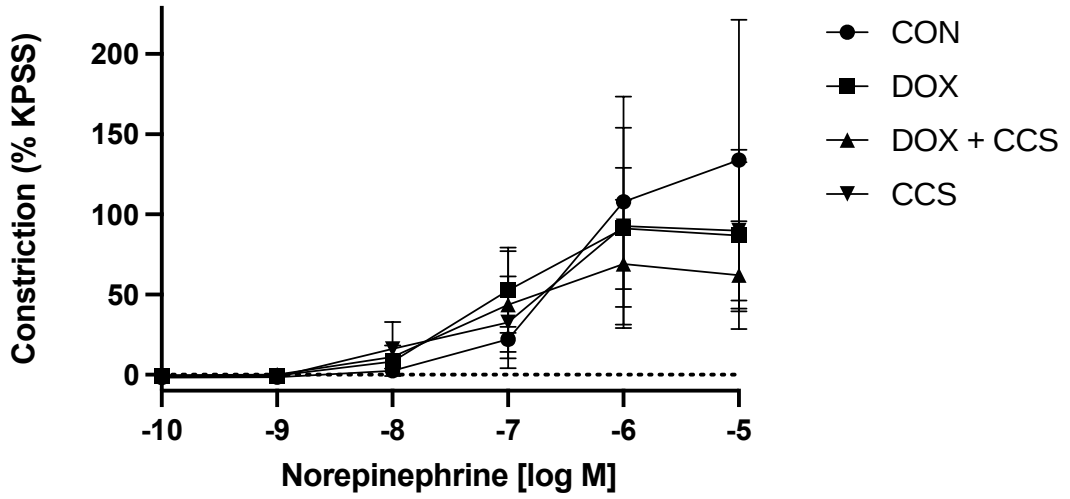

Concentration dose response to NE in aortic segments treated with vehicle (CON; n = 4), 2 µM doxorubicin (DOX; n = 5), 2 µM doxorubicin and 1 µM CCS-1477 (DOX + CCS; n = 5), or 1 µM CCS-1477 (CCS; n = 3). Data are mean ± SEM. $p > 0.05$.

Discussion

This study demonstrates that specific SNPs in the CBP gene encoding region may be associated with a decreased odds of diagnosis of a second malignancy in individuals with breast cancer after receiving doxorubicin. Though these SNPs are primarily associated with changes in the genetic sequence that do not alter the protein product, they may provide insight into predicting treatment outcomes. However, our study also suggests that there is no effect of p300/CBP inhibition on breast cancer cell sensitivity to acute DOX exposure *in vitro* and that there is no effect of acute DOX exposure or p300/CBP inhibition on aortic vascular function *ex vivo*. Overall, this study highlights genetic variation in CBP as a potential marker for odds of secondary malignancy, though modulation of p300/CBP may not directly impact immediate cellular sensitivity to doxorubicin or vascular function.

CBP/p300 SNPs

Candidate gene association studies represent a newer method of understanding the genetic basis of disease and can help lead to targeted interventions and risk stratification in patients. For example, the association of SNPs with higher odds of disease development can be leveraged to develop interventions that target the protein product related to the SNPs or to stratify patients at higher or lower risk of developing said disease. In our study, four CBP and no p300 polymorphisms were associated with lower risk of diagnosis of secondary malignancy in breast cancer patients receiving DOX. Since our findings suggest SNPs in the CBP region are associated with lower odds of diagnosis of secondary malignancy after DOX, it is possible that CBP could mediate resistance to DOX. Decreased CBP function could result in increased DNA damage from DOX and therefore, better response to treatment. In support of this, there is

evidence to suggest that p300/CBP are important mediators of DNA damage repair, and that their inhibition leads to greater levels of DNA damage [33-36].

Though the SNPs identified in our study are not directly associated with a different protein product, they may play an important regulatory role. For example, introns comprise half of the non-coding genome and an intronic variant may result in errors with splice site recognition and skipping of exons, which can lead to disease development [55]. Similarly, 3' UTR variants can alter mRNA stability or binding affinity of miRNAs, which can alter gene/protein expression, or alter drug/treatment susceptibility [56-60]. For example, SNPs in the 3' UTR of the NKX3-1 gene have been shown to increase miRNA binding, leading to downregulation of the gene, and were associated with risk of prostate cancer [61]. Thus, SNPs in the CBP gene encoding region could mediate the response to DOX through alterations in mRNA stability, miRNA binding, or other functional changes.

p300/CBP inhibition in cell culture

In vitro, inhibition of p300/CBP did not affect the efficacy of DOX in human breast cancer cells. Though the findings of part one of the present study suggest that p300/CBP may mediate the efficacy of DOX, the role of p300/CBP in cancer cell survival upon DOX exposure remains unclear, and may relate to their overlapping effects on DNA repair, oxidative stress, or senescence.

p300/CBP is important for successful DNA damage repair through either non-homologous end joining (NHEJ) or homologous recombination (HR) [33,34]. Knockdown of p300 can decrease the expression of HR-related proteins and lead to inefficient double-stranded break repair [35]. As such, this increases the amount of DNA damage and is expected to increase the

efficacy of DNA damaging agents. In pancreatic cancer cells, p300 inhibition has been shown to enhance the efficacy of the chemotherapy agent gemcitabine [62]. Though the mechanism of action of gemcitabine is different than that of DOX [63], it is suggested that the p300 dependent increase in the efficacy of gemcitabine is through inhibition of DNA repair [62]. As a whole, this suggests that inhibition of p300/CBP would decrease DNA damage repair capability, thereby increasing the efficacy of anti-cancer therapies. Evidence for the role of p300/CBP in mediating oxidative stress is less clear, but is an important consideration given that DOX induces damage, in part, through the generation of ROS. In a mouse model of diabetes, inhibition of p300/CBP has been demonstrated to decrease ROS production, potentially through a NOX-mediated mechanism [64], suggesting that p300/CBP may mediate oxidative stress. Interestingly, p300 overexpression has been shown to acetylate NRF2 and promote cell viability in response to oxidative stress [65], and p300/CBP inhibition also results in an attenuation of oxidative stress, while reducing pro-oxidant enzyme expression through an NF-κB-mediated mechanism [38]. Given these findings, albeit, not in cancer cells, it remains unclear whether p300/CBP inhibition might increase or decrease cell survival in response to DOX exposure through modulating oxidative stress. p300 knockdown has also been shown to inhibit cellular senescence [40], which is one mechanism by which DOX induces cellular damage [20,21]. If inhibition of p300/CBP reduces DOX-mediated senescence of breast cancer cells, this could negate any benefit of reduced DNA repair capabilities.

Vascular reactivity

The exact mechanisms resulting in DOX-induced vascular dysfunction are incompletely understood, but may be mediated in part by DNA damage, oxidative stress, and vascular cell senescence [13,22-32], all of which may be modulated by p300/CBP. We hypothesized that acute

exposure to DOX *ex vivo* would result in aortic vascular dysfunction, but this was not supported by our findings, as DOX did not cause any impairments in ACh or sodium nitroprusside-induced dilation, or NE-induced constriction. Prior work assessing DOX-mediated vascular dysfunction has shown impairments in ACh-mediated dilation [9-11,13,66-69]. However, to the best of our knowledge, in all but one study performed in mice [10], DOX was administered to animals *in vivo* prior to *ex vivo* assessments of aortic vascular function. As such, it is possible that acute *ex vivo* administration of DOX does not elicit impairments in ACh-mediated dilation, or that these alterations do not manifest within the timeline that we performed assessments of vascular function. Our findings of an un-altered response to sodium nitroprusside in response to DOX exposure is consistent with some studies showing no impact of DOX on endothelial-independent dilation[9-11], though some groups have demonstrated reductions in endothelium-dependent dilation to sodium nitroprusside after DOX exposure [67-69]. Reports differ on the impact of DOX on vascular smooth cell contraction in the aorta. Some findings suggest that DOX impairs aortic contraction to NE [70] and reduces sensitivity but not maximal contraction [71]. DOX is also shown to impair smooth muscle cell contraction of the aorta to PE [9-11,67-69], while others have shown both decreased and increased contraction to PE that depends upon the dose of DOX [72]. However, to our knowledge, this is the first study to assess cumulative dose response to NE in aortas exposed to DOX *ex vivo.* Given that DOX and p300/CBP both play a role in DNA damage, oxidative stress, and senescence, we also hypothesized that p300 inhibition might alter vascular function in aortic segments exposed to DOX. However, except for a decreased sensitivity to ACh in the CCS-1477 treated vessels from the 2 μM DOX group, *ex vivo* administration of CCS-1477 did not impact vascular function in the thoracic aorta, nor could we fully interpret any

relationship between p300/CBP inhibition and DOX, as DOX did not result in aortic vascular dysfunction.

Limitations

Though we were primarily interested in studying the diagnosis of secondary malignancy as a surrogate for predicting the efficacy of DOX, our analysis did not exclude individuals receiving other therapies. However, patient regimens rarely include only a single anti-cancer therapy, and our findings, in the context of other treatments, accurately represents patient populations. CCS-1477 inhibits both p300 and CBP, and as such, we included both in our analysis of SNPs. p300 and CBP have similar structures and are considered homologous proteins that are believed to function identically. However, there is some evidence to suggest that they serve non-redundant roles [73,74]. Though we cannot state that any of our *in vitro* or *ex vivo* findings are exclusively a result of either p300 or CBP inhibition, there is currently no commercially available drug that can inhibit either exclusively; as such, we included both in our SNPs analysis. Regarding our cell culture findings, 1 and 2 µM DOX reduced survival by nearly 89 and 97%, respectively. As such, there was little room to detect further decreases in survival through the addition of CCS-1477, but these doses were chosen based upon the reported IC_{50} for DOX in MDA MD 231 cells [75]. In addition, the exact role of p300/CBP inhibition in mediating DNA repair, oxidative stress, or senescence were not directly assessed in our study, which could provide important insight. Most studies investigating aortic vascular function *ex vivo* do so after *in vivo* dosing of DOX, and our *ex vivo* dosing protocol may not be an adequate stimulus to induce vascular dysfunction. However, we chose to expose vessels to DOX *ex vivo* to determine its effect independent of hemodynamic, metabolic, or humoral influences, in part because any

interaction between CCS-1477 and DOX *in vivo* is unknown. Our vascular reactivity assessments include a relatively small sample size, with a large standard error, particularly for NE dose responses. Additionally, there is a paucity of information regarding the acute effects of DOX on the vasculature (i.e., within hours of exposure), and further investigation is needed.

Conclusions

Taken together, our findings suggest that CBP genetic polymorphisms may have an important role in predicting or mediating the response to DOX. The exact mechanisms are unknown but may be due to alterations in gene expression or regulation, and should be investigated further. Our results also suggest that p300/CBP inhibition does not directly impact the survival of breast cancer cells *in vitro*, but whether it may modulate the effects of lower, clinically relevant doses of DOX are not known. Finally, we found that 24-hour exposure to DOX *ex vivo* does not impact aortic vascular function and that 24-hour exposure to CCS-1477 may impact vascular sensitivity to ACh, but largely does not impact aortic vascular function. Further investigation to determine the role of p300/CBP inhibition on the efficacy of other anti-cancer therapies, as well as cancer cell survival and vascular function *in vivo* is warranted.

References

1 Siegel, R. L., Giaquinto, A. N. & Jemal, A. Cancer statistics, 2024. *CA Cancer J Clin* **74**, 12-49 (2024). https://doi.org:10.3322/caac.21820

2 Lotrionte, M. *et al.* Review and meta-analysis of incidence and clinical predictors of anthracycline cardiotoxicity. *Am J Cardiol* **112**, 1980-1984 (2013). https://doi.org:10.1016/j.amjcard.2013.08.026

3 Cardinale, D., Iacopo, F. & Cipolla, C. M. Cardiotoxicity of Anthracyclines. *Front Cardiovasc Med* **7**, 26 (2020). https://doi.org:10.3389/fcvm.2020.00026

4 Curigliano, G. *et al.* Cardiotoxicity of anticancer treatments: Epidemiology, detection, and management. *CA Cancer J Clin* **66**, 309-325 (2016). https://doi.org:10.3322/caac.21341

5 Mulrooney, D. A. *et al.* Cardiac outcomes in a cohort of adult survivors of childhood and adolescent cancer: retrospective analysis of the Childhood Cancer Survivor Study cohort. *Bmj* **339**, b4606 (2009). https://doi.org:10.1136/bmj.b4606

6 Kremer, L. C., van Dalen, E. C., Offringa, M., Ottenkamp, J. & Voûte, P. A. Anthracycline-induced clinical heart failure in a cohort of 607 children: long-term follow-up study. *J Clin Oncol* **19**, 191-196 (2001). https://doi.org:10.1200/jco.2001.19.1.191

7 Herrmann, J. *et al.* Evaluation and management of patients with heart disease and cancer: cardio-oncology. *Mayo Clin Proc* **89**, 1287-1306 (2014). https://doi.org:10.1016/j.mayocp.2014.05.013

8 Plana, J. C., Thavendiranathan, P., Bucciarelli-Ducci, C. & Lancellotti, P. Multi-Modality Imaging in the Assessment of Cardiovascular Toxicity in the Cancer Patient. *JACC Cardiovasc Imaging* **11**, 1173-1186 (2018). https://doi.org:10.1016/j.jcmg.2018.06.003

9 Bosman, M. *et al.* Doxorubicin induces arterial stiffness: A comprehensive in vivo and ex vivo evaluation of vascular toxicity in mice. *Toxicol Lett* **346**, 23-33 (2021). https://doi.org:10.1016/j.toxlet.2021.04.015

10 Bosman, M. *et al.* Dexrazoxane does not mitigate early vascular toxicity induced by doxorubicin in mice. *Plos One* **18**, e0294848 (2023). https://doi.org:10.1371/journal.pone.0294848

11 Bosman, M. *et al.* Doxorubicin Impairs Smooth Muscle Cell Contraction: Novel Insights in Vascular Toxicity. *Int J Mol Sci* **22** (2021). https://doi.org:10.3390/ijms222312812

12 Chaosuwannakit, N. *et al.* Aortic stiffness increases upon receipt of anthracycline chemotherapy. *J Clin Oncol* **28**, 166-172 (2010). https://doi.org:10.1200/jco.2009.23.8527

13 Clayton, Z. S. *et al.* Doxorubicin-Induced Oxidative Stress and Endothelial Dysfunction in Conduit Arteries Is Prevented by Mitochondrial-Specific Antioxidant Treatment. *JACC CardioOncol* **2**, 475-488 (2020). https://doi.org:10.1016/j.jaccao.2020.06.010

14 Frye, J. N. *et al.* Vascular and autonomic changes in adult cancer patients receiving anticancer chemotherapy. *J Appl Physiol (1985)* **125**, 198-204 (2018). https://doi.org:10.1152/japplphysiol.00005.2018

15 Parr, S. K. *et al.* Anticancer Therapy-Related Increases in Arterial Stiffness: A Systematic Review and Meta-Analysis. *J Am Heart Assoc* **9**, e015598 (2020). https://doi.org:10.1161/jaha.119.015598

16 Reriani, M. K., Lerman, L. O. & Lerman, A. Endothelial function as a functional expression of cardiovascular risk factors. *Biomark Med* **4**, 351-360 (2010). https://doi.org:10.2217/bmm.10.61

17 Lakatta, E. G. & Levy, D. Arterial and cardiac aging: major shareholders in cardiovascular disease enterprises: Part I: aging arteries: a "set up" for vascular disease. *Circulation* **107**, 139-146 (2003). https://doi.org:10.1161/01.cir.0000048892.83521.58

18 Kciuk, M. *et al.* Doxorubicin-An Agent with Multiple Mechanisms of Anticancer Activity. *Cells* **12** (2023). https://doi.org:10.3390/cells12040659

19 Thorn, C. F. *et al.* Doxorubicin pathways: pharmacodynamics and adverse effects. *Pharmacogenet Genomics* **21**, 440-446 (2011). https://doi.org:10.1097/FPC.0b013e32833ffb56

20 Ewald, J. A., Desotelle, J. A., Wilding, G. & Jarrard, D. F. Therapy-induced senescence in cancer. *J Natl Cancer Inst* **102**, 1536-1546 (2010). https://doi.org:10.1093/jnci/djq364

21 Gewirtz, D. A., Holt, S. E. & Elmore, L. W. Accelerated senescence: an emerging role in tumor cell response to chemotherapy and radiation. *Biochem Pharmacol* **76**, 947-957 (2008). https://doi.org:10.1016/j.bcp.2008.06.024

22 Kong, C. Y. *et al.* Underlying the Mechanisms of Doxorubicin-Induced Acute Cardiotoxicity: Oxidative Stress and Cell Death. *Int J Biol Sci* **18**, 760-770 (2022). https://doi.org:10.7150/ijbs.65258

23 Linders, A. N. *et al.* A review of the pathophysiological mechanisms of doxorubicin-induced cardiotoxicity and aging. *NPJ Aging* **10**, 9 (2024). https://doi.org:10.1038/s41514-024-00135-7

24 Maejima, Y., Adachi, S., Ito, H., Hirao, K. & Isobe, M. Induction of premature senescence in cardiomyocytes by doxorubicin as a novel mechanism of myocardial damage. *Aging Cell* **7**, 125-136 (2008). https://doi.org:10.1111/j.1474-9726.2007.00358.x

25 Minotti, G., Menna, P., Salvatorelli, E., Cairo, G. & Gianni, L. Anthracyclines: molecular advances and pharmacologic developments in antitumor activity and cardiotoxicity. *Pharmacol Rev* **56**, 185-229 (2004). https://doi.org:10.1124/pr.56.2.6

26 Mitry, M. A. *et al.* Accelerated cardiomyocyte senescence contributes to late-onset doxorubicin-induced cardiotoxicity. *Am J Physiol Cell Physiol* **318**, C380-c391 (2020). https://doi.org:10.1152/ajpcell.00073.2019

27 Piegari, E. *et al.* Doxorubicin induces senescence and impairs function of human cardiac progenitor cells. *Basic Res Cardiol* **108**, 334 (2013). https://doi.org:10.1007/s00395-013-0334-4

28 Spallarossa, P. *et al.* Doxorubicin induces senescence or apoptosis in rat neonatal cardiomyocytes by regulating the expression levels of the telomere binding factors 1 and 2. *Am J Physiol Heart Circ Physiol* **297**, H2169-2181 (2009). https://doi.org:10.1152/ajpheart.00068.2009

29 Demaria, M. *et al.* Cellular Senescence Promotes Adverse Effects of Chemotherapy and Cancer Relapse. *Cancer Discov* **7**, 165-176 (2017). https://doi.org:10.1158/2159-8290.Cd-16-0241

30 Lyu, Y. L. *et al.* Topoisomerase IIbeta mediated DNA double-strand breaks: implications in doxorubicin cardiotoxicity and prevention by dexrazoxane. *Cancer Res* **67**, 8839-8846 (2007). https://doi.org:10.1158/0008-5472.Can-07-1649

31 Jirkovský, E. *et al.* Clinically Translatable Prevention of Anthracycline Cardiotoxicity by Dexrazoxane Is Mediated by Topoisomerase II Beta and Not Metal Chelation. *Circ Heart Fail* **14**, e008209 (2021). https://doi.org:10.1161/circheartfailure.120.008209

32 Clayton, Z. S. *et al.* Cellular Senescence Contributes to Large Elastic Artery Stiffening and Endothelial Dysfunction With Aging: Amelioration With Senolytic Treatment. *Hypertension* **80**, 2072-2087 (2023). https://doi.org:10.1161/hypertensionaha.123.21392

33 Ogiwara, H. & Kohno, T. CBP and p300 Histone Acetyltransferases Contribute to Homologous Recombination by Transcriptionally Activating the *BRCA1* and *RAD51* Genes. *Plos One* **7** (2012). https://doi.org:10.1371/journal.pone.0052810

34 Ogiwara, H. *et al.* Histone acetylation by CBP and p300 at double-strand break sites facilitates SWI/SNF chromatin remodeling and the recruitment of non-homologous end joining factors. *Oncogene* **30**, 2135-2146 (2011). https://doi.org:10.1038/onc.2010.592

35 Wallace, N. A., Robinson, K., Howie, H. L. & Galloway, D. A. β-HPV 5 and 8 E6 Disrupt Homology Dependent Double Strand Break Repair by Attenuating BRCA1 and BRCA2 Expression and Foci Formation. *Plos Pathog* **11** (2015). https://doi.org:10.1371/journal.ppat.1004687

36 Dutto, I., Scalera, C. & Prosperi, E. CREBBP and p300 lysine acetyl transferases in the DNA damage response. *Cell Mol Life Sci* **75**, 1325-1338 (2018). https://doi.org:10.1007/s00018-017-2717-4

37 Chiu, J., Khan, Z. A., Farhangkhoee, H. & Chakrabarti, S. Curcumin prevents diabetes-associated abnormalities in the kidneys by inhibiting p300 and nuclear factor-kappaB. *Nutrition* **25**, 964-972 (2009). https://doi.org:10.1016/j.nut.2008.12.007

38 Kim, J. Y., Jo, J., Leem, J. & Park, K. K. Inhibition of p300 by Garcinol Protects against Cisplatin-Induced Acute Kidney Injury through Suppression of Oxidative Stress, Inflammation, and Tubular Cell Death in Mice. *Antioxidants (Basel)* **9** (2020). https://doi.org:10.3390/antiox9121271

39 Lan, F., Hu, Y., Tang, D., Cai, J. & Zhang, Q. Transcription coactivator p300 promotes inflammation by enhancing p65 subunit activation in type 2 diabetes nephropathy. *Int J Clin Exp Pathol* **12**, 1826-1834 (2019).

40 Sen, P. *et al.* Histone Acetyltransferase p300 Induces De Novo Super-Enhancers to Drive Cellular Senescence. *Mol Cell* **73**, 684-698.e688 (2019). https://doi.org:10.1016/j.molcel.2019.01.021

41 Zhang, E. *et al.* Metformin and Resveratrol Inhibited High Glucose-Induced Metabolic Memory of Endothelial Senescence through SIRT1/p300/p53/p21 Pathway. *Plos One* **10**, e0143814 (2015). https://doi.org:10.1371/journal.pone.0143814

42 Asgari, M. M., Eide, M. J., Warton, E. M. & Fletcher, S. W. Validation of a large basal cell carcinoma registry. *J Registry Manag* **40**, 65-69 (2013).

43 Senior, R. *et al.* Evaluation of SNOMED CT Grouper Accuracy and Coverage in Organizing the Electronic Health Record Problem List by Clinical System: Observational Study. *JMIR Med Inform* **12**, e51274 (2024). https://doi.org:10.2196/51274

44 Uno, H. *et al.* Determining the Time of Cancer Recurrence Using Claims or Electronic Medical Record Data. *JCO Clin Cancer Inform* **2**, 1-10 (2018). https://doi.org:10.1200/cci.17.00163

45 infection, W. W. G. o. t. C. C. a. M. o. C.-. A minimal common outcome measure set for COVID-19 clinical research. *Lancet Infect Dis* **20**, e192-e197 (2020). https://doi.org:10.1016/s1473-3099(20)30483-7

46 Yuan, Q. *et al.* Performance of a Machine Learning Algorithm Using Electronic Health Record Data to Identify and Estimate Survival in a Longitudinal Cohort of Patients With Lung Cancer. *JAMA Netw Open* **4**, e2114723 (2021). https://doi.org:10.1001/jamanetworkopen.2021.14723

47 Hassett, M. J. *et al.* eSyM: An Electronic Health Record-Integrated Patient-Reported Outcomes-Based Cancer Symptom Management Program Used by Six Diverse Health Systems. *JCO Clin Cancer Inform* **6**, e2100137 (2022). https://doi.org:10.1200/cci.21.00137

48 Feoktistova, M., Geserick, P. & Leverkus, M. Crystal Violet Assay for Determining Viability of Cultured Cells. *Cold Spring Harb Protoc* **2016**, pdb.prot087379 (2016). https://doi.org:10.1101/pdb.prot087379

49 Franken, N. A., Rodermond, H. M., Stap, J., Haveman, J. & van Bree, C. Clonogenic assay of cells in vitro. *Nat Protoc* **1**, 2315-2319 (2006). https://doi.org:10.1038/nprot.2006.339

50 Wenceslau, C. F. *et al.* Guidelines for the measurement of vascular function and structure in isolated arteries and veins. *Am J Physiol Heart Circ Physiol* **321**, H77-h111 (2021). https://doi.org:10.1152/ajpheart.01021.2020

51 Gross, A., Tönjes, A. & Scholz, M. On the impact of relatedness on SNP association analysis. *BMC Genet* **18**, 104 (2017). https://doi.org:10.1186/s12863-017-0571-x

52 Graffelman, J., Jain, D. & Weir, B. A genome-wide study of Hardy-Weinberg equilibrium with next generation sequence data. *Hum Genet* **136**, 727-741 (2017). https://doi.org:10.1007/s00439-017-1786-7

53 Azzawi, M. in *Handbook of Vascular Biology Techniques* (eds Mark Slevin & Garry McDowell) 65-79 (Springer Netherlands, 2015).

54 Griffiths, K. & Madhani, M. The Use of Wire Myography to Investigate Vascular Tone and Function. *Methods Mol Biol* **2419**, 361-376 (2022). https://doi.org:10.1007/978-1-0716-1924-7_23

55 Lin, H. *et al.* RegSNPs-intron: a computational framework for predicting pathogenic impact of intronic single nucleotide variants. *Genome Biol* **20**, 254 (2019). https://doi.org:10.1186/s13059-019-1847-4

56 Mayr, C. What Are 3' UTRs Doing? *Cold Spring Harb Perspect Biol* **11** (2019). https://doi.org:10.1101/cshperspect.a034728

57 Steri, M., Idda, M. L., Whalen, M. B. & Orrù, V. Genetic variants in mRNA untranslated regions. *Wiley Interdiscip Rev RNA* **9**, e1474 (2018). https://doi.org:10.1002/wrna.1474

58 Hong, D. & Jeong, S. 3'UTR Diversity: Expanding Repertoire of RNA Alterations in Human mRNAs. *Mol Cells* **46**, 48-56 (2023). https://doi.org:10.14348/molcells.2023.0003

59 Rykova, E., Ershov, N., Damarov, I. & Merkulova, T. SNPs in 3'UTR miRNA Target Sequences Associated with Individual Drug Susceptibility. *Int J Mol Sci* **23** (2022). https://doi.org:10.3390/ijms232213725

60 Hrdlickova, B., de Almeida, R. C., Borek, Z. & Withoff, S. Genetic variation in the non-coding genome: Involvement of micro-RNAs and long non-coding RNAs in disease. *Biochim Biophys Acta* **1842**, 1910-1922 (2014). https://doi.org:10.1016/j.bbadis.2014.03.011

61 Zhang, N. *et al.* Genome-Wide 3'-UTR Single Nucleotide Polymorphism Association Study Identifies Significant Prostate Cancer Risk-Associated Functional Loci at 8p21.2 in Chinese Population. *Adv Sci (Weinh)* **9**, e2201420 (2022). https://doi.org:10.1002/advs.202201420

62 Ono, H., Basson, M. D. & Ito, H. P300 inhibition enhances gemcitabine-induced apoptosis of pancreatic cancer. *Oncotarget* **7**, 51301-51310 (2016). https://doi.org:10.18632/oncotarget.10117

63 Mini, E., Nobili, S., Caciagli, B., Landini, I. & Mazzei, T. Cellular pharmacology of gemcitabine. *Ann Oncol* **17 Suppl 5**, v7-12 (2006). https://doi.org:10.1093/annonc/mdj941

64 Lazar, A. G., Vlad, M. L., Manea, A., Simionescu, M. & Manea, S. A. Activated Histone Acetyltransferase p300/CBP-Related Signalling Pathways Mediate Up-Regulation of NADPH Oxidase, Inflammation, and Fibrosis in Diabetic Kidney. *Antioxidants (Basel)* **10** (2021). https://doi.org:10.3390/antiox10091356

65 Ganner, A. *et al.* The acetyltransferase p300 regulates NRF2 stability and localization. *Biochem Biophys Res Commun* **524**, 895-902 (2020). https://doi.org:10.1016/j.bbrc.2020.02.006

66 Duquaine, D. *et al.* Rapid-onset endothelial dysfunction with adriamycin: evidence for a dysfunctional nitric oxide synthase. *Vasc Med* **8**, 101-107 (2003). https://doi.org:10.1191/1358863x03vm476oa

67 Gibson, N. M., Greufe, S. E., Hydock, D. S. & Hayward, R. Doxorubicin-induced vascular dysfunction and its attenuation by exercise preconditioning. *J Cardiovasc Pharmacol* **62**, 355-360 (2013). https://doi.org:10.1097/FJC.0b013e31829c9993

68 Hayward, R. *et al.* Tissue retention of doxorubicin and its effects on cardiac, smooth, and skeletal muscle function. *J Physiol Biochem* **69**, 177-187 (2013). https://doi.org:10.1007/s13105-012-0200-0

69 Olukman, M. *et al.* Reversal of doxorubicin-induced vascular dysfunction by resveratrol in rat thoracic aorta: Is there a possible role of nitric oxide synthase inhibition? *Anadolu Kardiyol Derg* **9**, 260-266 (2009).

70 Dalske, H. F. & Hardy, K. Effect of low-dose doxorubicin on calcium content and norepinephrine response in rat aorta. *Eur J Cancer Clin Oncol* **24**, 979-983 (1988). https://doi.org:10.1016/0277-5379(88)90146-0

71 Ahmadiasl, N., Rostami, A., Mohammadi, N. M. & Rajabi, F. Effects of noradrenaline and KCl on peripheral vessels in doxorubicin induced model of heart failure. *Pathophysiology* **8**, 259-262 (2002). https://doi.org:10.1016/s0928-4680(02)00012-3

72 Shen, B., Ye, C. L., Ye, K. H., Zhuang, L. & Jiang, J. H. Doxorubicin-induced vasomotion and [Ca(2+)](i) elevation in vascular smooth muscle cells from C57BL/6 mice. *Acta Pharmacol Sin* **30**, 1488-1495 (2009). https://doi.org:10.1038/aps.2009.145

73 Santer, F. R. *et al.* Inhibition of the acetyltransferases p300 and CBP reveals a targetable function for p300 in the survival and invasion pathways of prostate cancer cell lines. *Mol Cancer Ther* **10**, 1644-1655 (2011). https://doi.org:10.1158/1535-7163.Mct-11-0182

74 Kalkhoven, E. CBP and p300: HATs for different occasions. *Biochem Pharmacol* **68**, 1145-1155 (2004). https://doi.org:10.1016/j.bcp.2004.03.045

75 Pilco-Ferreto, N. & Calaf, G. M. Influence of doxorubicin on apoptosis and oxidative stress in breast cancer cell lines. *Int J Oncol* **49**, 753-762 (2016). https://doi.org:10.3892/ijo.2016.3558

Chapter 4 - Tumor arteriolar function in an orthotopic model of breast cancer

Abstract

Many pre-clinical models of cancer are used to investigate interventions aimed at enhancing treatment outcomes. However, most of these models utilize an ectopic, rather than orthotopic, tumor location. Evidence suggests that tumor location may impact cancer signaling and tumor hemodynamics, which are of critical importance when researching modalities to improve cancer therapies. As such, we sought to characterize the vasculature and muscle mass changes in an orthotopic model of breast cancer. We hypothesized that compared to healthy host tissue, tumor arterioles would exhibit impaired α-adrenergic and myogenic vasoconstriction, and that the orthotopic model would result in some features of cachexia, which have been shown to occur in humans and pre-clinical models of cancer, independent of treatment. Though myogenic constriction was unaltered, there were impairments in α-adrenergic vasoconstriction of tumor arterioles compared to healthy host tissue. This is valuable information for guiding research into interventions that depend on tumor hemodynamics and taken together with previous findings, suggests that tumor blood flow could be preferentially increased through interventions such as exercise. Our model also suggests that some features of cachexia are present, which extends previous findings from orthotopic models of prostate cancer.

Introduction

Though the 5-year overall survival is over 90% for individuals diagnosed with breast cancer, survival rates decrease drastically for those with advanced disease. Several features of the tumor microenvironment can contribute to reduced treatment efficacy, malignant progression, and poor patient prognosis [1-10]. Two of the key features of the tumor microenvironment implicated in treatment failure are aberrant tumor vasculature and tumor hypoxia, which can lead to inadequate drug delivery [8,11], poor response to radiation therapy [1,3,12], and a shift towards a more aggressive phenotype [4,7,13-16].

Though it has long been understood that the vasculature of solid tumors is irregular [3,5,17-22], it is poorly modeled in most pre-clinical cancer models. Solid tumors can be highly angiogenic [5,6,8,23,24] and co-opt existing vessels of the host tissue vasculature [25,26]. Because hemodynamics vary greatly by host tissue bed (e.g., renal vs. skin circulation), functional differences in both the newly formed and co-opted vessels can be expected to vary greatly given the vascular bed it originates in. A study by Fukumura et al., demonstrated that liver cancer cells grown in the liver vs. subcutaneous tissue exhibited vastly different vascular morphology and function [27]. In addition, work from Garcia et al., suggests that host-tissue hemodynamics critically influence the vascular function of solid tumors in rats and that compared to ectopic models, orthotopic models have differing impacts on the response to interventions like exercise [28]. This builds upon the work of McCullough et al., who demonstrated that orthotopic tumor blood flow may increase in response to exercise, despite growing in a host tissue that exhibits unchanging or decreased blood flow during or after exercise [29,30]. However, most pre-clinical models are ectopic; that is, the tumor does not grow in the tissue of origin. Most often, tumors are grown subcutaneously in either the hindlimb or flank, in part because the procedures are

generally easier to perform than those for orthotopic injections, making it easier to inoculate many animals [31,32]. A shift toward using orthotopic models is important for better exploring interventions that rely on alterations in tumor blood flow, such as heat therapy or exercise.

Another important consequence of cancer progression that may be impacted by tumor location and the tumor microenvironment, and not adequately reflected in ectopic pre-clinical models, is cancer cachexia. As many as 80% of patients diagnosed with cancer experience cachexia with losses in cardiac and skeletal muscle mass [33,34] and prior research in pre-clinical orthotopic models of prostate cancer have shown that cancer, independent of treatment, leads to cardiac and skeletal muscle atrophy [35,36]. Of particular importance, the development of cachexia may be influenced by circulating factors released by tumor cells [37-39], which can be significantly impacted by tumor location [40]. As such, whether a pre-clinical model of breast cancer induces cachexia is an important issue to consider in pre-clinical cancer research, particularly when investigating interventions that may impact cardiac and skeletal muscle mass (e.g., exercise).

To our knowledge, this is the first study to investigate tumor vascular function in an orthotopic model of breast cancer in rats. Given the importance of tumor growth location to the development of the vasculature and microenvironment and evidence that orthotopic prostate tumor vessels exhibit impairments in vascular function, we sought to determine whether there were impairments in orthotopic breast tumor vascular function. We hypothesized that compared to healthy mammary vessels, tumor vessels would exhibit reduced responses to norepinephrine, as well as reduced myogenic constriction. We also hypothesized that breast cancer, independent of treatment, would result in cardiac and skeletal muscle atrophy.

Methods

Animal Handling and Tissue Acquisition

All procedures were approved by the Kansas State University Institutional Animal Care and Use Committee and carried out in accordance with the National Institutes of Health Guide for the Care and Use of Laboratory Animals. Healthy retired breeder female Fischer 344 rats (n = 11) obtained from Charles River Laboratories (Wilmington, MA) were housed and maintained in a temperature controlled (23 ± 2°C) room with a 12:12-h light-dark cycle, with water and standard rat chow provided *ad libitum*.

Orthotopic Tumor Model

The Mat B III breast cancer adenocarcinoma cell line (ATCC, Manassas, VA) was used in this study, which is a Fischer 344-derived cell line commonly used in pre-clinical models of breast cancer. Mat B III cells were maintained in McCoy's 5A medium (ATCC), supplemented with 10% fetal bovine serum (FBS) and 2 mM l-glutamine (Fisher Scientific, Hampton, NH), and grown in a humidified incubator maintained at 37º C with 5% CO_2/room air balance. Cells were harvested via trypsinization and centrifugation once reaching 75-80% confluency. Cells were then resuspended in sterile saline and prepared as 0.05 ml aliquots containing $6x10^3$ cells for injection.

Rats were anesthetized with a 5%/O_2 balance isoflurane anesthesia and maintained at 2%/O_2 balance. The left or right abdominal or upper inguinal nipple (#4 or 5; selected for largest size [41] and less likely to interfere with ambulation) was located and cells were injected directly through the nipple and into the mammary duct using a sterile insulin syringe (28 G). The needle was held in place for 1-2 seconds after injection and slowly removed to prevent leakage of cells.

A second injection was performed on the contralateral side if leakage of fluid out of the nipple was observed immediately after injection. Post-operative monitoring occurred 3 times/week until tumors were palpable, after which monitoring occurred daily. Rats were euthanized once tumors reached 1.5-2 cm (Kansas State University IACUC guideline #18, Tumor Burdens in Animals), 17-24 days after injection.

Tissue Acquisition and Tumor Vascular Function

We assessed tumor feed arterioles and healthy mammary arterioles using the *ex vivo* isolated microvessel technique to characterize the tumor vasculature. After euthanasia, tumors were carefully exposed and the feed arteriole was excised, cleaned of adipose tissue, and placed in cold (4º C) physiological saline solution (PSS) containing the following in mM concentration: 145 NaCl, 4.7 KCl, 2.0 $CaCl_2$, 1.17 $MgSO_4$, 1.2 NaH_2PO_4, 5.0 glucose, 2.0 pyruvate, 0.02 EDTA, 3.0 3-(*N*-morpholino)propanesulfonic acid (MOPS) buffer, and 1 g/100 ml bovine serum albumin, at a pH of 7.4. Control vessels were obtained from tumor-free animals by dissecting around the cranial inguinal nipple and isolating the feed arteriole. Vessels were then placed in a Lucite chamber containing warm (37º C) PSS equilibrated with room air, cannulated on glass micropipettes and secured with nylon suture (11-0 ophthalmic suture, Alcon Laboratories, Inc., Fort Worth, TX), and placed on an inverted microscope (Olympus IX70, Tokyo, Japan) equipped with a video camera (Panasonic BP310, Newark, NJ) and video caliper (Colorado Video, Longmont, CO) to record diameter. Vessels were pressurized to 90 cm H_2O and tested for leaks. Any vessel unable to maintain diameter was discarded. Leak-free vessels were allowed to equilibrate for one hour in warm PSS and develop spontaneous tone.

Cumulative dose response

After spontaneous tone developed, vasoconstrictor response to cumulative additions of the α-adrenoreceptor agonist norepinephrine (NE; 10^{-9} to 10^{-4}) was assessed. After each addition of NE, vessels were allowed three minutes to reach a steady state before measuring diameter.

Myogenic and passive-pressure response

After completion of cumulative dose-response curves, vessels were washed and allowed to return to baseline tone. We then assessed the myogenic response to increases in intraluminal pressure from 0 to 140 cm H_2O, in 20 cm H_2O increments. Vessel diameter was recorded for three minutes after each increase in pressure. The passive pressure-diameter response was then evaluated after a 60-minute incubation in calcium-free PSS. Vessels were again exposed to increases in intraluminal pressure from 0 to 140 cm H_2O, in 20 cm H_2O increments. Maximal diameter was then determined in calcium-free PSS containing 100 μM sodium nitroprusside (SNP) at a pressure of 90 cm H_2O.

Data Analysis and Statistics

All statistical analyses were performed using Prism (Version 10, GraphPad Software, San Diego, CA) data analysis software. Student's T-test was performed to determine the significance of any differences in body weight or muscle mass between groups (a paired t-test was performed to compare body weight in tumor-bearing animals over time). Vasodilatory responses were recorded as intraluminal diameter and expressed as a percentage of maximal relaxation according to the following:

$$\text{relaxation (\%)} = (D_s - D_b) / (D_m - D_b) * 100$$

where D_s is the steady state diameter recorded after addition of ACh, D_b is the initial diameter recorded before the first addition of ACh, and D_m is the maximal diameter recorded at 90 cm H_2O in calcium-free PSS. Vasoconstrictor responses to NE were recorded as intraluminal diameter and expressed as a percentage of maximal response according to the following:

$$\text{constriction (\%)} = (D_i - D_{ss}) / D_i * 100$$

where D_i is the initial diameter before first addition of NE and D_{ss} is the steady state diameter recorded after each addition of NE. Active myogenic responses after intraluminal pressure increases were normalized according to the following:

$$\text{normalized diameter} = (ID_{ss} - ID_{90})$$

where ID_{ss} is the steady state diameter at a given pressure step and ID_{90} is the diameter measured during the passive pressure response at 90 cm H_2O. Resting myogenic tone is expressed as a percentage change in diameter relative to passive myogenic tone and normalized to the diameter at 90 cm H_2O. Two-way analysis of variance (ANOVA) with repeated measures was used to determine differences between vessels from control and tumor-bearing animals for all measures. Post hoc comparisons were made using Holm-Sidak test to correct for multiple comparisons. All data are presented as mean ± SEM. Significance was set as $p \leq 0.05$.

Results

Animal Characteristics

There was no difference in body mass between control (CON) and tumor-bearing (TB) animals and no significant change in body mass over time in TB animals (Figure 4.1). Heart mass, left ventricle mass, and right ventricle mass were not different between groups (Table 4.1). Heart, left ventricle, and right ventricle masses were also normalized to body mass to account for possible differences in growth between control and tumor-bearing animals. There were no differences between heart mass, left ventricle mass, or right ventricle mass when normalized to body mass (Figure 4.2, Table 4.1). Skeletal muscle masses were also normalized to body mass. Gastrocnemius/body mass ratio was not different between groups, but gastrocnemius mass, plantaris mass, soleus mass, soleus/body mass ratio, and plantaris/body mass ratio were significantly decreased in tumor-bearing animals (all $p \leq 0.05$; Table 4.1, Figure 4.3). Body mass, heart mass, and left ventricle mass were not correlated with tumor mass (all $p > 0.05$; Figure 4.4). There were no correlations between gastrocnemius, soleus, or plantaris mass with tumor mass (all $p > 0.05$; Figure 4.5).

Vascular Function

To determine vasoactive responsiveness, we assessed vasoconstriction to the α-adrenoreceptor agonist norepinephrine in isolated arterioles from mammary tissue of healthy animals and from tumor-bearing animals. There were no differences in maximal constriction (58.9 ± 16.1 vs. 40.7 ± 14.0%; Figure 4.6) or sensitivity (log EC_{50}, -6.602 [95% CI, -7.251 to -5.938] vs. -7.084 [95% CI, -8.209 to -5.982]) to NE between control and tumor-bearing animals, respectively ($p > 0.05$). Compared to control, there was a significant interaction effect between

dose and group (CON vs. TB; $p \leq 0.05$; Figure 4.6), but there were no individual differences at any dose (all $p > 0.05$). There were no differences in active or passive pressure-diameter responses or resting myogenic tone between arterioles from control and tumor-bearing animals across the physiological range of pressures ($p > 0.05$; Figure 4.7).

Table 4.1. Animal Characteristics

	CON (n = 4)	TB (n = 6)	p-value	effect size (Hedge's g)
Mass (g)				
Body	219 ± 15.3	212 ± 18.2	0.55	0.44
Heart	0.657 ± 0.07	0.605 ± 0.07	0.28	0.75
Left ventricle	0.473 ± 0.04	0.442 ± 0.05	0.25	0.68
Right ventricle	0.103 ± 0.02	0.103 ± .02	0.99	0.002
Gastrocnemius	0.937 ± 0.05	0.795 ± 0.07 *	0.01	2.30
Soleus	0.090 ± 0.004	0.076 ± 0.06 *	0.005	2.50
Plantaris	0.019 ± 0.007	0.017 ± 0.01 *	0.003	2.76
Tumor	n/a	4.48 ± 1.3		
Tumor burden (% body mass)	n/a	2.16 ± 0.81		
Muscle mass normalized to body mass (mg/g)				
Heart/body mass	2.99 ± 0.20	2.85 ± 0.15	0.25	0.82
Left ventricle/body mass	2.16 ± 0.15	2.09 ± 0.15	0.49	0.47
Right ventricle/body mass	0.47 ± 0.08	0.49 ± 0.06	0.73	0.29
Gastrocnemius/body mass	4.28 ± 0.16	3.81 ± 0.50	0.22	0.90
Soleus/body mass	0.41 ± 0.03	0.36 ± 0.03 *	0.02	1.67
Plantaris/body mass	0.89 ± 0.03	0.81 ± 0.05 *	0.03	1.84

Data are mean ± SD. *significant vs. CON ($p \leq 0.05$)

Figure 4.1. Body mass

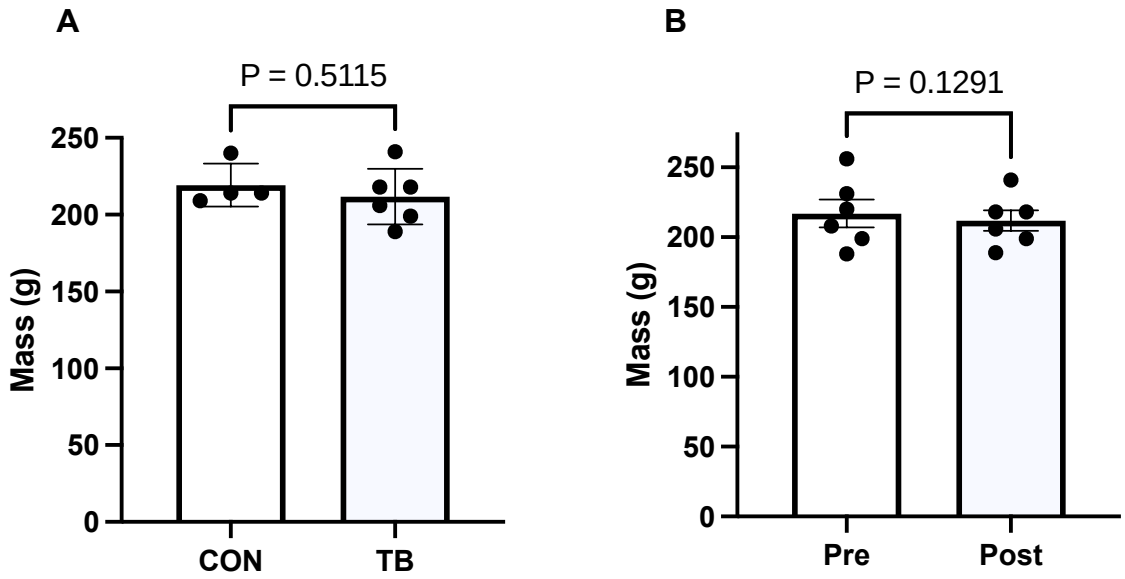

There were no differences in body mass between control (CON; n = 4) and tumor-bearing (TB; n = 6) animals (**A**) and body mass pre- to post- within TB animals (**B**). Data are mean ± SD. All p > 0.05).

Figure 4.2. Heart, left ventricle, and right ventricle mass normalized to body mass

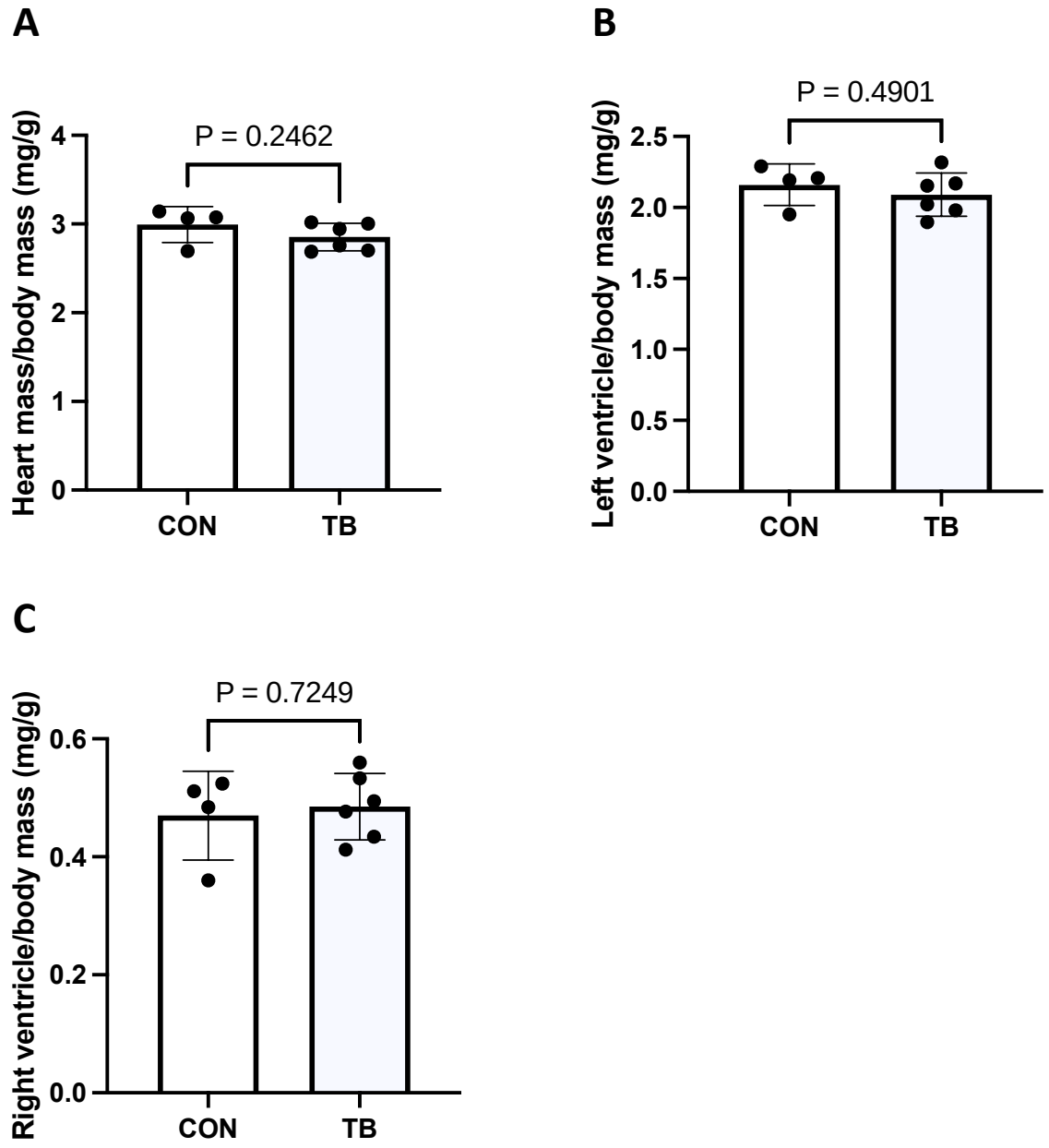

Heart (**A**), left ventricle (LV; **B**), and right ventricle (RV; **C**) mass normalized to body mass were not different between control (CON; n = 4) and tumor-bearing (TB; n = 6). Data are mean ± SD. All $p > 0.05$.

Figure 4.3. Soleus, plantaris, and gastrocnemius mass normalized to body mass

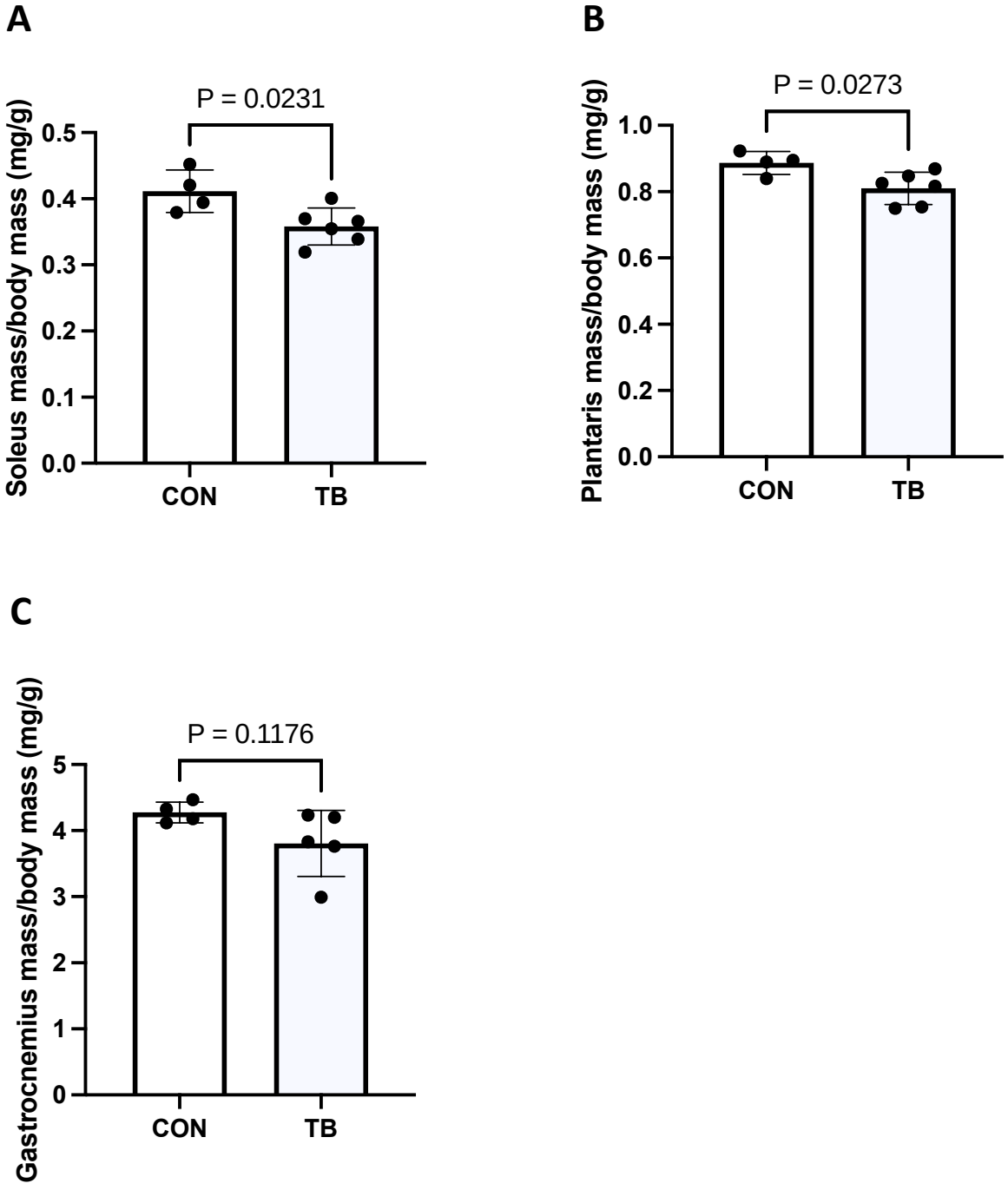

Soleus (**A**) and plantaris (**B**) mass were significantly lower in tumor-bearing (TB; n = 6) vs. control (CON; n = 4) animals when normalized to body mass ($p \leq 0.05$). Gastrocnemius mass (**C**) was not different between groups when normalized to body mass ($p > 0.05$). Data are mean ± SD.

Figure 4.4. Body mass, heart mass, and left ventricle mass relationship to tumor mass

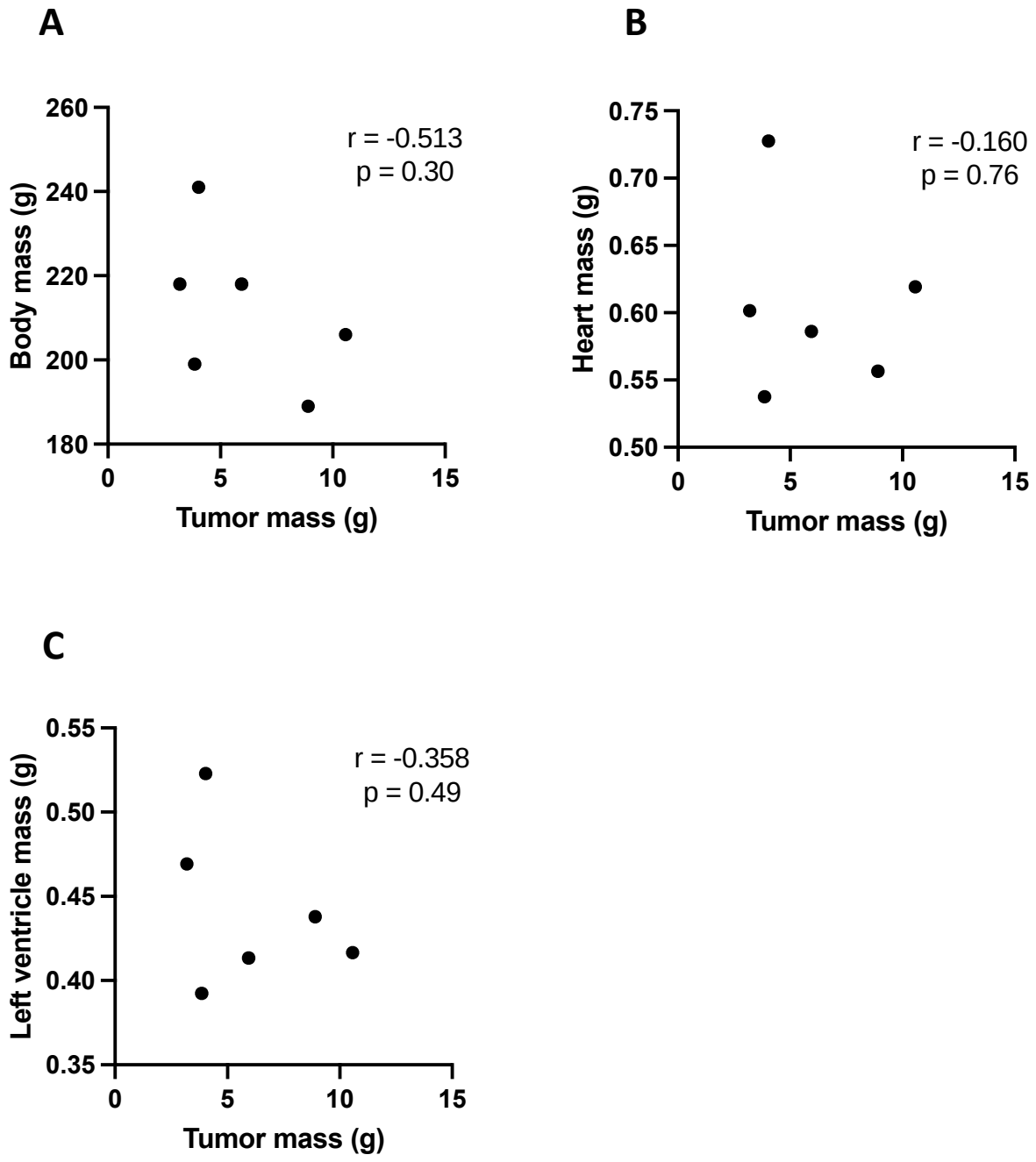

Body mass (**A**), heart mass (**B**), and left ventricle mass (**C**) were not correlated with tumor mass (n = 6).

Figure 4.5. Soleus, plantaris, and gastrocnemius mass relationship to tumor mass

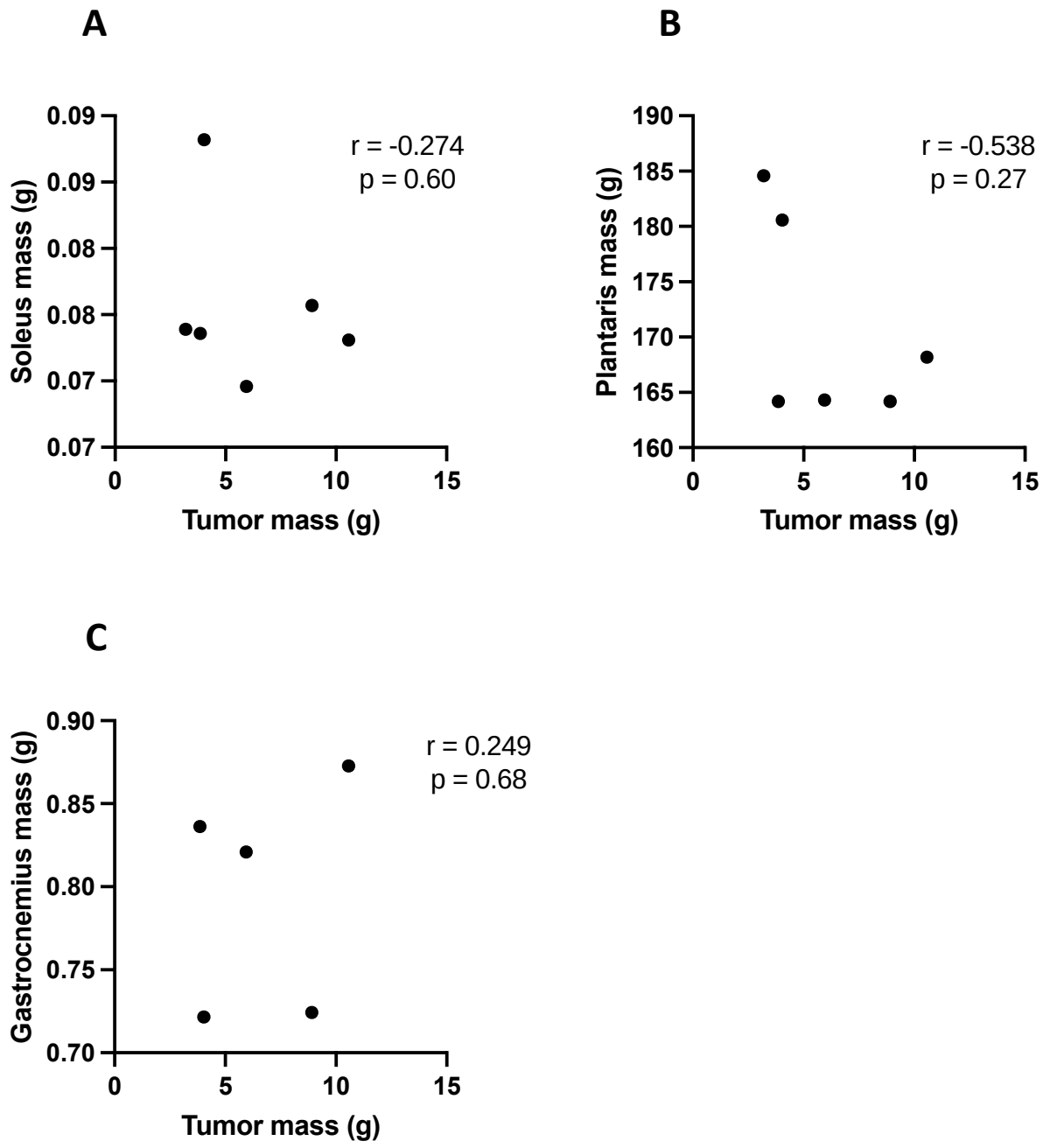

Soleus (**A**), plantaris (**B**), and gastrocnemius (**C**) were not correlated with tumor mass (n = 6).

Figure 4.6. Responses to norepinephrine

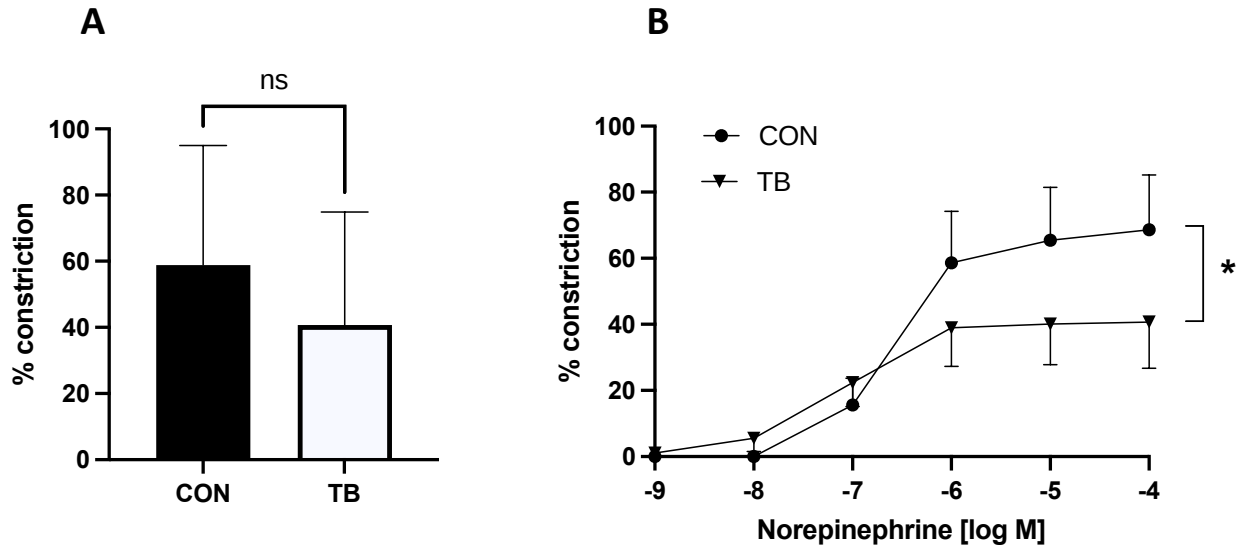

There was no difference in maximal constriction between control (CON; n = 4) and tumor-bearing (TB; n = 6; **A**, $p > 0.05$). There was a significant interaction between dose and tumor status in the norepinephrine dose response (**B**, $p \leq 0.05$).

Figure 4.7. Myogenic response

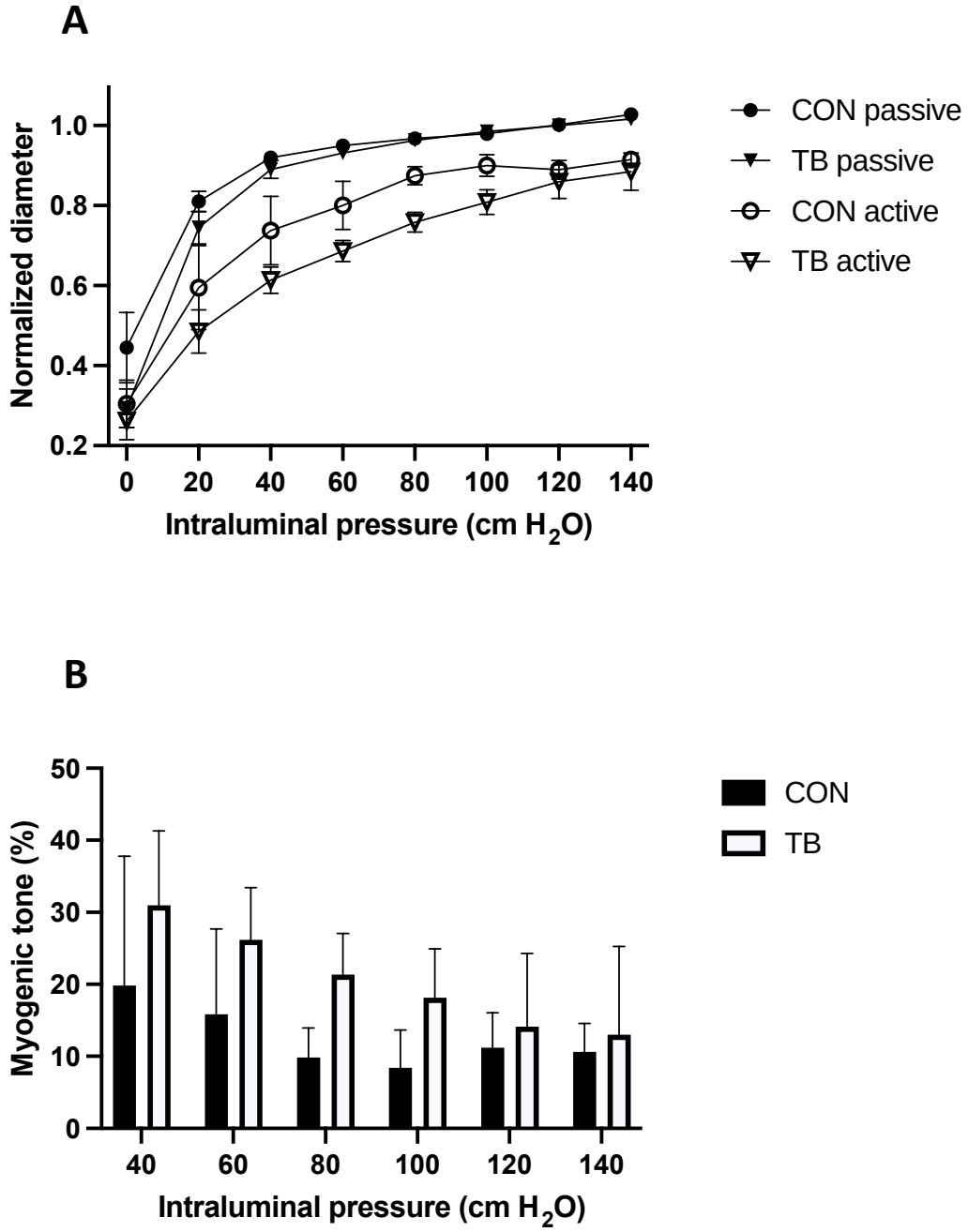

There were no differences in myogenic vasoconstriction (**A**) or resting myogenic tone (**B**) between control (CON; n = 4) or tumor-bearing (TB; n = 6); $p > 0.05$).

Discussion

To our knowledge, this is the first study to characterize the tumor vasculature and cardiac and skeletal muscle mass changes, independent of cancer treatment, in an orthotopic model of breast cancer. Notably, there were no differences in heart, left ventricle, or right ventricle mass between healthy and tumor-bearing animals, even when normalized to body mass. However, there skeletal muscle mass was a significantly lower in tumor-bearing animals, including when normalized to body mass, for both the soleus and plantaris, and this was accompanied by an overall loss in body weight averaging ~5%, which may be indicative of cachexia [42]. Despite these changes, no differences were observed in active or passive response to increasing intraluminal pressure or resting myogenic tone. There was, however, a significant interaction between dose and group (CON vs. TB) in α-adrenergic mediated vasoconstriction, suggesting potential impairment in α-adrenergic vasoconstriction at higher doses of NE. This finding has clinical relevance for designing and implementing interventions and adjuvant therapies that modify or depend on host-tissue and tumor hemodynamics. Additionally, a lack of vasoconstriction in the tumor feed arteriole compared to healthy tissue suggests that interventions like exercise may preferentially enhance tumor blood flow relative to other tissues.

Cancer cachexia

In humans, cancer cachexia is defined as a weight loss greater than 5%, or a weight loss between 2 and 5%, accompanied by sarcopenia [42]. The tumor-bearing rats in our study experienced a weight loss averaging 5% when comparing tumor-free body mass, and 2.1% with a reduced skeletal muscle mass compared to control animals, suggesting that our model *could* induce cachexia, but further investigation is needed to determine whether sarcopenia occurred.

Depending on the cancer site, cachexia occurs in 40-80% of patients and is responsible for 20% of cancer-related deaths [33,34]. Although the mechanisms are complex, inflammatory factors secreted by cancer cells represent a potential pathway mediating cachexia. For example, TNF-α, IL-6, and IL-1 are all secreted from tumor cells [43] and promote the initiation of cachexia [37-39]. Thus, our findings suggest that the orthotopic breast cancer model may represent the complex interaction between the tumor microenvironment and cancer cachexia.

Tumor vascular dysfunction: implications for treatment efficacy and metastatic potential

A hallmark feature of solid tumors is hypoxia, generally classified as pressure of oxygen (PO_2) < 10 mmHg [2]. As a tumor develops, it rapidly outgrows its existing vascular supply, necessitating compensation by co-opting surrounding vasculature and initiating new vessel growth [6,8,23,24]. However, this pathological angiogenesis leads to a dysfunctional vascular network, characterized by increased permeability, gaps in smooth muscle and endothelial cell layers, and vessel tortuosity [3,8,21]. These abnormalities in the newly co-opted or formed vessels result in a tumor vascular network characterized by limitations in perfusion and diffusion [2,6], potentiating tumor hypoxia. Critically, tumor hypoxia leads to radiation resistance, negatively impacting treatment success and patient outcomes [1,3,4,7-10] and triggers a cascade of hypoxia-mediated signaling that drives genetic adaptation and potentiates cancer cell survival [4,13-16].

Radioresistance arises in hypoxic tumors, in part, due to the dependence of radiation-induced DNA damage on the presence of oxygen, and due to hypoxia-mediated proteomic and genomic changes. Radiation therapy both directly and indirectly damages the structure of DNA, primarily through the induction of DNA DSBs [44-46]. Direct DNA damage occurs through

ionization of the DNA backbone, while indirect DNA damage results from damage by free radicals, produced primarily by water radiolysis. In both scenarios, molecular oxygen is a central contributor to the permanence or fixation of DNA damage [47,48]. Prior research suggests that radiation is up to 3 times more effective in a normoxic environment [48,49]. This effect, known as the oxygen-enhancement ratio (OER), suggests that simply increasing the PO_2 of a tumor will result in an increased efficacy of radiation therapy. However, increasing tumor oxygenation may be difficult given the aberrant nature of the tumor vasculature, and hypoxia-mediated proteomic and genomic changes further contribute to radioresistance. In addition, limited tumor blood flow, independent of tumor hypoxia, may be a significant barrier to the success of chemotherapy, as inadequate blood flow would result in decreased delivery of chemotherapy to the tumor.

Given the potential role of the tumor vasculature in cancer treatment, the finding that breast tumor arterioles may have a diminished vasoconstriction to norepinephrine is significant. In healthy tissue, perfusion is well-regulated to meet tissue-specific needs. For example, the metabolic demands of skeletal muscle necessitate an increase in skeletal muscle blood flow during exercise. Consequently, vascular beds of inactive tissues experience a decrease in blood flow, achieved in part by a sympathetically mediated vasoconstriction [50]. Because sympathetically mediated vasoconstriction is impaired in breast tumor arterioles, interventions that would typically result in a decrease in blood flow to the host tissue may result in increased blood flow to the tumor. A diminished α-adrenergic vasoconstriction compared to healthy host tissue, along with increased tumor blood flow and reduced hypoxia, was evidenced by McCullough et al in an orthotopic model of prostate cancer [30]. They demonstrated that prostate tumor arterioles exhibit a 95% blunted α-adrenergic vasoconstriction, accompanied by a 200% increase in tumor blood flow during moderate-intensity endurance exercise [30]. The increased

blood flow and resultant reduction in tumor hypoxia may improve the efficacy of radiation therapy and reduce metastatic potential.

In addition to improving treatment efficacy, decreased tumor hypoxia may promote a less aggressive cancer phenotype. In an environment where O_2 demand exceeds O_2 supply, cancer cells must reduce O_2 consumption and adapt to lower PO_2 to survive. This adaptation is primarily driven by an upregulation of HIF-1α signaling. Under normoxic conditions, HIF-1α expression is regulated by the presence of oxygen. When adequate O_2 is present, proline residues on HIF-1α are hydroxylated by prolyl-4-hydroxylase domain (PHD) proteins. In turn, this allows binding to the VHL component of E3 ubiquitin ligases, leading to proteasomal degradation, which maintains a homeostatic level of HIF-1α [51-54]. Under hypoxic conditions however, PHD function is diminished and is unable to hydroxylate HIF-1α. HIF-1α instead dimerizes with HIF-1β and forms a complex with other transcriptional coactivators (such as p300) at HRE [55] and drives transcription of genes responsible for metabolic adaptations (e.g. transcriptional activation of glycolytic enzymes, inhibition of mitochondrial respiration, etc.), angiogenesis, ROS homeostasis, cell proliferation, apoptosis, and more [56,57]. It would be expected that interventions such as exercise could be utilized to take advantage of diminished tumor arteriolar vasoconstriction, thereby increasing tumor blood flow and decreasing tumor hypoxia, which is supported by the finding of McCullough et al that there was a 50% reduction in tumor hypoxia after moderate-intensity exercise [30].

Experimental Considerations

Our study has a few experimental considerations. First, we only assessed two aspects of vascular function, and there are many other factors to consider that impact tumor vascular

function, such as vasodilatory pathways, vessel density, and neurohumoral influences. Secondly, we did not measure tumor hypoxia or blood flow in our study. The reductions in α-adrenergic vasoconstriction in our study were not as pronounced as those observed by McCullough et al [30] (nor accompanied by altered myogenic vasoconstriction), and it is possible that the resting tumor PO_2 and blood flow in the orthotopic breast tumor differ from that of the prostate. However, most solid tumors are considered hypoxic [16] and have a median PO_2 lower than their tissue of origin [2]. We did not perform any molecular studies to investigate the mechanisms of cachexia, which could provide insight to whether our model induces clinically defined cachexia observed in patients. Lastly, we did not compare the effects of ectopic vs. orthotopic tumor location on vascular function or cachexia, which is an important follow-up to our study to determine whether tumor vascular function or development of cachexia differs between orthotopic and ectopic models.

Conclusions

In summary, our findings suggest that the orthotopic model of breast cancer induces impaired α-adrenergic vasoconstriction and skeletal muscle atrophy, but does not induce impairments in myogenic tone or result in cardiac atrophy. Though the exact mechanisms underlying these changes are incompletely understood, our model confirms previous findings from orthotopic prostate cancer models [28-30,35,36] and suggests that vascular impairments of the orthotopic breast tumor may be similar to that of the prostate. As such, our model can be utilized to explore interventions that may modulate tumor blood flow, and the possibility of cachexia occurring suggests that our model may mirror some of the changes experienced by patients that depend in part on the tumor microenvironment. Further studies should be performed to

characterize other aspects of the orthotopic breast tumor environment, as well as changes in skeletal muscle.

References

1 Höckel, M., Schlenger, K., Mitze, M., Schäffer, U. & Vaupel, P. Hypoxia and Radiation Response in Human Tumors. *Semin Radiat Oncol* **6**, 3-9 (1996). https://doi.org:10.1053/srao0060003

2 Höckel, M. & Vaupel, P. Tumor hypoxia: definitions and current clinical, biologic, and molecular aspects. *J Natl Cancer Inst* **93**, 266-276 (2001). https://doi.org:10.1093/jnci/93.4.266

3 Vaupel, P. Tumor microenvironmental physiology and its implications for radiation oncology. *Semin Radiat Oncol* **14**, 198-206 (2004). https://doi.org:10.1016/j.semradonc.2004.04.008

4 Vaupel, P. The role of hypoxia-induced factors in tumor progression. *Oncologist* **9 Suppl 5**, 10-17 (2004). https://doi.org:10.1634/theoncologist.9-90005-10

5 Vaupel, P. & Harrison, L. Tumor hypoxia: causative factors, compensatory mechanisms, and cellular response. *Oncologist* **9 Suppl 5**, 4-9 (2004). https://doi.org:10.1634/theoncologist.9-90005-4

6 Vaupel, P., Kallinowski, F. & Okunieff, P. Blood-Flow, Oxygen and Nutrient Supply, and Metabolic Microenvironment of Human-Tumors - a Review. *Cancer Res* **49**, 6449-6465 (1989).

7 Vaupel, P., Mayer, A. & Höckel, M. Tumor hypoxia and malignant progression. *Methods Enzymol* **381**, 335-354 (2004). https://doi.org:10.1016/s0076-6879(04)81023-1

8 Siemann, D. W. The unique characteristics of tumor vasculature and preclinical evidence for its selective disruption by Tumor-Vascular Disrupting Agents. *Cancer Treat Rev* **37**, 63-74 (2011). https://doi.org:10.1016/j.ctrv.2010.05.001

9 Walsh, J. C. *et al.* The clinical importance of assessing tumor hypoxia: relationship of tumor hypoxia to prognosis and therapeutic opportunities. *Antioxid Redox Signal* **21**, 1516-1554 (2014). https://doi.org:10.1089/ars.2013.5378

10 Turaka, A. *et al.* Hypoxic prostate/muscle PO2 ratio predicts for outcome in patients with localized prostate cancer: long-term results. *Int J Radiat Oncol Biol Phys* **82**, e433-439 (2012). https://doi.org:10.1016/j.ijrobp.2011.05.037

11 Koch, S., Mayer, F., Honecker, F., Schittenhelm, M. & Bokemeyer, C. Efficacy of cytotoxic agents used in the treatment of testicular germ cell tumours under normoxic and

hypoxic conditions in vitro. *Br J Cancer* **89**, 2133-2139 (2003). https://doi.org:10.1038/sj.bjc.6601375

12 Hill, R. P. *et al.* Hypoxia and Predicting Radiation Response. *Semin Radiat Oncol* **25**, 260-272 (2015). https://doi.org:10.1016/j.semradonc.2015.05.004

13 Rofstad, E. K. Microenvironment-induced cancer metastasis. *Int J Radiat Biol* **76**, 589-605 (2000). https://doi.org:10.1080/095530000138259

14 Subarsky, P. & Hill, R. P. The hypoxic tumour microenvironment and metastatic progression. *Clin Exp Metastasis* **20**, 237-250 (2003). https://doi.org:10.1023/a:1022939318102

15 Milosevic, M., Fyles, A., Hedley, D. & Hill, R. The human tumor microenvironment: invasive (needle) measurement of oxygen and interstitial fluid pressure. *Semin Radiat Oncol* **14**, 249-258 (2004). https://doi.org:10.1016/j.semradonc.2004.04.006

16 Bristow, R. G. & Hill, R. P. Hypoxia, DNA repair and genetic instability. *Nat Rev Cancer* **8**, 180-192 (2008). https://doi.org:10.1038/nrc2344

17 Konerding, M. A. *et al.* Evidence for characteristic vascular patterns in solid tumours: quantitative studies using corrosion casts. *Br J Cancer* **80**, 724-732 (1999). https://doi.org:10.1038/sj.bjc.6690416

18 Carmeliet, P. & Jain, R. K. Angiogenesis in cancer and other diseases. *Nature* **407**, 249-257 (2000). https://doi.org:10.1038/35025220

19 Jain, R. K. Determinants of tumor blood flow: a review. *Cancer Res* **48**, 2641-2658 (1988).

20 Baish, J. W. *et al.* Role of tumor vascular architecture in nutrient and drug delivery: an invasion percolation-based network model. *Microvasc Res* **51**, 327-346 (1996). https://doi.org:10.1006/mvre.1996.0031

21 Baluk, P., Morikawa, S., Haskell, A., Mancuso, M. & McDonald, D. M. Abnormalities of basement membrane on blood vessels and endothelial sprouts in tumors. *Am J Pathol* **163**, 1801-1815 (2003). https://doi.org:10.1016/S0002-9440(10)63540-7

22 Yancopoulos, G. D. *et al.* Vascular-specific growth factors and blood vessel formation. *Nature* **407**, 242-248 (2000). https://doi.org:10.1038/35025215

23 Semenza, G. L. Targeting HIF-1 for cancer therapy. *Nat Rev Cancer* **3**, 721-732 (2003). https://doi.org:10.1038/nrc1187

24 Folkman, J. Tumor angiogenesis. *Adv Cancer Res* **43**, 175-203 (1985). https://doi.org:10.1016/s0065-230x(08)60946-x

25 Holash, J. *et al.* Vessel cooption, regression, and growth in tumors mediated by angiopoietins and VEGF. *Science* **284**, 1994-1998 (1999). https://doi.org:10.1126/science.284.5422.1994

26 Küsters, B. *et al.* Vascular endothelial growth factor-A(165) induces progression of melanoma brain metastases without induction of sprouting angiogenesis. *Cancer Res* **62**, 341-345 (2002).

27 Fukumura, D., Yuan, F., Monsky, W. L., Chen, Y. & Jain, R. K. Effect of host microenvironment on the microcirculation of human colon adenocarcinoma. *Am J Pathol* **151**, 679-688 (1997).

28 Garcia, E. *et al.* Blood flow responses to mild-intensity exercise in ectopic vs. orthotopic prostate tumors; dependence upon host tissue hemodynamics and vascular reactivity. *J Appl Physiol (1985)* **121**, 15-24 (2016). https://doi.org:10.1152/japplphysiol.00266.2016

29 McCullough, D. J., Nguyen, L. M., Siemann, D. W. & Behnke, B. J. Effects of exercise training on tumor hypoxia and vascular function in the rodent preclinical orthotopic prostate cancer model. *J Appl Physiol (1985)* **115**, 1846-1854 (2013). https://doi.org:10.1152/japplphysiol.00949.2013

30 McCullough, D. J., Stabley, J. N., Siemann, D. W. & Behnke, B. J. Modulation of blood flow, hypoxia, and vascular function in orthotopic prostate tumors during exercise. *J Natl Cancer Inst* **106**, dju036 (2014). https://doi.org:10.1093/jnci/dju036

31 Caceres, S. *et al.* Tumor Growth Progression in Ectopic and Orthotopic Xenografts from Inflammatory Breast Cancer Cell Lines. *Vet Sci* **8** (2021). https://doi.org:10.3390/vetsci8090194

32 de Jong, M. & Maina, T. Of mice and humans: are they the same?--Implications in cancer translational research. *J Nucl Med* **51**, 501-504 (2010). https://doi.org:10.2967/jnumed.109.065706

33 Argilés, J. M., Busquets, S., Stemmler, B. & López-Soriano, F. J. Cancer cachexia: understanding the molecular basis. *Nat Rev Cancer* **14**, 754-762 (2014). https://doi.org:10.1038/nrc3829

34 Rao, V. K., Das, D. & Taneja, R. Cancer Cachexia: Signaling and Transcriptional Regulation of Muscle Catabolic Genes. *Cancers (Basel)* **14** (2022). https://doi.org:10.3390/cancers14174258

35 Baumfalk, D. R. *et al.* Effects of prostate cancer and exercise training on left ventricular function and cardiac and skeletal muscle mass. *J Appl Physiol (1985)* **126**, 668-680 (2019). https://doi.org:10.1152/japplphysiol.00829.2018

36 Esau, P. J. *et al.* Prostate cancer reduces endurance exercise capacity in association with reductions in cardiac and skeletal muscle mass in the rat. *Am J Cancer Res* **7**, 2566-2576 (2017).

37 Tisdale, M. J. Are tumoral factors responsible for host tissue wasting in cancer cachexia? *Future Oncol* **6**, 503-513 (2010). https://doi.org:10.2217/fon.10.20

38 Inácio Pinto, N. *et al.* Cancer as a Proinflammatory Environment: Metastasis and Cachexia. *Mediators Inflamm* **2015**, 791060 (2015). https://doi.org:10.1155/2015/791060

39 Zhou, J., Liu, B., Liang, C., Li, Y. & Song, Y. H. Cytokine Signaling in Skeletal Muscle Wasting. *Trends Endocrinol Metab* **27**, 335-347 (2016). https://doi.org:10.1016/j.tem.2016.03.002

40 Matsuyama, T. *et al.* Tumor inoculation site affects the development of cancer cachexia and muscle wasting. *Int J Cancer* **137**, 2558-2565 (2015). https://doi.org:10.1002/ijc.29620

41 Hvid, H., Thorup, I., Sjögren, I., Oleksiewicz, M. B. & Jensen, H. E. Mammary gland proliferation in female rats: effects of the estrous cycle, pseudo-pregnancy and age. *Exp Toxicol Pathol* **64**, 321-332 (2012). https://doi.org:10.1016/j.etp.2010.09.005

42 Fearon, K. *et al.* Definition and classification of cancer cachexia: an international consensus. *Lancet Oncol* **12**, 489-495 (2011). https://doi.org:10.1016/s1470-2045(10)70218-7

43 Mantovani, G. *et al.* Serum levels of leptin and proinflammatory cytokines in patients with advanced-stage cancer at different sites. *J Mol Med (Berl)* **78**, 554-561 (2000). https://doi.org:10.1007/s001090000137

44 Desouky, O., Ding, N. & Zhou, G. Targeted and non-targeted effects of ionizing radiation. *Journal of Radiation Research and Applied Sciences* **8**, 247-254 (2015). https://doi.org:https://doi.org/10.1016/j.jrras.2015.03.003

45 Ward, J. F. DNA damage produced by ionizing radiation in mammalian cells: identities, mechanisms of formation, and reparability. *Prog Nucleic Acid Res Mol Biol* **35**, 95-125 (1988). https://doi.org:10.1016/s0079-6603(08)60611-x

46 van Gent, D. C., Hoeijmakers, J. H. & Kanaar, R. Chromosomal stability and the DNA double-stranded break connection. *Nat Rev Genet* **2**, 196-206 (2001). https://doi.org:10.1038/35056049

47 Riley, P. A. Free-Radicals in Biology - Oxidative Stress and the Effects of Ionizing-Radiation. *Int J Radiat Biol* **65**, 27-33 (1994). https://doi.org:Doi 10.1080/09553009414550041

48 Rockwell, S., Dobrucki, I. T., Kim, E. Y., Marrison, S. T. & Vu, V. T. Hypoxia and Radiation Therapy: Past History, Ongoing Research, and Future Promise. *Curr Mol Med* **9**, 442-458 (2009). https://doi.org:Doi 10.2174/156652409788167087

49 Gray, L. H., Conger, A. D., Ebert, M., Hornsey, S. & Scott, O. C. The concentration of oxygen dissolved in tissues at the time of irradiation as a factor in radiotherapy. *Br J Radiol* **26**, 638-648 (1953). https://doi.org:10.1259/0007-1285-26-312-638

50 Rowell, L. *Human cardiovascular control*. Vol. 268 (Oxford University Press, 1993).

51 Ohh, M. *et al.* Ubiquitination of hypoxia-inducible factor requires direct binding to the beta-domain of the von Hippel-Lindau protein. *Nat Cell Biol* **2**, 423-427 (2000). https://doi.org:10.1038/35017054

52 Cockman, M. E. *et al.* Hypoxia inducible factor-alpha binding and ubiquitylation by the von Hippel-Lindau tumor suppressor protein. *J Biol Chem* **275**, 25733-25741 (2000). https://doi.org:10.1074/jbc.M002740200

53 Tanimoto, K., Makino, Y., Pereira, T. & Poellinger, L. Mechanism of regulation of the hypoxia-inducible factor-1 alpha by the von Hippel-Lindau tumor suppressor protein. *EMBO J* **19**, 4298-4309 (2000). https://doi.org:10.1093/emboj/19.16.4298

54 Gorres, K. L. & Raines, R. T. Prolyl 4-hydroxylase. *Crit Rev Biochem Mol Biol* **45**, 106-124 (2010). https://doi.org:10.3109/10409231003627991

55 Weidemann, A. & Johnson, R. S. Biology of HIF-1α. *Cell Death Differ* **15**, 621-627 (2008). https://doi.org:10.1038/cdd.2008.12

56 Rey, S., Schito, L., Koritzinsky, M. & Wouters, B. G. Molecular targeting of hypoxia in radiotherapy. *Adv Drug Deliver Rev* **109**, 45-62 (2017). https://doi.org:10.1016/j.addr.2016.10.002

57 Eales, K. L., Hollinshead, K. E. R. & Tennant, D. A. Hypoxia and metabolic adaptation of cancer cells. *Oncogenesis* **5** (2016). https://doi.org:10.1038/oncsis.2015.50

Chapter 5 - Conclusions

Despite the many advances in anti-cancer therapies over the last several decades, many individuals diagnosed with cancer experience treatment failure. As such, the development of treatment adjuvants is important for improving patient outcomes. The most diagnosed cancers in the United States are prostate and breast cancer, and both are frequently treated with radiation. Breast cancer is also commonly treated with the anthracycline chemotherapy doxorubicin. As such, we focused our studies on factors that may improve the efficacy of these treatments. A potential candidate to modulate the efficacy of both treatments is p300/CBP, a histone acetyltransferase known to interact with a multitude of transcription factors and modulate the expression of many genes. Thus, in the first two studies of this dissertation, we explored the role of p300/CBP in mediating the response to radiation and doxorubicin. To better explore interventions that impact the efficacy of anti-cancer therapies, the final study seeks to characterize the vasculature and skeletal muscle mass changes in an orthotopic model of breast cancer.

In Chapter 2, we found that SNPs in both the p300 and CBP gene encoding regions are associated with the odds of diagnosis of secondary malignancy in both prostate and breast cancer patients, among all treatments, as well as among those who received radiation. This suggests that p300/CBP may, in part, mediate the response to radiation and other anti-cancer therapies. Further investigation into the role of these particular SNPs may provide valuable insight on potential treatment options and may help to predict patient responses to specific treatments. Though our cell culture findings did not support a role of pharmacological inhibition of p300/CBP for enhancing the efficacy of radiation, valuable insight can be gained from performing these studies *in vivo.* In Chapter 3, we explored the association between p300/CBP SNPs and the odds of

secondary diagnosis in individuals with breast cancer who received doxorubicin. We found that there is an association between several CBP, but no p300, SNPs and the odds of diagnosis. This suggests a potential role of CBP in mediating the efficacy of doxorubicin. These findings can be further explored to develop new treatments and predict patient responses. Following these results, we explored the role of pharmacological inhibition of p300/CBP in the response of breast cancer cells to doxorubicin *in vitro.* We found that p300/CBP inhibition did not affect breast cancer cell survival after exposure to doxorubicin. Given that doxorubicin profoundly impacts the cardiovascular system, also explored the impact of doxorubicin and p300/CBP inhibition on aortic vascular function, finding that neither doxorubicin nor p300/CBP inhibition impacted aortic vascular function *ex vivo*. Further investigations should be performed to gain insight into the impact of doxorubicin and p300/CBP on aortic vascular function *in vivo.* Finally, in Chapter 4, we found that breast tumor arterioles exhibit some impairments in α-adrenergic vasoconstriction, which may be a potential impairment through which tumor blood flow can be modulated. Secondly, we found that an orthotopic model of breast cancer may result in some characteristics of cachexia, which occurs in as many as 80% of cancer patients and can be influenced by the tumor microenvironment. As such, this model may be valuable for studying interventions which impact tumor blood flow and the tumor microenvironment.

Taken together, we feel this work provides a basis for investigating the precise role of p300 and CBP in the efficacy of anti-cancer therapies, which may provide valuable information to improve treatment responses, as well as a potential means of stratifying patients to determine optimal treatment regimens. While some of our hypotheses were not supported, we hope that our findings can provide insight into further research and new strategies to improve patient outcomes.